Cloning and characterization of *Escherichia coli fosA* and *Mycobacterium tuberculosis mmr* antimicrobial resistance genes

By
Kieran A. Milner

A Thesis
Submitted to the Faculty of Graduate Studies
in Partial Fulfillment of the Requirements for the Degree of

Master of Science

Department of Medical Microbiology and Infectious Diseases
Rady Faculty of Health Sciences
University of Manitoba
Winnipeg, Manitoba, Canada

Abstract

The overuse of antimicrobials in medicine and agriculture has led to the emergence of antimicrobial resistant bacteria, which are difficult to treat and incur significant healthcare costs. The purpose of this thesis was to characterize important antimicrobial resistance genes (*fosA* and *mmr*) from two organisms identified as pathogens of concern by the World Health Organization; *Escherichia coli* and *Mycobacterium tuberculosis*. The goal of these two studies was to distinguish the antimicrobial resistant phenotypes of these genes to clinically relevant antimicrobial agents and learn more about their drug selectivity, their structure-function, and their phylogenetic relationships to previously characterized representative homologs.

The first objective was to characterize the fosfomycin resistance (*fosA*) genes from three Canadian clinical *E. coli* isolates with high-level fosfomycin resistance (MIC >512 µg/mL). Whole genome sequencing was performed on these isolates which uncovered *fosA3*, *fosA8*, and a novel gene *fosA7.5*. The *fosA3*, *fosA8*, and three *fosA7.5* variants ($fosA7.5^{WT}$, $fosA7.5^{Q86E}$, $fosA7.5^{W92G}$) were individually cloned and over-expressed in *E. coli* K-12 BW25113. Antimicrobial susceptibility testing using Clinical and Laboratory Standards Institute (CLSI) methodology was performed to confirm the role of these *fosA* genes in conferring fosfomycin resistance. Each gene was found to confer high level fosfomycin resistance, with the exception of $fosA7.5^{W92G}$ which did not confer resistance to fosfomycin. Phylogenetic comparison, protein sequence alignment, and homology modelling of the FosA7.5 variants identified amino acid residues that distinguish this sub-family and play an important role in the active site of these enzymes.

The second objective was to characterize the small multidrug resistance (SMR) family efflux gene *mmr* (Rv3065) from *M. tuberculosis* H37Rv using *M. smegmatis* as a model organism for expression. The *mmr* gene was electroporated into *M. smegmatis* mc^24517, and compared to eight other representative SMR genes (*emrE, qacE, qacF, gdx, qacC, qacG, qacH,* and *qacJ*) which were cloned in either *E. coli* K-12 BW25113 or *B. subtilis* MGNA-A001. CLSI broth microdilution antimicrobial susceptibility was used to determine substrate specificity differences between over-expressed efflux pumps. Only *mmr* was shown to confer 2-4 fold reduced susceptibility to erythromycin, clarithromycin, azithromycin, roxithromycin, and clindamycin. Phylogenetic analysis, amino acid sequence alignments, and homology modelling of Mmr to previously characterized SMR family representatives identified several conserved regions and multiple residue differences that may explain the differences in Mmr macrolide selectivity.

Acknowledgements

First I would like to acknowledge my family; my mother Jennifer Milner, my grandparents John F. Milner and Sylvia Milner, my aunt Traci Milner, and my uncle John E. Milner. Thank you all for supporting me, providing me with guidance, and for encouraging me to follow my passion.

I'm grateful to Drs. Meenu Sharma and Denice Bay for giving me the opportunity to work in their laboratories and for providing me with guidance and support throughout my Master's degree. It's been a pleasure to work with my supervisors on our research projects. I also sincerely wish to thank my committee members Drs. Ann Karen Brassinga and George Zhanel for all of their thoughtful suggestions and helpful assistance at our meetings.

Many thanks to my collaborators Drs. David Alexander, Andrew Walkty, James Karlowsky, and Michael Mulvey for their valuable contributions to our research and this thesis. Thanks to Nancy Laing and the scientists of the Canadian Antimicrobial Resistance Alliance, Cadham Provincial Laboratory, and National Microbiology Laboratory for their assistance with my research and training.

Thanks to Angela Nelson and the other hardworking MMID staff for all of their administrative assistance, and for making our time in the MSc program as graduate students much easier to navigate. Thanks should also go to Dr. Jason Kindrachuk and his lab members Brayden Shindell and Andrew Webb for routinely helping me with my experiments, providing troubleshooting advice, and for generously sharing their laboratory resources with me.

I would like to thank Dr. Richard Sparling for inspiring me, as well as many others to continue studying microbiology. I will never forget his engaging undergraduate lectures, and I'm grateful to have worked with him on a research project course prior to beginning my MSc. I'd also like to extend another acknowledgement to Dr. George Zhanel for his fantastic lectures and excellent mentorship during my time in his graduate courses and the MSc program.

A final thanks to all of my friends, past and present lab members, and wonderful people in my life Branden Gregorchuk, Shelby Reimer, Carmine Slipski, Ali Doucet, Kari Green, Shiv Bhanot, Blaine Stenson, Kabir Bhanot, and Mitchell Beavis for all of their assistance with my experiments and coursework, and for helping me make it through the rigors of my degree. I couldn't have made it here without all of your support. Thank you everyone.

To my family, Jennifer Milner, John F. Milner, Sylvia Milner,
John E. Milner, Traci Milner, and Max Milner.

"There is nothing in the dark that isn't there when the lights are on."
-Rodman Edward "Rod" Serling (1924-1975)

Table of Contents

Abstract ii

Acknowledgements iii

Table of Contents v

List of Tables viii

List of Figures ix

List of Abbreviations x

Contributions of Authors xii

Chapter 1: Antimicrobial resistance review 1

1.1. Background 1

1.2. Antimicrobial resistance in *Escherichia coli* 2

1.2.1. Pathogenicity and treatment of *E. coli* 2

1.2.2. Resistance to fosfomycin 3

1.3. Antimicrobial resistance in *Mycobacterium tuberculosis* 5

1.3.1. Pathogenicity and treatment of *M. tuberculosis* 5

1.3.2. Resistance to antituberculosis drugs 6

1.3.3. Contribution of efflux pumps to antimicrobial resistance 10

1.3.4. *M. smegmatis* as a model for *M. tuberculosis* protein characterization 14

1.4. Thesis objectives 14

1.4.1. Chapter 3 rationale and hypothesis 15

1.4.2. Chapter 4 rationale and hypothesis 15

Chapter 2: Methods 17

2.1. Chemicals and media used in this study 17

2.2. Bacterial strains and culture conditions 17

2.3. *E. coli* clinical isolate whole genome sequencing 19

2.4. *fosA* and SMR protein sequence sources 19

2.5. Construction of plasmids 22
2.6. Construction of expression strains 24
2.7. Determination of protein accumulation 25
2.8. Antimicrobial susceptibility tests (AST) 27
2.9. Multiple sequence alignments and phylogenetic analyses 29
2.10. Homology modelling of FosA and SMR protein sequences 29

Chapter 3: Identification and characterization of a novel FosA7 member from fosfomycin resistant clinical *Escherichia coli* isolates from Canadian hospitals 31
3.1. Introduction 31
3.2. Results and Discussion 31
3.2.1. Phylogenetic analysis of *fos* genes reveals multiple *fosA* types in Canadian isolates. 31
3.2.2. *fosA* genes confer similar fosfomycin resistance MIC values 37
3.2.3. FosA homology models demonstrate close overall alignment to each other 38
3.3. Conclusions 42

Chapter 4: Characterization of the *Mycobacterium tuberculosis* Mmr efflux pump in *M. smegmatis* reveals a macrolide selectivity when compared to other small multidrug resistance efflux pump family members 43
4.1. Introduction 43
4.2. Results and Discussion 45
4.2.1. Mmr is closely related to members of the small multidrug pump (SMP) SMR subclass 45
4.2.2. Mmr possesses key residue differences suggesting it may confer altered substrate selectivity as compared to other characterized SMP subclass members 48
4.2.3. Mmr confers reduced susceptibility to macrolides and lincosamides in *M. smegmatis* 51
4.2.4. Homology modelling of Mmr demonstrates structural relatedness to other SMR protein homology models 55
4.3. Conclusions 58

Chapter 5: Discussion of Chaper 3-4 findings, concluding remarks, and future directions 59
5.1. Summary and impact of Chapters 3 and 4 findings 59
5.2. Study limitations 60
5.3. Future directions 61
5.4. Conclusion 62

References 63

Appendix A – Accession numbers utilized in this study 83

Appendix B – Fasta files for gene synthesis 86

Appendix C – Homology model active sites 88

List of Tables

1.1.	List of antimicrobials currently used for the treatment of tuberculosis.	7
2.1.	Sequences, strains, and plasmids examined in this study.	20
2.2.	Parental plasmids, cut sites, and affinity tag sequences for genes cloned in this study.	23
3.1.	Resistance genes and plasmids identified in the three *E. coli* CANWARD isolates.	33
3.2.	Fosfomycin susceptibility testing results for *E. coli* transformants.	40
4.1.	Antimicrobial susceptibility testing results for *M. smegmatis*, *E. coli*, and *B. subtilis* SMR transformants.	53

List of Figures

1.1.	Structural diagram of FosA-catalyzed inactivation of fosfomycin.	4
1.2.	Schematic representation of the mycobacterial cell wall and residing efflux pumps.	9
1.3.	Topology diagram of the SMR family efflux pump Mmr from *M. tuberculosis*.	12
2.1.	Cartoon diagram of plasmids used in this study.	18
3.1.	Phylogenetic and sequence analysis of clinically isolated *E. coli* FosA sequences and their comparison to previously identified FosA variants.	34
3.2.	Multiple sequence alignment of FosA1-A12 protein sequence variants.	36
3.3.	Induction of FosA proteins in *E. coli* transformants.	39
3.4.	Structural visualization of FosA protein homology models generated by I-TASSER.	41
4.1.	Phylogenetic tree of SMR efflux pump family variants.	46
4.2.	Phylogenetic tree of representative Mmr homologs from Actinobacteria.	47
4.3.	Multiple sequence alignment of SMR proteins cloned and analyzed in this study.	49
4.4.	Multiple sequence alignment of Mmr homologs from Actinobacteria representatives.	50
4.5.	Induction of SMR proteins in *M. smegmatis* and *B. subtilis* transformants.	53
4.6.	Structural visualization of Mmr and related SMR efflux protein homology models generated by I-TASSER.	56

List of Abbreviations

ABC	ATP-Binding Cassette
ACR	Acriflavine
AMR	Antimicrobial resistance
AST	Antimicrobial susceptibility testing
ATCC	American Type Culture Collection
ATP	Adenosine triphosphate
AZM	Azithromycin
BDQ	Bedaquiline
BLAST	Basic Local Alignment Search Tool
bp	Base pair(s)
CAMHA	Cation-adjusted Mueller-Hinton agar
CAMHB	Cation-adjusted Mueller-Hinton broth
cAMP	Cyclic adenosine monophosphate
CARD	Comprehensive Antibiotic Resistance Database
CFU	Colony forming units
CLI	Clindamycin
CLR	Clarithromycin
CLSI	Clinical and Laboratory Standards Institute
C-terminus	Carboxy-terminus
DAEC	Diffusely adherent *E. coli*
DMSO	Dimethyl sulfoxide
DNA	Deoxyribonucleic acid
DTT	Dithiothreitol
EBR	Ethidium bromide
EDTA	Ethylenediaminetetraacetic acid
EMB	Ethambutol
ERY	Erythromycin
ESBL	Extended-spectrum β-lactamase
EAEC	Enteroaggregative *E. coli*
EHEC	Enterohaemorrhagic *E. coli*
EIEC	Enteroinvasive *E. coli*
EPEC	Enteropathogenic *E. coli*
ETEC	Enterotoxigenic *E. coli*
GDM	Guanidinium Exporter
His_6	Hexahistidine
HIV	Human immunodeficiency virus
HRP	Horseradish peroxidase
INH	Isoniazid
IPTG	Isopropyl β-D-1-thiogalactopyranoside
IRIDA	Integrated Rapid Infectious Disease Analysis
I-TASSER	Iterative Threading Assembly Refinement
kb	Kilobase pair(s)
LB	Luria-Bertani
LZD	Linezolid
M	Molar

List of Abbreviations (Continued)

MATE	Multidrug and Toxic Compound Extrusion
MDR	Multidrug resistant
MEGA	Molecular Evolutionary Genetics Analysis
MFS	Major Facilitator Superfamily
mg	Milligram(s)
MIC	Minimum inhibitory concentration
mL	Millilitre(s)
MLST	Multi-locus sequence typing
mM	Millimolar
MOPS	Morpholinepropanesulfonic acid
MXF	Moxifloxacin
NCBI	National Center for Biotechnology Information
nm	Nanometer(s)
NMEC	Neonatal meningitis *E. coli*
NTM	Non-tuberculosis mycobacteria
OD	Optical density
PAGE	Polyacrylamide gel electrophoresis
PBS	Phosphate-buffered saline
PMSF	Phenylmethylsulfonyl fluoride
PSI	Pounds per square inch
PSMR	Paired Small Multidrug Resistance
QUAST	Quality Assessment Tool for Genome Assemblies
RIF	Rifampin
RMSD	Root mean square deviation
RNA	Ribonucleic acid
RND	Resistance-Nodulation-Division
ROX	Roxithromycin
RPM	Revolutions per minute
rRNA	Ribosomal RNA
SDS	Sodium dodecyl sulfate
SMP	Small Multidrug Pump
SMR	Small Multidrug Resistance
SUG	Suppressor of *groEL* Mutations
TB	Tuberculosis
TCE	2,2,2-trichloroethanol
TMH	Transmembrane helix
Tris	Tris(hydroxymethyl)aminomethane
µg	Microgram(s)
µL	Microliter(s)
UPEC	Uropathogenic *E. coli*
UV	Ultraviolet
v/v	Volume per volume
WHO	World Health Organization
w/v	Weight per volume
XDR	Extensively drug resistant

Contributions of Authors

Chapter 1: Kieran A. Milner (KAM): Thesis writing. Denice C. Bay (DCB): Thesis editing. Meenu K. Sharma (MKS): Thesis editing. Andrew Walkty (AW): Assisted in writing the *E. coli* and fosfomycin resistance sections for journal publication.

Chapter 2: KAM: Thesis writing, transformation of bacteria, protein isolations, SDS-PAGE and Western Blotting, antimicrobial susceptibility tests, multi-sequence alignments and phylogenetic analyses, homology modelling. DCB: Project advisor, design of plasmid constructs, thesis editing. David Alexander (DA): Whole genome sequencing, assisted with phylogenetic analyses of *fosA* genes, assisted with writing the methods sections for *E. coli* clinical isolate whole genome sequencing, *fosA* and SMR protein sequence sequence sources, and multi-sequence alignments and phylogenetic analyses. AW: Assisted with writing the CANWARD section. MKS: Project advisor, manuscript writing. George G. Zhanel (GGZ): Fosfomycin antimicrobial susceptibility testing, assisted with writing the antimicrobial susceptibility tests section.

Chapter 3: This chapter was published as a manuscript in the journal Antimicrobial Agents and Chemotherapy (DOI: https://doi.org/10.1128/AAC.00865-20). KAM: Thesis writing, performed experiments and conducted data analyses as outlined in chapter 2. DCB: Project advisor, design of plasmid constructs, assisted with writing the results sections and thesis editing. MKS: Project advisor, assisted with writing the results sections and thesis editing. AW: Assisted with writing the results sections. DA: Assisted with writing the results sections. GGZ: Assisted with writing the results sections.

Chapter 4: KAM: Performed all experiments, data analysis, and thesis writing. DCB: Project advisor, thesis editing. MKS: Project advisor, thesis editing.

Chapter 5: KAM: Thesis writing. DCB: Thesis editing. MKS: Thesis editing.

1. Chapter 1: Antimicrobial resistance review

1.1. Background

Overuse and misuse of antimicrobials in medicine and agriculture has led to the emergence of antimicrobial resistance (AMR) in bacteria, which represents a critical threat to human health (1). In 2014, the World Health Organization (WHO) warned of a "post-antibiotic era" due to the decreasing effectiveness and ineffectiveness of many antimicrobials (2). AMR leads to infections that are more difficult to treat than those caused by susceptible organisms, and these infections incur increased healthcare costs due to the need for more expensive second-line drugs, additional diagnostic tests, and longer treatment durations with less effective therapeutics (1, 3). This emphasizes the importance of understanding bacterial AMR mechanisms in greater depth.

In 2016, the World Health Assembly adopted the WHO's End TB strategy for ending the global tuberculosis epidemic, but the continuing emergence of AMR in *Mycobacterium tuberculosis* poses a major challenge to the targets set by the End TB strategy (1). To support the Global Action Plan on Antimicrobial Resistance developed by the World Health Assembly in 2015, the WHO also created a Priority Pathogens List (PPL) to guide research related to other AMR bacteria (1). In this report, the WHO identified carbapenem-resistant *Acinetobacter baumannii*, carbapenem-resistant *Pseudomonas aeruginosa*, and carbapenem and 3rd generation cephalosporin-resistant *Enterobacteriaceae* as critical priorities for the development of new antibiotics (1).

This thesis investigates mechanisms of resistance in two different species of bacteria recognized by the WHO as priority genera for research related to AMR; *M. tuberculosis* and *Escherichia coli* (1). Although *E. coli* and *M. tuberculosis* are very different bacterial pathogens, both species utilize AMR genes that could be explored through similar methodological approaches. Bacteria develop AMR through several major mechanisms including drug degradation, drug modifications, target site alterations, decreased permeability, and reduced drug accumulation through the use of efflux pumps (4). The pathogenicity, treatment, and respective AMR mechanisms of *E. coli* and *M. tuberculosis* are reviewed herein. For *E. coli*, this thesis focuses on enzymatic inactivation of fosfomycin by FosA proteins, while for *M. tuberculosis*, efflux-mediated resistance to macrolides related to the expression of the small multidrug resistance family efflux pump Mmr is explored.

1.2. Antimicrobial resistance in *Escherichia coli*

1.2.1. Pathogenicity and treatment of *E. coli*

The Gram-negative bacillus *E. coli* is a facultative anaerobe with both commensal and pathogenic activity (5). *E. coli* is notable for being one of the most well-studied bacterial species and is a widely used model organism for laboratory experiments. For example, *E. coli* K-12 BW25113 is the parental strain of the Keio collection of single gene knockout strains. It is a useful model organism for studying genes, for molecular analysis, and functional characterization since it is non-pathogenic and its physiology and genetic mechanisms are some of the most well understood among bacteria (6). *E. coli* also causes several diseases including intestinal infections, urinary tract infections, and meningitis (7). Pathogenic strains of *E. coli* can be classified into eight pathovars based on serological characteristics and virulence strategies; enteroaggregative *E. coli* (EAEC), enterohaemorrhagic *E. coli* (EHEC), enteroinvasive *E. coli* (EIEC), enteropathogenic *E. coli* (EPEC), enterotoxigenic *E. coli* (ETEC), diffusely adherent *E. coli* (DAEC), uropathogenic *E. coli* (UPEC), and neonatal meningitis *E. coli* (NMEC) (7). A variety of antimicrobials can be used to treat *E. coli* infections caused by these pathogenic variants, such as β-lactams, fluoroquinolones, and aminoglycosides (8). However, in response to the selective pressure of antimicrobials, *E. coli* strains have developed AMR to these compounds through mechanisms such as drug-inactivating enzymes (β-lactamases), target site alterations, and efflux pumps (8).

E. coli is the primary cause of urinary tract infections, which are one of the most common types of bacterial infections in humans, globally (9). Urinary tract infections account for more than 8 million physician visits in the United States, annually (7, 10). AMR isolates of *E. coli*, including extended–spectrum β-lactamase (ESBL) producers are of particular concern as they are frequently recovered from clinical specimens (11, 12). Between 2011-2013 the International Network for Optimal Resistance Monitoring program reported a 12% proportion of ESBL phenotype isolates for *E. coli* collected from hospitals in the United States (12). Treatment of infections caused by ESBL and multidrug resistant (MDR) *E. coli*, which are resistant to multiple antimicrobials can be problematic for clinicians, as there may be limited therapeutic options (11). β-lactams and fluoroquinolones have been used historically to treat urinary tract infections, but the emergence of resistance to these agents has resulted in nitrofurantoin and trimethoprim/ sulfamethoxazole becoming the currently recommended first-line agents (13).

In recent years, there has also been renewed interest in the use of fosfomycin for the treatment of urinary tract infections (14). Fosfomycin is a phosphoenolpyruvate analogue (**Figure 1.1**) that was originally discovered in 1969, but it fell into disuse due to the superior pharmacological properties and clinical effectiveness of other antimicrobials (15). With the emergence of AMR outpacing the development of newer antimicrobials, older therapeutics such as fosfomycin have seen a resurgence in use (15). The chemical structure of fosfomycin contains a stable epoxide group and a phosphonic acid moiety (15). Fosfomycin disrupts bacterial cell wall synthesis by inhibiting UDP–N–acetylglucosamine–3–enolpyruvyl transferase (MurA), an enzyme involved in the synthesis of N–acetylmuramic acid (15). MurA catalyzes an addition-elimination reaction with phosphoenolpyruvate and UDP-N-acetylglucosamine to form UDP-N-acetylglucosamine-enolpyruvate (15). In a recent surveillance study on Canadian *E. coli* clinical isolates, including MDR and ESBL–producing isolates, fosfomycin demonstrated high *in vitro* activity (99.2% of isolates susceptible) (16). In Canada, fosfomycin is available in both oral and intravenous formulations (14, 15). In adults, a single 3 g dose of oral fosfomycin is currently recommended by the Infectious Diseases Society of America as a first-line treatment of uncomplicated bacterial cystitis, while the intravenous formulation (1 hour infusions 3 times daily for 7 days) has demonstrated efficacy in the treatment of complicated urinary tract infections (including pyelonephritis) (17, 18).

1.2.2. Resistance to fosfomycin

E. coli strains with resistance to fosfomycin were described as early as 1972 (19), and resistance can occur through several different mechanisms. Firstly, mutations may occur in glycerol–3–phosphate (*glpT*) and hexose phosphate (*uhpT*) transporter genes required for fosfomycin uptake into the bacterial cell, which results in lower intracellular levels of fosfomycin (20). Secondly, mutations may also occur in genes which affect the cellular concentration of cyclic adenosine monophosphate (cAMP), including phosphoenolpyruvate-protein phosphotransferase (*ptsI*) and adenylate cyclase (*cyaA*), since reduced cAMP levels down-regulates *glpT* and *uhpT* expression. Next, mutations can occur in MurA which decrease the binding affinity of fosfomycin, such as substitution of Cys115 with aspartic acid (20). Lastly, *E. coli* can develop resistance to fosfomycin through the acquisition of a fosfomycin inactivating (*fos*) enzyme (15). Of these four

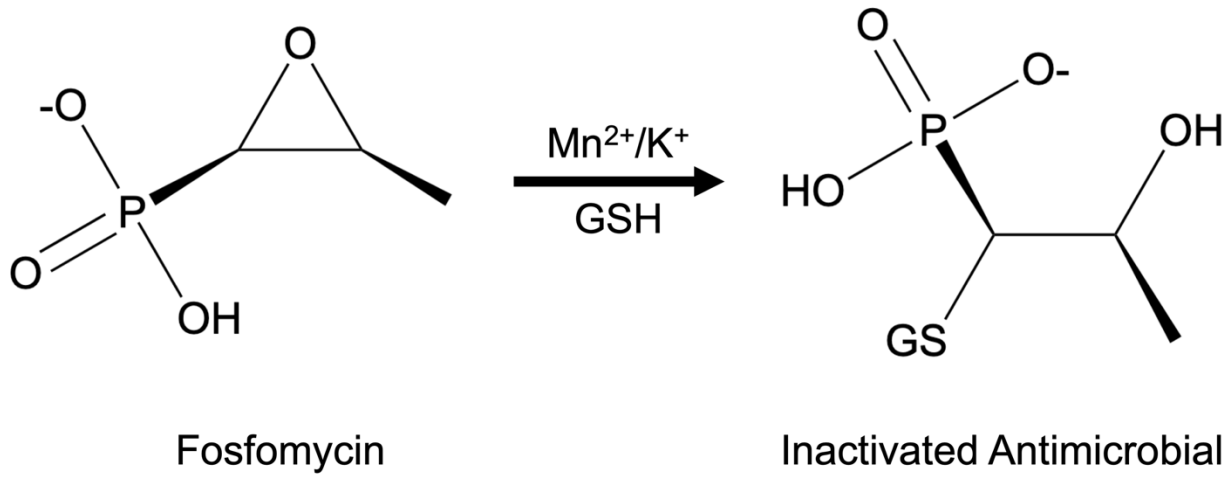

Figure 1.1. Structural diagram of FosA-catalyzed inactivation of fosfomycin. FosA is an Mn^{2+} and K^{+} dependent glutathione transferase enzyme which catalyzes the conjugation of fosfomycin with glutathione (GSH), opening the epoxide ring and rendering the antimicrobial inactive (15). During the nucleophilic attack on fosfomycin by glutathione, Mn^{2+} acts as a Lewis acid, while K^{+} balances the negative charge of the active site (21).

main resistance mechanisms, fosfomycin inactivating enzymes encoded by *fos* genes are of notable concern (22). *fos* genes are found on plasmids that can mobilize and transfer them between different Gram-negative pathogens (14, 15). More than 10 different Fos enzyme variants have been described (e.g., FosA-E, FosG-I, FosK-L, FosX) (23, 24). The most common and clinically relevant group of Fos variants found in Gram-negative bacteria are FosA, which are around 140 amino acids in length. *fosA* genes are frequently identified in Enterobacterales species, specifically *Enterobacter* spp., *Klebsiella* spp., *Kluyvera* spp., and *Leclercia adecarboxylata* which are thought to be the natural reservoir of horizontally transmitted *fosA* genes (25–27). *fosA* genes are also widely distributed among Enterobacteriaceae (25), and can be transferred to species such as *E. coli* through plasmids that contain other AMR genes such as ESBL or carbapenemase enzymes (14, 15, 23). This is clinically worrisome as the treatment options for patients that develop infections from these MDR and *fosA* expressing *E. coli* isolates may be very limited (11).

Fosfomycin inactivating enzymes are members of the glyoxyalase superfamily and work by catalyzing the conjugation of fosfomycin with a nucleophile, such as glutathione (FosA), bacillithiol (FosB), or water (FosC) (15). Resultingly, the epoxide ring is opened and the antimicrobial is rendered inactive (**Figure 1.1**) (15). The glutathione transferase FosA functions as a homodimer, which uses several residues at each of its two active sites to bind fosfomycin (Y9, Y65, K93, S97, S101, Y103, R122) (21). An Mn^{2+} ion is required at the FosA active site, which acts as a lewis acid during the nucleophilic attack on fosfomycin by glutathione (21). Additionally, a K^{+} ion is used to balance the negative charge of the active site and increase the enzyme's rate of reaction (21). Currently, resistance to fosfomycin mediated by FosA activity is rare in clinical isolates of *E. coli* (22, 28), but ongoing surveillance is important to ensure fosfomycin remains an effective first-line therapy for urinary tract infections.

1.3. Antimicrobial resistance in *Mycobacterium tuberculosis*

1.3.1. Pathogenicity and treatment of *M. tuberculosis*

M. tuberculosis is an obligate intracellular pathogen and the causative agent of tuberculosis (TB), a disease which typically affects the lungs (pulmonary TB) but can also affect other organs (extrapulmonary TB) (29). TB is responsible for approximately 2 million deaths annually, most of which occur in developing countries, and is associated with overcrowding, poor nutrition, and many other risk factors including co-infection with human immunodeficiency virus (HIV) (29).

According to the WHO Global Tuberculosis Report from 2020, in 2019 TB resulted in 1.2 million deaths among HIV-negative people and 208,000 deaths in HIV-positive people (30). In Canada, the incidence and mortality rates for TB are relatively low at 4.6 per 100,000 when compared to global statistics, but the annual number of cases has been increasing among Canadian-born First Nations (23.8 per 100,000), Inuit (170.1 per 100,000) and Métis people (2.1 per 100,000) (31, 32).

The main route of entry for *M. tuberculosis* infection is through the respiratory tract, where it is inhaled via aerosolized particles spread by infected individuals (33). In the lower airways, innate immune responses usually clear the infection, but *M. tuberculosis* is capable of subverting host defenses and surviving intracellularly within the lungs (29). For example, mannose-capped lipoarabinomannan present on the *M. tuberculosis* cell surface inhibits phagosome maturation, cytokine production, and antigen presentation within phagocytes (34). Individuals exposed to *M. tuberculosis* have an average lifetime risk of 10% for developing active TB, while 90% either eliminate the pathogen or experience an asymptomatic infection known as latent TB (30). Latent TB may reactivate and progress to active TB if the person's immune system becomes weakened in the future (30). The standard antimicrobial regimen for the treatment of active TB involves a combination of the first line antituberculosis drugs rifampin, isoniazid, pyrazinamide, and ethambutol for 2 months followed by an additional four month course of rifampin and isoniazid (35). Resistance to these agents has emerged over time, and second-line antimicrobials such as bedaquiline, moxifloxacin, linezolid, clofazimine, cycloserine, terizidone, delamanid, imipenem-cilastatin, meropenem, amikacin, streptomycin, ethionamide, prothionamide, and *p*-aminosalicylic acid are frequently used in alternative treatment regimens in cases where first line agents are ineffective (**Table 1.1**) (36, 37).

1.3.2. Resistance to antituberculosis drugs

Resistant strains of *M. tuberculosis* have become the leading cause of mortality related to AMR globally (30). Selective pressure from antimicrobials, inadequate treatments due to patient non-adherence, and inappropriate regimens due to the lack of susceptibility testing before treatment can all contribute to the development of AMR in *M. tuberculosis* (38). Multi-drug resistant TB (MDR-TB) is defined as resistance to the first line antituberculosis drugs rifampin and isoniazid, while extensively drug-resistant TB (XDR-TB) is defined as rifampin-resistant TB

Table 1.1. List of antimicrobials currently used for the treatment of tuberculosis.

Category	Family	Drug[a]	Process Inhibited	Target
Nucleic acid synthesis inhibitors	Aminosalicylic acids	*p*-Aminosalicylic acid	Folate synthesis	Dihydrofolate reductase (39)
	Ansamycins	Rifampin	RNA synthesis	RNA polymerase (40)
		Rifapentine	RNA synthesis	RNA polymerase (40)
		Rifabutin	RNA synthesis	RNA polymerase (40)
	Diarylquinolones	Bedaquiline	ATP synthesis	ATP synthase (41)
	Fluoroquinolones	Moxifloxacin	DNA synthesis	DNA gyrase (42)
		Levofloxacin	DNA synthesis	DNA gyrase (42)
Protein synthesis inhibitors	Aminoglycosides	Amikacin	Translation (elongation)	16S rRNA (43)
		Streptomycin	Translation (elongation)	16S rRNA (43)
	Oxazolidinones	Linezolid	Translation (initiation)	23S rRNA (44)
	Pyrazines	Pyrazinamide	Trans-translation	Ribosomal protein S1 (45)
Cell wall synthesis inhibitors	β-lactams	Imipenem-Cilastatin	Peptidoglycan synthesis	Transpeptidase (46)
		Meropenem	Peptidoglycan synthesis	Transpeptidase (46)
	Ethylenediamines	Ethambutol	Arabinogalactan synthesis	Arabinosyltransferase (47)
	Isoxazolines	Cycloserine	Peptidoglycan synthesis	Alanine racemase/Alanine-alanine ligase (48)
		Terizidone	Peptidoglycan synthesis	Alanine racemase/Alanine-alanine ligase (48)
	Nitroimidazoles	Pretomanid	Mycolic acid synthesis	Multiple (49)
		Delamanid	Mycolic acid synthesis	Multiple (50)
	Pyridine derivatives	Isoniazid	Mycolic acid synthesis	InhA[b] (51)
		Ethionamide	Mycolic acid synthesis	InhA (51)
		Prothionamide	Mycolic acid synthesis	InhA (51)
	Riminophenazines	Clofazimine	Cell membrane integrity	Multiple (52)

[a]**First-line medicines:** Rifampin, isoniazid, pyrazinamide, ethambutol. Grouping of second-line medicines for multidrug resistant (MDR) TB treatment regimens is as follows - **Group A medicines** (highly effective, include all three): levofloxacin or moxifloxacin, bedaquiline, linezolid. **Group B medicines** (conditionally recommended, add one or both): clofazimine, cycloserine or terizidone. **Group C medicines** (last-line, add to complete the regimen and when medicines from Group A or B cannot be used): ethambutol, delamanid, pyrazinamide, imipenem-cilastatin or meropenem, amikacin or streptomycin, ethionamide or prothionamide, *p*-aminosalicylic acid (30).

[b]2-trans-enoyl-acyl carrier protein reductase

or MDR-TB with additional resistance to any fluoroquinolone and at least one additional Group A second-line drug (levofloxacin, moxifloxacin, bedaquiline, or linezolid) (**Table 1.1**) (53). More than 484,000 people developed drug-resistant TB infections in 2018 globally, which resulted in 214,000 deaths (30). Treatment courses for these AMR strains are only around 55% and 34% successful for MDR-TB and XDR-TB respectively, and can last up to 24 months compared to 6-9 months for pansusceptible strains (30). Thus, owing to the high treatment costs, drug intolerance and toxicity, and low success rates of available treatment courses, the emergence of AMR in *M. tuberculosis* represents a major global health challenge.

M. tuberculosis possesses intrinsic resistance to many antimicrobials due in part to the unique structure of its cell envelope. The cell wall of *M. tuberculosis* is multi-layered and comprised of a layer of peptidoglycan, a layer of arabinogalactan with covalently linked mycolic acids, and an outer layer of glycolipids with associated proteins (**Figure 1.2**) (54). The outer lipids intercalate with the mycolic acids forming a structure resembling the outer membrane of Gram-negative bacteria, but one which is 10-100 fold more impermeable to hydrophilic compounds (55). As a result, *M. tuberculosis* possesses two hydrophilic barriers which reduces permeability to many different classes of antimicrobials. Furthermore, the transpeptidases present in the *M. tuberculosis* genome form non-classical 3,3 transpeptide bonds in their peptidoglycan as opposed to 4,3 bonds found in other bacteria. These peptidoglycan bonding differences limit the effectiveness of β-lactams such as carbapenems, which are last line antimicrobials for the treatment of XDR-TB (56).

There are also several acquired or adaptive mechanisms of resistance that *M. tuberculosis* and other mycobacteria can use to evade the action of antimicrobials such as the alteration of drug targets, the production of drug-modifying enzymes, and the reduced accumulation of antimicrobials through efflux pump over-expression (56). Efflux-mediated resistance has garnered more attention recently due to the ability of many pumps to confer reduced susceptibility to a wide variety of antimicrobials (57, 58). In addition to their role as resistance determinants, some *M. tuberculosis* efflux pumps are virulence factors (58). Although the role of efflux pumps in causing infection are not well understood, several transporter proteins (eg. Rv1272c, Rv1747, Rv3781, Rv1410c) are associated with intracellular survival within macrophages (59). Therefore, efflux pump proteins play a key role in both the pathogenesis of *M. tuberculosis* and the emergence of AMR strains.

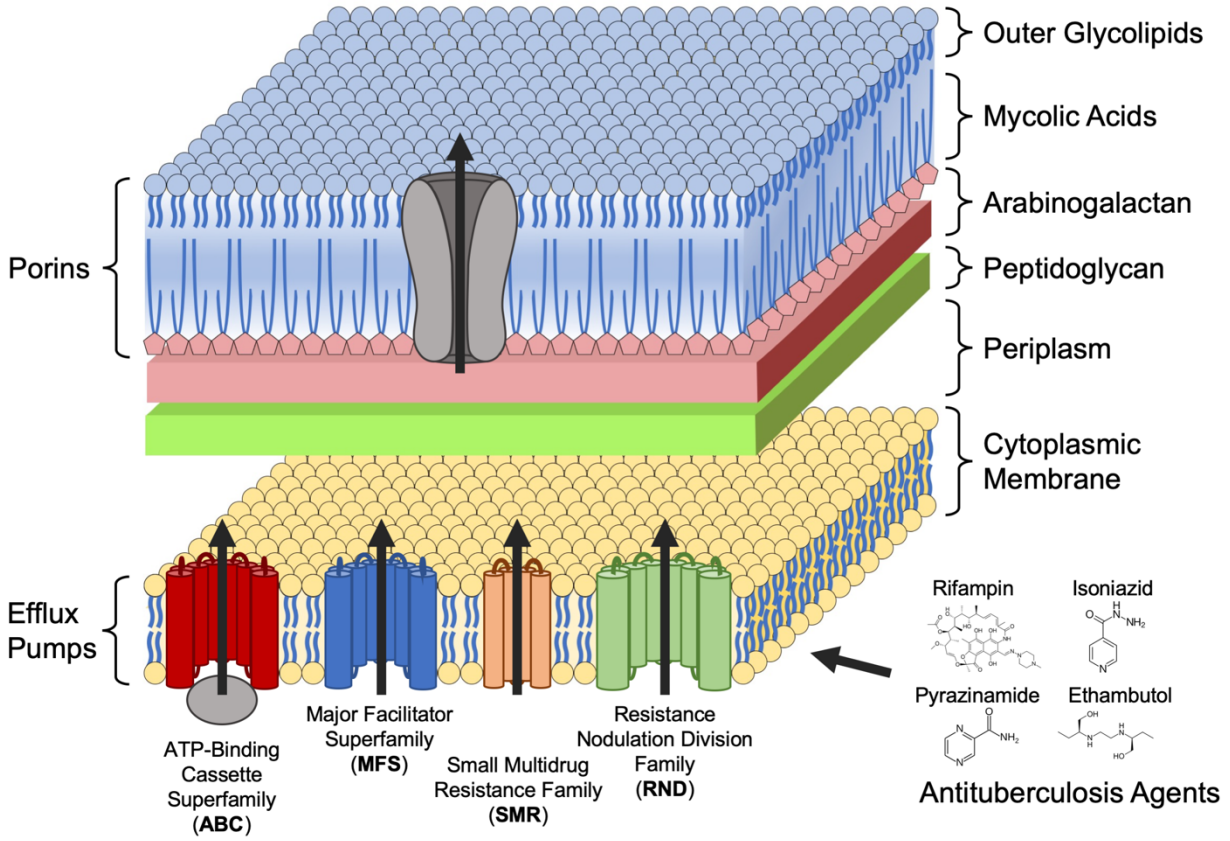

Figure 1.2. Schematic representation of the mycobacterial cell wall and residing efflux pumps. Efflux pump transmembrane helices are represented by cylinders. Arrows represent efflux of antituberculosis drugs, resulting in reduced susceptibility to these antimicrobials (54, 60).

1.3.3. Contribution of efflux pumps to antimicrobial resistance

Bacteria use efflux pumps to expel antimicrobials, and their increased activity can occur through mutations in their efflux pump gene(s), or more commonly through changes in the regulatory element DNA or transcriptional factors controlling their expression (61–63). Effluxpumps in the *M. tuberculosis* genome are responsible for both intrinsic drug tolerance and adaptive high-level resistance (64). During treatment courses for drug-susceptible *M. tuberculosis* strains, it is suggested that populations of drug-tolerant bacteria may persist through macrophage-induced efflux pump expression, which increases the duration of treatment needed to completely eradicate the organism (58). Additionally, efflux pump over-expression in *M. tuberculosis* can confer high-level resistance to certain antituberculosis drugs by transporting them out of the cell and limiting their access to intracellular targets (57). There are five major transporter families in bacteria: the ATP-Binding Cassette family (ABC), the Major Facilitator Superfamily (MFS), the Multidrug and Toxic Compound Extrusion family (MATE), the Small Multidrug Resistance family (SMR), and the Resistance-Nodulation-Cell Division family (RND) (65). With the current exception of MATE family efflux pumps, all of these transporter families have been shown to play a role in antimicrobial extrusion in *M. tuberculosis* (60).

ABC transporters are the most abundant family of efflux pumps in *M. tuberculosis* and represent around 2.5% of the total genomic content in this organism (65). They usually consist of two transmembrane domains and two nucleotide binding domains that form a tetramer at the cytoplasmic membrane (65). In ABC transporters, the nucleotide binding subunits hydrolyze ATP to fuel substrate transport, whereas the other efflux families in *M. tuberculosis* utilize a proton or sodium motive force for energy (65). An important ABC transporter identified in *M. tuberculosis* is Rv1217c-1218c, which is up-regulated in rifampin and isoniazid-resistant strains (66). Additionally, strains of *M. tuberculosis* with this efflux pump inactivated showed a 2-fold decrease in the MICs of rifampin and clofazimine (67).

MFS transporters are comprised of 12-14 transmembrane α-helices connected by several hydrophilic loops (65). The MFS efflux pump Rv1258c enhances AMR as well as the intracellular survival of *M. tuberculosis* within macrophages (65). Rv1258c is up-regulated during exposure to antimicrobials including isoniazid (68). *M. tuberculosis* Rv1258c knockout mutants displayed a 2-fold decrease in the MIC of rifampin, amikacin, and gentamycin, as well as an 8-fold decrease in spectinomycin MIC (67). Additional evidence for the role of Rv1258c in antimicrobial efflux

comes from research using *Mycobacterium bovis*; over-expression of the Rv1258c homolog caused a 4-fold increase in tetracycline and streptomycin MICs, and its deletion mutant exhibited increased susceptibility to these antimicrobials (69).

RND efflux systems are commonly found in the genomes of Gram-negative bacteria, but they are also present in *M. tuberculosis* (65). The presence of RND pumps in *M. tuberculosis* is likely due to the unique structure of the mycobacterial cell envelope and its similarities to the Gram-negative cell wall (65). In Gram-negative bacteria, RND pumps form a tripartite structure comprised of an integral membrane transporter, an outer membrane channel, and a periplasmic adaptor (65). In *M. tuberculosis* RND pumps may exist as single component efflux pumps, since homologs for the Gram-negative outer membrane proteins and periplasmic adaptors have not been identified in sequenced genomes (65). Most of the RND pumps in *M. tuberculosis* belong to the mycobacterial membrane protein large (MmpL) sub-family and have been shown to influence both mycobacterial virulence and antimicrobial efflux (65). For example, MmpL7 (Rv2942) is essential for the intracellular survival of *M. tuberculosis* during infection and it is up-regulated in isoniazid-exposed strains of *M. tuberculosis* (70). When over-expressed in the model organism *Mycobacterium smegmatis* (also known as *Mycolicibacterium smegmatis*) (71), MmpL7 increased the MIC values of isoniazid and ethionamide by 16-fold and 4-fold respectively (72).

The last major class of efflux proteins found in *M. tuberculosis* belong to the SMR family. SMR proteins are one of the smallest known multidrug efflux transporters in bacteria, ranging from 100-170 amino acids in length (73). They are comprised of 4 transmembrane α-helices which multimerize into dimers and potentially larger oligomers, allowing them to export a variety of structurally dissimilar antimicrobials out of the cell including cationic and lipophilic compounds (**Figure 1.3**) (73). SMR efflux pumps can be classified into three major subfamilies based on their substrate selectivity, function, and homology: 1) The small multidrug pump (SMP) subclass, with *E. coli* EmrE as the archetypical member, 2) the suppressor of *groEL* mutations subclass (SUG) recently renamed as the riboswitch-regulated guanidinium-exporter (GDM) subclass (74), the most well-characterized member being *E. coli* Gdx/SugE, and 3) the paired SMR (PSMR) subclass which requires expression of two genes to confer AMR (eg. *E. coli* MdtIJ and *Bacillus subtilis* EbrAB) (75). SMR proteins adopt a dimeric, oppositely oriented, antiparallel "dual" topology in the plasma membrane, where the same SMP or GDM protein can insert into the membrane in

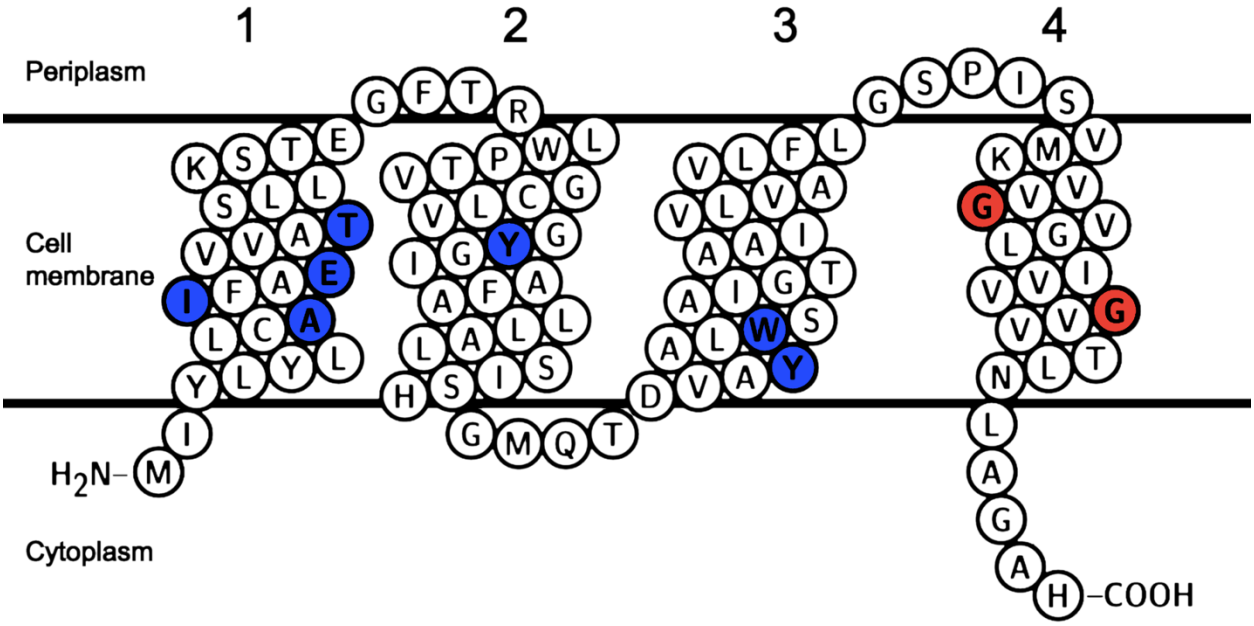

Figure 1.3. Topology diagram of the SMR family efflux pump Mmr from *M. tuberculosis*. Transmembrane helices are labeled 1-4. Residues predicted to be involved in substrate binding are highlighted in blue. Residues predicted to be involved in transporter multimerization are highlighted in red (76, 77). The image was generated using Protter version 1.0 (78).

opposite orientations relative to their amino and carboxyl termini (79).

With respect to Mycobacterial SMR members, *mmr* (Rv3065) is the only predicted SMR gene identified in the *M. tuberculosis* genome. When over-expressed in *M. smegmatis*, Mmr has demonstrated resistance to the biocide tetraphenylphosphonium, intercalating dyes ethidium bromide and acriflavine, antimicrobial erythromycin, and staining dyes safranin O and pyronin Y (80). *mmr*-knockout mutants in *M. tuberculosis* also exhibited reduced susceptibility to ethidium bromide, tetraphenylphosphonium, and the antiseptic cetyltrimethylammonium bromide (81). Although Mmr has been shown to confer resistance to a range of structurally diverse compounds including the antimicrobial erythromycin, it is unclear if it confers resistance to any clinically relevant antitubercular drugs.

SMP members expel diverse substrates including quaternary ammonium compounds, cationic dyes, and antimicrobials. In contrast, SMR efflux pumps belonging to the GDM and PSMR subclasses often transport a more narrow range of substrates. For example, PSMR members such as YkkCD that have closer homology to GDM members have a substrate recognition limited to guanidinium compounds (82, 83). In comparison, the PSMR of *E. coli* MdtIJ has a closer homology to SMP members but expels toxic polyamine compounds like spermidine in addition to some cationic biocides (84). SMR family efflux pumps possess several conserved residues and consensus motifs according to alignments of large SMR sequence datasets based on previous bioinformatic studies (85). Additionally, site-directed mutagenesis studies of EmrE have identified several residues comprising the substrate binding pocket (A9, I10, E13, T17, Y39, Y60, W63; numbered according to the Mmr protein sequence) (86–91), as well as amino acids implicated in SMR protein multimerization (G90, G97) (76, 77). Replacement of individual residues in EmrE has also been shown in previous studies to influence its substrate selectivity (92, 93). For example, Serine 43 (S43) in EmrE is responsible for a methyl viologen resistance phenotype which is lost when altered (93). There are currently many gaps in knowledge regarding how SMR family efflux pumps and their residues specifically contribute to the transport of clinically relevant antimicrobials, particularly in mycobacteria including *M. tuberculosis*. It is unclear what specific amino acid residues in SMR proteins may be involved in the recognition and transport of antimicrobials. Since SMR amino acid sequence identities can vary substantially, even within Enterobacterial orders, it is difficult to predict SMR substrate selectivity directly from their sequences (92, 94).

1.3.4. *M. smegmatis* as a model for *M. tuberculosis* protein characterization

While most efflux pump characterization is conducted in the Gram-negative bacterium *E. coli*, the dramatic differences in membrane architecture and codon bias between *E. coli* and *M. tuberculosis* often result in the formation of insoluble inclusion bodies when *M. tuberculosis* membrane proteins are expressed in *E. coli* (95). This makes *E. coli* a poor model for mycobacterial gene expression. *M. smegmatis* is an established model system that overcomes the aforementioned limitations of *E. coli* due to its similar genetic background and closer membrane architecture resemblance to *M. tuberculosis* (95, 96). It is a member of the rapidly growing mycobacteria group and is a faster growing species than *M. tuberculosis* taking 2-3 days to grow versus 1-3 weeks (97). It is also non-pathogenic allowing for safer experimental work in biocontainment safety level 1-2 facilities as compared to containment level 3 requirements for *M. tuberculosis* (98, 99). *M. smegmatis* mc^2155 is a strain with high transformation efficiency, which makes it an ideal model organism for our research since it is easier to genetically manipulate than *M. tuberculosis* and faster to cultivate (95, 100). *M. smegmatis* $mc^2$4517 is a derivative of mc^2155 that possesses a T7 RNA polymerase gene under the control of the *M. smegmatis* acetamidase promotor on an integrative plasmid pYUB1232 (101). Expression of the T7 RNA polymerase gene on pYUB1232 can be induced with acetamide, which allows for the expression of other transformed genes cloned with a T7 promotor and terminator in the IPTG-inducible pYUB28b plasmid (102). This dual-induction system reduces leaky expression in *M. smegmatis* and helps to prevent unregulated efflux gene over-production, which may be toxic to cells over long periods of time.

1.4. Thesis objectives

The purpose of this thesis was to characterize the AMR genes from two important pathogens recognized by the WHO as a priority for research related to AMR; *M. tuberculosis* and *E. coli* (1). Both species have AMR genes that could be explored using similar methodological approaches. AMR genes of interest from each of these pathogens were cloned and expressed in their respective drug-susceptible model species to elucidate their AMR phenotypes. Chapter 3 of this thesis describes the characterization of cloned cytoplasmic *fosA* genes from Canadian clinical *E. coli* isolates in the *E. coli* K-12 BW25113 model organism. Chapter 4 details the characterization of the *M. tuberculosis* SMR family efflux pump *mmr* cloned and expressed in the

model mycobacterial species *M. smegmatis* mc^{2}155. The goal of both studies was to distinguish the AMR phenotypes of these genes to clinically relevant antimicrobial agents in an effort learn more about their drug selectivity, their structure-function, and their phylogenetic relationships to characterized representative homologs.

1.4.1. Chapter 3 rationale and hypothesis

In this chapter, we characterize three *fosA* genes from Canadian *E. coli* isolates using the laboratory strain *E. coli* K-12 BW25113. Here, *fosA* genes were cloned, over-expressed and subjected to antimicrobial susceptibility testing. Three fosfomycin-resistant *E. coli* clinical isolates which exhibited high-level fosfomycin resistance (MIC of >512 μg/mL) were selected from the CANWARD collection (103) for characterization. We hypothesize that cloned and over-expressed *fosA* genes with affinity tags in *E. coli* K-12 BW25113 can be used to clearly distinguish fosfomycin antimicrobial susceptibilities when compared to previously established *fosA* variant representatives. We also discuss the phylogenetics, amino acid sequence diversity, and protein structural relationships of the three FosA members identified from *E. coli* clinical isolates to determine their relationship to previously documented FosA1-A12 members. The outcome of this chapter will identify and characterize the novel *fosA* genes currently disseminated in Canadian clinical *E. coli* isolates and confirm their phenotypic contributions as fosfomycin resistance determinants.

1.4.2. Chapter 4 rationale and hypothesis

In this chapter, we characterize *mmr* cloned from *M. tuberculosis* H37Rv for expression in the *M. smegmatis* mc^{2}155 model system. The *M. tuberculosis* Mmr efflux pump was the focus of this study, as a literature scan indicated that certain SMR members confer reduced susceptibility to erythromycin when over-expressed (80, 104). We hypothesize that cloned and over-expressed *mmr* in *M. smegmatis* will confer increased resistance to macrolides as well as other structurally related antimicrobial compounds. The *mmr* gene was cloned and over-expressed in *M. smegmatis* mc^{2}155, and compared to other cloned SMR family efflux pump genes expressed in either *E. coli* K-12 BW25113 (*emrE*, *qacE, qacF*, *gdx*) or *B. subtilis* MGNA-A001 (*qacC, qacG, qacH, qacJ*) for comparative analysis. Phylogenetic and protein sequence analysis of *mmr* in relation to previously characterized and sequenced representative Gram-negative, Gram-positive, and

mycobacterial SMR homologs was conducted to establish Mmr SMR subclass homology. Our studies of the Mmr efflux pump expands current knowledge of its substrate specificity, structural homology, and its role in conferring AMR in *M. tuberculosis*. The outcome of this chapter confirms macrolides are Mmr pump substrates when compared to other SMR family members and identifies SMR residues and motifs that may contribute to macrolide selectivity.

2. Chapter 2: Methods

2.1. Chemicals and media used in this study

Cation adjusted Mueller-Hinton broth and kanamycin were purchased from MilliporeSigma (St. Louis, MO, USA). Tryptone, yeast extract, hygromycin, tween-80, acetamide, azithromycin, roxithromycin, and ethidium bromide were purchased from Thermo Fisher Scientific (Waltham, MA, USA). Rifampin, isoniazid, and bedaquiline were purchased from MedChemExpress (Monmouth Junction, NJ, USA). Ethambutol was purchased from Becton, Dickinson and Company (Franklin Lakes, NJ, USA). Clarithromycin, clindamycin, linezolid, and moxifloxacin were purchased from Tecoland (Irvine, CA, USA). Ampicillin and erythromycin were purchased from VWR (Radnor, PA, USA). Isopropyl β-D-1-thiogalactopyranoside (IPTG) was purchased from Cedarlane (Burlington, ON, Canada). Acriflavine was purchased from Tokyo Chemical Industries USA (Portland, OR, USA). Fosfomycin was supplied by Paladin Labs (Montreal, QC, Canada). Remaining chemicals, buffers, and media were purchased from Thermo Fisher Scientific and VWR.

2.2. Bacterial strains and culture conditions

The strains and plasmids used in this study are listed in **Table 2.1.** *E. coli* K-12 BW25113 and *E. coli* DH5α were obtained from the Coli Genetic Stock Centre (Yale University, CT, USA) (6). *B. subtilis* MGNA-A001 was obtained from the National Institute of Genetics (Japan) (105). *E. coli* and *B. subtilis* strains were grown at 37°C in either Luria–Bertani (LB) broth with aeration at 170 RPM, LB agar, cation adjusted Mueller-Hinton broth (CAMHB) with aeration at 170 RPM, or cation adjusted Mueller-Hinton agar (CAMHA). Ampicillin (100 µg/mL), hygromycin (200 µg/mL), and kanamycin (50 µg/mL) were included in all media where applicable to maintain transformed plasmids in *E. coli*, and chloramphenicol (5 µg/mL) was used to maintain plasmids in *B. subtilis* (**Figure 2.1**). Gene expression from transformed plasmids (pYUB28b, pMS119EH, and pHT01) was induced with IPTG at a final concentration of 1 mM (238 µg/mL).

The *M. smegmatis* mc^2155 (ATCC 700084) strain was obtained from Cedarlane (Burlington, ON, Canada). All *M. smegmatis* strains were grown at 37°C in CAMHB with aeration at 170 RPM, or on CAMHA. Tween-80 was added to *M. smegmatis* broth cultures at a final concentration of 0.05% (v/v) to reduce cell clumping (96). Hygromycin (50 µg/mL for broth, 100 µg/mL for agar) and kanamycin (20 µg/mL for broth, 40 µg/mL for agar) were added to media to

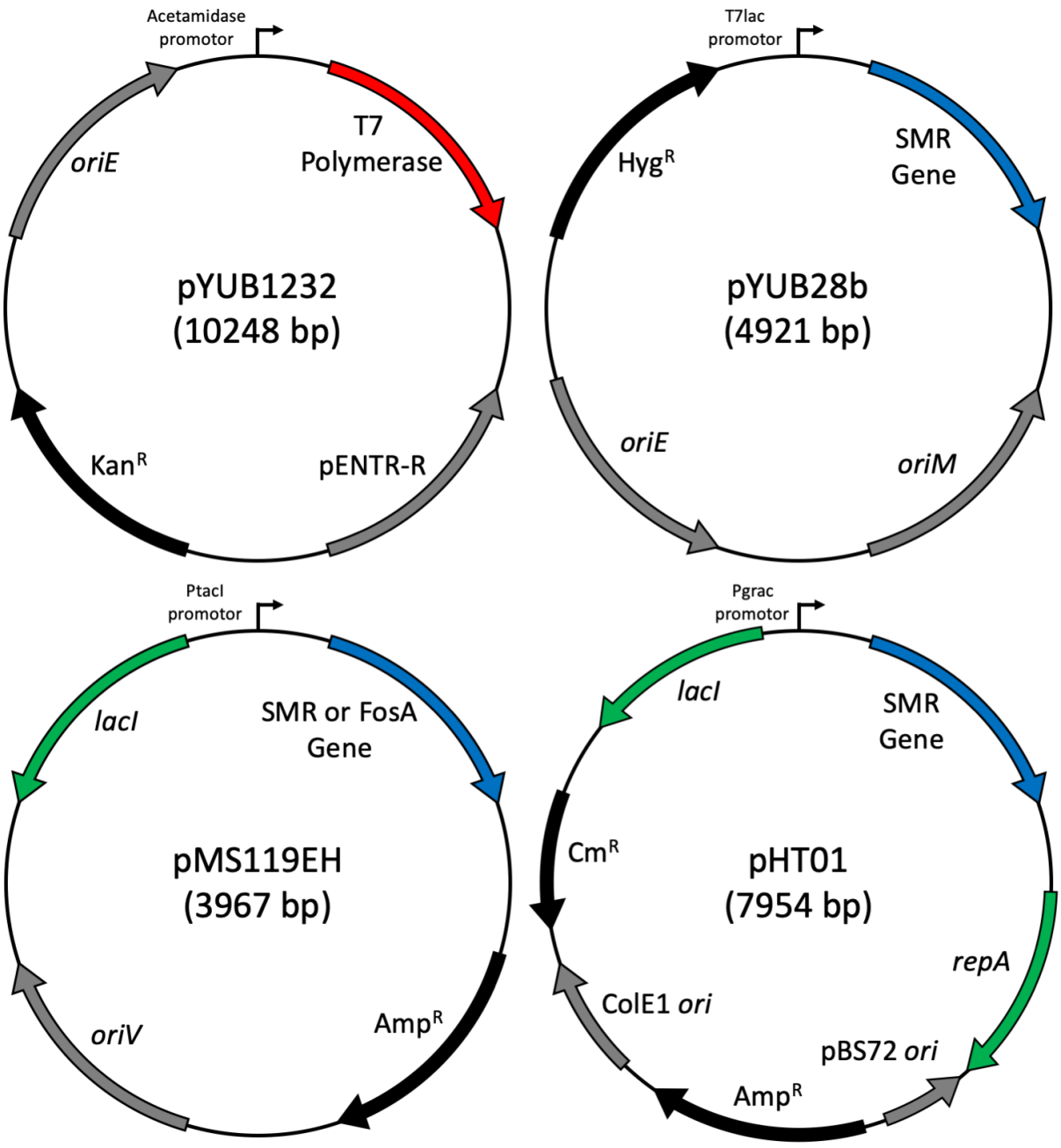

Figure 2.1. Cartoon diagram of plasmids used in this study. Black arrows represent resistance genes for selection. Grey arrows indicate replicative or integrative elements. Blue arrows represent cloned *fosA* or SMR efflux pump genes. The red arrow represents the T7 RNA polymerase gene. Green arrows represent genes for plasmid regulation (101, 102, 106, 107).

maintain transformed plasmids in *M. smegmatis* (**Figure 2.1**). Gene expression from *M. smegmatis* plasmid transformants was induced with 0.2% (w/v) acetamide and 1 mM IPTG.

The *E. coli* clinical isolates used in this study were obtained from the CANWARD collection (108). Briefly, CANWARD is an ongoing surveillance study of AMR in Canadian hospitals (108). All isolates undergo susceptibility testing at a central laboratory in Winnipeg, Manitoba (Health Sciences Centre) using reference methods as described by the Clinical and Laboratory Standards Institute (CLSI) (109). Between 2007 and 2016, three *E. coli* isolates (two from urine and one from blood; EC623771-EC623773) showed high resistance to fosfomycin (MIC of >512 μg/mL) and hence, were selected for further evaluation (see Chapter 3).

2.3. *E. coli* clinical isolate whole genome sequencing

Whole genome sequencing of the three fosfomycin–resistant *E. coli* isolates was performed on an Illumina MiSeq system by the Cadham Provincial Laboratory (Winnipeg, MB, Canada). Briefly, DNA libraries were prepared with Nextera XT reagents and then sequenced using V2 chemistry. Sequencing data has been deposited in GenBank as BioProject PRJNA511988 (author: David Alexander). The accession numbers for *E. coli* strains EC623771 (*fosA3*), EC623772 (*fosA7.5*^{Q86E}), and EC623773 (*fosA8*) are SAMN13659120, SAMN13659121, and SAMN13659122, respectively. Genome assembly and annotation were performed with the Integrated Rapid Infectious Disease Analysis (IRIDA) platform (version 19.09) (110). Briefly, this pipeline combines Shovill assembly, with Prokka annotation and Quality Assessment Tool (QUAST) genome assembly assessment (111). To determine whether the *fosA7.5*^{Q86E} gene from *E. coli* EC623772 was located on a plasmid or chromosome, resequencing of *E. coli* EC623772 was performed on a MinION system (Oxford Nanopore Technologies) by the Andrew Cameron laboratory at the University of Regina (Regina, SK, Canada), and assembly was performed with Flye (version 2.8.1) (112).

2.4. *fosA* and SMR protein sequence sources

The *fosA* and SMR sequences used in this study were obtained from published literature (26–28, 104, 113–119) and public sequence archives/databases, including the National Center for Biotechnology Information (NCBI) Bacterial Antimicrobial Resistance Reference Gene

Table 2.1. Sequences, strains, and plasmids examined in this study.

Strains used	Characteristics	Source
E. coli EC623771	Fosfomycin–resistant isolate	CANWARD
E. coli EC623772	Fosfomycin–resistant isolate	CANWARD
E. coli EC623773	Fosfomycin–resistant isolate	CANWARD
E. coli K-12 BW25113	*F*$^{-}$, Δ*(araD–araB)567*, Δ*lacZ4787(::rrnB–3)*, λ^{-}, *rph–1*, Δ*(rhaD–rhaB)568*, *hsdR514*	(6)
E. coli pMS119EH	*E. coli* BW25113 transformed with pMS119EH	This study
E. coli FosA3	*E. coli* BW25113 transformed with pFosA3	This study
E. coli FosA8	*E. coli* BW25113 transformed with pFosA8	This study
E. coli FosA7.5^{WT}	*E. coli* BW25113 transformed with pFosA7.5^{WT}	This study
E. coli FosA7.5^{Q863}	*E. coli* BW25113 transformed with pFosA7.5^{Q86E}	This study
E. coli FosA7.5^{W92G}	*E. coli* BW25113 transformed with pFosA7.5^{W92G}	This study
E. coli EmrE	*E. coli* BW25113 transformed with pEmrE	This study
E. coli QacE	*E. coli* BW25113 transformed with pQacE	This study
E. coli QacF	*E. coli* BW25113 transformed with pQacF	This study
E. coli Gdx	*E. coli* BW25113 transformed with pGdx	This study
B. subtilis MGNA-A001	*trpC2*	(105)
B. subtilis pHT01	*B. subtilis* MGNA-A001 transformed with pHT01	This study
B. subtilis QacJ	*B. subtilis* MGNA-A001 transformed with pQacJ	This study
B. subtilis QacC	*B. subtilis* MGNA-A001 transformed with pQacC	This study
B. subtilis QacH	*B. subtilis* MGNA-A001 transformed with pQacH	This study
B. subtilis QacG	*B. subtilis* MGNA-A001 transformed with pQacG	This study
M. smegmatis mc^{2}155	High frequency transformation mutant derived from *M. smegmatis* mc^{2}154	(120)
M. smegmatis mc^{2}4517	*M. smegmatis* mc^{2}155 transformed with pYUB1232	(101)
M. smegmatis pYUB28b	*M. smegmatis* mc^{2}4517 transformed with pYUB28b	This study
M. smegmatis Mmr	*M. smegmatis* mc^{2}4517 transformed with pMmr	This study
Plasmids used		
pMS119EH	NruI–NdeI deletion of pJF119EH vector	(121)
pFosA3	C–terminus His6–tagged *fosA3* (EC623771) gene cloned into pMS119EH	This study
pFosA8	C–terminus His6–tagged *fosA8* (EC623773) gene cloned into pMS119EH	This study
pFosA7.5^{WT}	C–terminus His6–tagged *fosA7.5^{WT}* (WP_000941933.1) gene cloned into pMS119EH	This study
pFosA7.5^{Q86E}	C–terminus His6–tagged *fosA7.5^{Q86E}* (EC623772) gene cloned into pMS119EH	This study
pFosA7.5^{W92G}	C–terminus His6–tagged *fosA7.5^{W92G}* (WP_094163054.1) gene cloned into pMS119EH	This study
pEmrE	*emrE* gene cloned into pMS119EH	(122)
pQacE	*qacE* gene cloned into pMS119EH	(123)
pQacF	*qacF* gene cloned into pMS119EH	(123)
pGdx	*gdx/sugE* gene cloned into pMS119EH	(75)
pHT01	Derivative of pNDH33 vector	(107)
pQacJ	*qacJ* gene cloned into pHT01	This study

pQacC	*qacC* gene cloned into pHT01	This study
pQacH	*qacH* gene cloned into pHT01	This study
pQacG	*qacG* gene cloned into pHT01	This study
pYUB1232	*M. smegmatis* acetamidase promotor and T7 polymerase cloned into pMV306	(101)
pYUB28b	NcoI and BlpI digestion of pYUB1049 ligated to multiple cloning site from pET28b	(102)
pMmr	C–terminus *myc*-His6–tagged *mmr* gene cloned into pYUB28b	This study

Abbreviations: His_6; hexahistidine, C–terminus; carboxy–terminus

Database (BioProject PRJNA313047) and the Comprehensive Antibiotic Resistance Database (CARD; https://card.mcmaster.ca/). The NCBI Basic Local Alignment Search Tool (BLAST) was used to retrieve homologous *fosA* and SMR sequences with e-values of $\leq 10^{-3}$ and query coverage of ≥80% as the cut-off values for identification (124). A list of the *fosA* and SMR sequences referenced in this study as well as their accession numbers is given in **Table S1** (**Appendix A**). *fosA* sequences in the datasets for clinical *E. coli* isolates EC623771, EC623772, and EC623773 were analyzed by ResFinder on the Center for Genomic Epidemiology website (https://cge.cbs.dtu.dk/services/). Annotated contigs from whole genome sequencing data were reviewed for genes labelled '*fosA*' or 'glutathione transferase', and contig sequences were compared to a reference set of *fosA* sequences using Geneious version 7.0 (https:// geneious.com).

2.5. Construction of plasmids

Synthesis and cloning of *fosA* and SMR genes into the expression plasmids pMS119EH, pYUB28b, and pHT01 was performed using BioBasic Inc. Gene Synthesis services (Markham, ON, Canada). Genes were synthesized using the plasmids and cut sites listed in **Table 2.2**. Each *fosA* gene was synthesized with an in–frame C–terminal hexahistidine affinity tag, while *mmr* was synthesized with a C-terminal *myc*-hexahistidine affinity tag (see **Appendix B** for gene synthesis fasta files). The *myc* tag added to the membrane protein Mmr was used as a linker to space the hexahistidine tag from the cell membrane (88).

The *E. coli-M. smegmatis* shuttle plasmid pYUB28b (hygromycin resistant) and the *E. coli-B. subtilis* shuttle plasmid pHT01 (ampicillin and chloramphenicol resistant) were obtained from Addgene (Watertown, MA, USA). pYUB28b possesses a T7lac promoter, while pHT01 uses a Pgrac promoter comprised of the *B. subtilis groES-groEL* operon fused to the *lac* operator. pMS119EH (ampicillin resistant) was obtained from the authors of Strack *et al.* 1992 (121) and contains a PtacI promoter, which is a fusion of the *E. coli lac* and *trp* operon promoters. The kanamycin-resistant *E. coli-M. smegmatis* shuttle plasmid pYUB1232 (101) that possesses an acetamide-inducible T7 polymerase gene was generously provided by the William Jacobs laboratory (Albert Einstein College of Medicine, NY, USA). All plasmid constructs were verified by Sanger sequencing (**Figure 2.1**).

Table 2.2. Parental plasmids, cut sites, and affinity tag sequences for genes cloned in this study.

Gene	Plasmid	Restriction Endonuclease Cut Sites (5', 3')	Affinity Tag Sequence[a]
mmr	pYUB28b	XbaI, SmaI	EFEAYVEQKLISEEDLNSAVDHHHHHH
fosA3	pMS119EH	EcoRI, XbaI	GGSHHHHHHS
fosA8	pMS119EH	EcoRI, XbaI	GGSHHHHHHS
fosA7.5^{WT}	pMS119EH	EcoRI, XbaI	GGSHHHHHHS
fosA7.5^{Q86E}	pMS119EH	EcoRI, XbaI	GGSHHHHHHS
fosA7.5^{W92G}	pMS119EH	EcoRI, XbaI	GGSHHHHHHS
emrE	pMS119EH	XbaI, HindIII	n/a[b]
qacE	pMS119EH	XbaI, PstI	n/a
qacF/L	pMS119EH	XbaI, PstI	n/a
gdx/sugE	pMS119EH	XbaI, PstI	n/a
qacC	pHT01	XbaI, SmaI	n/a
qacG	pHT01	XbaI, SmaI	n/a
qacH	pHT01	XbaI, SmaI	n/a
qacJ	pHT01	XbaI, SmaI	n/a

[a]Affinity tag sequences were added in frame after the C-terminus codon of each cloned gene
[b]None added

2.6. Construction of expression strains

pYUB1232, pYUB28b, pMS119EH, pHT01 and cloned constructs derived from these parental plasmids were transformed into *E. coli* DH5α competent cells for long term cryo-storage using standard protocols (125). pMS119EH and cloned construct plasmids used for gene expression and AMR characterization were transformed into *E. coli* K-12 BW25113 using the same standard methods. In brief, an overnight culture of *E. coli* was used to inoculate 100 mL LB broth. The culture was grown until reaching an optical density at 600 nm (OD_{600}) of 0.3 units (measured using a Syngery Neo2 microplate reader, BioTek Instruments), then cultures were incubated on ice for 15 min. Cells in culture were pelleted by centrifugation (3000 x g, 10 min) and resuspended in 10 mL transformation buffer 1 (30 mM potassium acetate, 100 mL rubidium chloride, 10 mM calcium chloride, 50 mM manganese(II) chloride, 15% [v/v] glycerol, pH 5.8) for 15 min on ice. Afterwards, cells were pelleted by centrifugation (3000 x g, 10 min) and resuspended in 8 mL transformation buffer 2 (10 mM morpholinepropanesulfonic acid [MOPS], 75 mM calcium chloride, 10 mM rubidium chloride, 15% [v/v] glycerol, pH 6.5). 50 µL aliquots of *E. coli* competent cells were mixed with 2 µL of plasmid DNA (10 ng/µL) and placed on ice for 5 min. Cells were heat shocked at 42°C for 1 min, then mixed with 1 mL LB broth and incubated at 37°C for 1 h. Afterwards, cells were plated on LB agar with antibiotic selection and incubated for 16 h. For each transformation, a single colony was used to inoculate 5 mL LB broth with antibiotic selection. All *E. coli* transformants were cryopreserved at -80°C in LB with dimethyl sulfoxide (DMSO) added to a final concentration of 8% (v/v).

Electrocompetent *M. smegmatis* cells were prepared using a standard protocol (102). Briefly, a single *M. smegmatis* colony grown on CAMHA was used to inoculate 10 mL of CAMHB with 0.05% (v/v) tween-80. Cells were grown for 16-24 h with shaking at 170 rpm then standardized to OD_{600} 1.0 units, and 1 mL of standardized culture was used to inoculate 100 mL of CAMHB with 0.05% tween-80. The culture was incubated at 37°C until reaching approximately OD_{600} 0.5-0.8 units. Afterwards, the culture was incubated on ice for 1.5 h, then cells were harvested by centrifugation (3000 x g, 10 min). Cells were washed 3 times with ice cold 10% (v/v) glycerol and resuspended to a total final volume of 5 mL with 10% (v/v) glycerol. 200 µL aliquots of the resulting electrocompetent cells were frozen at -80°C for at least 24 h prior to electroporation.

Electrocompetent *B. subtilis* cells were prepared using a standard protocol (126). Briefly, an overnight culture of *B. subtilis* was used to inoculate 100 mL of LB with 7.5% (v/v) glycine betaine and 0.5 M sorbitol added. The culture was grown to approximately OD_{600} 0.5 units, then incubated on ice for 10 min. Cells were recovered by centrifugation (3000 x g, 10 min), washed 3 times with ice cold electroporation buffer (10% [v/v] glycerol, 7.5% [v/v] glycine betaine, 0.5 M sorbitol, 0.5 M mannitol), and resuspended to a final volume of 1 mL in electroporation buffer. 50 µL aliquots of electrocompetent *B. subtilis* were frozen at -80ºC.

M. smegmatis and *B. subtilis* strains were electroporated using a Bio-Rad Gene Pulser. Aliquots of electrocompetent cells were mixed with 1-5 µL of plasmid DNA (approximately 5 µg total DNA) and incubated on ice for 5 min, then transferred to a chilled 0.2 cm gap electroporate cuvette. Cells were subjected to a single electric pulse for transformation; V=2.5 kV, Q=25 µF, R=1000 Ω for *M. smegmatis*, V=2.1 kV, Q=25 µF, R=200 Ω for *B. subtilis* (102, 126). Afterwards, the cells were transferred to 5 mL of recovery media which was CAMHB with 0.05% (v/v) tween-80 for *M. smegmatis*, or LB with 0.5 M sorbitol and 0.38 M mannitol for *B. subtilis*. These recovery media cultures were incubated for 2-3 h at 37ºC with aeration at 170 RPM for *M. smegmatis*, and without shaking for *B. subtilis*. Cells were harvested by centrifugation and plated onto CAMHA or LB agar with appropriate plasmid antibiotic selection for 3-5 days for *M. smegmatis*, or 24 h for *B. subtilis*. Single colonies were used to inoculate 5 mL of CAMHB with 0.05% (v/v) tween-80 or LB broth with antibiotic selection, and the resulting cultures were cryopreserved at -80ºC in CAMHB with 16% (v/v) glycerol or LB with 8% (v/v) DMSO. pYUB1232 was electroporated into *M. smegmatis* mc^2155 to generate the expression strain mc^24517 (101). *M. smegmatis* mc^24517 was electroporated with pYUB28b to generate a control transformant, or with pMmr to generate a transformant over-expressing the *mmr* gene. *B. subtilis* was electroporated with pHT01 and the cloned constructs as listed in **Table 2.1**.

2.7. Determination of protein accumulation

For *E. coli fosA* transformants, overnight (16 h) cultures grown in LB broth with 100 µg/mL ampicillin were standardized to OD_{600} 1.0 units. 50 µL of cells were used to inoculate 5 mL LB broth with 100 µg/mL ampicillin, and cultures were incubated at 37ºC until reaching OD_{600} 0.5 units. Cultures were removed from the incubator, induced with 1 mM IPTG, and incubated at 25ºC for 3 h to reduce the chances of inclusion body formation. 2 mL of cells were harvested by

centrifugation (15,000 x g, 1 min), re–suspended in 0.4 mL of urea buffer (100 mM monosodium phosphate, 10 mM tris(hydroxymethyl)aminomethane [Tris], 8M urea, pH 8.0) to denature cellular proteins, and vortexed briefly. The urea buffered cell supernatants were recovered after centrifugation at 15,000 x g for 10 min.

For cell membrane isolations of each SMR transformant, an overnight culture was used to inoculate 20 mL of CAMHB or LB broth with appropriate antibiotic selection to maintain plasmids. Cultures were grown for 24 h, the culture suspension was standardized to OD_{600} 1.0 units, and 10 mL of standardized culture was used to inoculate 500 mL of CAMHB or LB broth with antibiotic selection. *E. coli* and *B. subtilis* cultures were grown until reaching approximately OD_{600} 0.5 units, then induced with 1 mM IPTG and incubated at 25°C for another 3-6 h. *M. smegmatis* cultures were incubated at 37°C without induction for 24 h, then induced with 0.2% (w/v) acetamide and 1 mM IPTG for an additional 24 h at 37°C. Afterwards, cells were pelleted by centrifugation (3,000 x g, 10 min). *M. smegmatis* and *B. subtilis* cells were each re-suspended in 30 mL of phosphate-buffered saline ethylenediaminetetraacetic acid (PBS-EDTA) buffer (137 mM sodium chloride, 2.7 mM potassium chloride, 10 mM disodium phosphate, 1.8 mM monopotassium phosphate, 1 mM EDTA, 0.1 mM phenylmethylsulfonyl fluoride [PMSF], pH 7.4) while *E. coli* was re-suspended in 30 mL of SMR-A buffer (50 mM MOPS, 5 mM EDTA, 1 mM dithiothreitol [DTT], 8% [v/v] glycerol, 0.1 mM PMSF, pH 7.0). Cell suspensions were disrupted by French Press between 1,000 and 1,500 pounds per square inch (PSI) a total of three times, and unbroken cells were removed by centrifugation (3,000 x g, 10 min). The membrane fractions were separated from the cytosol by centrifugation (30,000 x g, 1 h), washed once to remove contaminating material, and resuspended in 5 mL PBS-EDTA or SMR-A buffer.

Protein concentration from extractions was determined using a modified Lowry protein assay (127). 10 µL of quantified protein extracts (10-25 µg) were mixed with 15 µL sodium dodecylsulfate–tricine polyacrylamide gel electrophoresis (SDS-tricine-PAGE) loading dye (100 mM DTT, 150 mM Tris-HCl [pH 7.0], 12% [w/v] SDS, 30% [v/v] glycerol, 0.05% [w/v] Coomassie brilliant blue G250 dye) and heated to 95°C for 5 min. Samples were separated using SDS-tricine-PAGE with a 12% (w/v) acrylamide gel for FosA protein samples and 16% (w/v) acrylamide gels for SMR samples (128). Fractionated proteins were visualized with ultraviolet (UV) light (at 310 nm) using 2,2,2–trichloroethanol (TCE) at a final concentration of 0.5% (v/v) (129). *M. smegmatis* membrane isolations and *E. coli fosA* extractions were also analyzed using

Western Blotting (130). Proteins from these samples were transferred onto a nitrocellulose membrane and blocked for 1 h in Tris–buffered saline (20 mM Tris, 500 mM sodium chloride, pH 7.5) containing 5% (w/v) skim milk powder. Afterwards, the membrane was washed in Tris–buffered saline containing 0.05% (v/v) tween–20, and incubated with an anti–hexahistidine horseradish peroxidase (HRP)–conjugated antibody (Thermo Fisher Scientific) for 2 h. Protein expression was colorimetrically detected using the HRP conjugate substrate kit (Bio–Rad Laboratories) according to the recommended manufacturer procedures.

2.8. Antimicrobial susceptibility tests (AST)

In vitro susceptibility of *E. coli fosA* transformants to fosfomycin was determined as per CLSI agar dilution (109, 131), CLSI disk diffusion (131, 132), and Etest (bioMérieux, Marcy l'Etoile, France) with minor modifications described as follows. CAMHA dilution plates (supplemented with 25 µg/mL of glucose–6–phosphate) contained doubling–dilutions of fosfomycin from 0.5 to 512 µg/mL (109, 131). 200 µg fosfomycin disks (containing 50 µg of glucose–6–phosphate) (131, 132) and Etest were tested using CAMHA. Inoculated agar plates were incubated in ambient air at 35°C ± 2°C for 16–18 h. Fosfomycin AST were determined in triplicate for each transformant using each of the three susceptibility testing methods. Agar dilution AST and disk diffusion zone sizes were interpreted using CLSI definitions and directives (131). Etest endpoints were interpreted according to manufacturer instructions. CLSI fosfomycin agar dilution MIC breakpoints (≤64 µg/mL = susceptible, 128 µg/mL = intermediate, ≥256 µg/mL = resistant) and disk diffusion zone size breakpoints (≥16 mm = susceptible, 13–15 mm = intermediate, ≤12 mm = resistant) were used to interpret the results of fosfomycin AST.

AST of *E. coli* and *B. subtilis* SMR transformants to erythromycin, clarithromycin, azithromycin, roxithromycin, clindamycin, and ethidium bromide was carried out using CLSI broth microdiluton methods for aerobically growing bacteria (109) with minor modifications. In brief, *E. coli* or *B. subtilis* cultures grown in LB broth were incubated at 37°C until exceeding the turbidity equivalent of a 0.5 McFarland standard. Cultures were pelleted by centrifugation (15,000 x g, 1 min) and re-suspended in CAMHB to match the turbidity of a 0.5 McFarland standard. Three biological replicates were prepared for each strain to be tested, and the inoculum density of each replicate was verified by plating onto CAMHA. Cultures were inoculated into CAMHB, and 50 µL was added to 96-well microdilution plates containing 50 µL of serial 2-fold dilutions of

antimicrobial agents to achieve a final cell concentration of $5x10^5$ colony forming units (CFU)/mL. Plates were sealed in plastic ziplock bags and incubated at 37°C in ambient air for 16-24 h. MIC endpoints were determined according to CLSI directives (131). MICs were calculated and defined as the lowest concentration of an antimicrobial that completely inhibits visible growth.

M. smegmatis AST to rifampin, isoniazid, ethambutol, moxifloxacin, bedaquiline, linezolid, acriflavine, erythromycin, clarithromycin, azithromycin, roxithromycin, and clindamycin was performed as per the CLSI broth microdilution method for rapidly growing mycobacteria (133) with minor modifications. In brief, half a loopful of *M. smegmatis* culture grown on CAMHA was transferred to a 2 mL cryovial containing 1 mL of sterile water and approximately 100 µL of 0.5 mm sterile glass beads (MilliporeSigma). The mixture was vigorously vortexed for 20 seconds, then allowed to stand until the beads and larger particles settled. The supernatant was extracted and adjusted visually to a 0.5 McFarland standard turbidity equivalent using sterile water, and the inoculum density was verified by plating onto CAMHA. Cell suspensions were inoculated into CAMHB, and 50 µL was added to 96-well microdilution plates containing 50 µL of serial 2-fold dilutions of antimicrobial agents to achieve a final cell concentration of $5x10^5$ CFU/mL. Each transformant was tested in biological triplicate. Plates were covered with gas permeable adhesive seals (Thermo Fisher Scientific) and incubated at 30°C in ambient air for 3-5 days. MIC endpoints and results were recorded in accordance with CLSI guidelines (133). If sufficient growth was observed in the inoculated growth control wells, MICs were recorded on day 3. If growth in the positive control wells was insufficient, plates were re-incubated and MIC measurements were taken at day 4 or 5 when positive control wells showed growth. If negative control wells showed growth or inoculated quality control strain wells did not fall within the indicated MIC range, the AST procedure was repeated from the beginning. MICs were calculated and defined as the lowest concentration of an antimicrobial that completely inhibits visible growth (133). Erm(38)-mediated inducible macrolide resistance was not tested by incubating plates for 14 days, as CLSI guidelines for testing macrolide susceptibility in rapidly growing mycobacteria does not include *M. smegmatis* isolates (133).

Quality control strains for AST included ATCC strains *E. coli* 25922, *Pseudomonas aeruginosa* 27853, *Staphylococcus aureus* 29213, and *Enterococcus faecalis* ATCC 29212. At least one quality control strain was included on each microdilution plate to verify an acceptable range of the antimicrobial being tested wherever possible. It should be noted that antibiotics for

plasmid selection were included in all media when appropriate to maintain transformed plasmids in some strains (**Table 2.1**); kanamycin and hygromycin for *M. smegmatis*, ampicillin for *E. coli*, and chloramphenicol for *B. subtilis*. Additionally, acetamide and/or IPTG were added to induce gene expression. Specifically, 0.2% (w/v) acetamide was included to induce T7 polymerase expression in *M. smegmatis*, while 1 mM IPTG was included to induce *fosA* and efflux gene over-expression in all transformants.

2.9. Multiple sequence alignments and phylogenetic analyses

Multiple sequence alignments and phylogenetic analyses of FosA protein sequences (**Table S1** in **Appendix A**) were performed with Molecular Evolutionary Genetics Analysis (MEGA7) software version 7.0 (134). Protein dendrograms (shown in **Figures 3.1A and 3.1B**) were constructed using the Neighbor-Joining method, where branch node confidence intervals were assigned using the interior branch test with 500 replicates (135, 136). The sequence alignment of FosA proteins shown in **Figure 3.1C** was generated using Clustal Omega (137) and visualized by Jalview version 2.10.5 software (138).

Multiple sequence alignments of SMR efflux pump protein sequences (shown in **Figures 4.1 and 4.2**) were generated using Clustal Omega (137) to compare Mmr and other mycobacterial sequences to previously functionally characterized representatives from other species. SMR representatives and homologs listed in **Table S1** in **Appendix A** from select genera were included in alignments and phylogenetic trees. Alignments were visualized by Jalview version 2.10.5 software (138). Maximum Likelihood phylogenetic analyses (shown in **Figures 4.3 and 4.4**) were performed using PhyML version 3.0 (139) with 1000 bootstrap replications to determine Mmr homolog relatedness to known SMR family representatives.

2.10. Homology modelling of FosA and SMR protein sequences

For FosA sequences, the crystal structure of FosA1 ($FosA^{Tn2921}$, PDB: 1NBP) from *Serratia marcescens* (140) was the closest template, with root mean square deviation (RMSD) values of 2.3 ± 1.8 Å to 2.6 ± 2.0 Å and C–scores between 1.03-1.19. Homology modelling of all proteins was performed using the Iterative Threading Assembly Refinement (I–TASSER) homology modelling online webserver (141). The overlapped superposition of all FosA homology

model sequences generated by I–TASSER (**Figure 3.3**) was created using PyMOL software version 2.2.3 (142).

I-TASSER analysis of Mmr and other SMR members identified that the crystal structure of SMR protein Gdx-clo (PDB: 6WK8) from *Clostridium* (79) was the closest structural homolog to the proteins submitted for modelling, based their calculated RMSD values (ranging from 2.1 ± 1.6 Å to 3.4 ± 2.4 Å) and C-scores (values ranging from 0.39 to 1.07). SMR protein overlay structural diagram PDB files generated from this analysis (shown in **Figure 4.6**) were derived from PyMOL software version 2.2.3 (142).

3. Chapter 3: Identification and characterization of a novel FosA7 member from fosfomycin resistant clinical *Escherichia coli* isolates from Canadian hospitals

3.1. Introduction

Infections caused by ESBL-producing or MDR *E. coli* can be problematic as there may be limited therapeutic options (22). With a renewed interest in the use of fosfomycin for treatment of urinary tract infections (15), the possible emergence of fosfomycin resistance in uropathogenic *E. coli* is important to discern. Of the three known mechanisms of fosfomycin resistance discussed earlier in Chapter 1, Fos enzymes are of greatest concern, since the *fos* genes that encode them can be found on plasmids allowing for their dissemination by horizontal gene transfer (14, 15). A current literature review shows that fosfomycin resistance and *fosA* sequences in *E. coli* clinical are rare in Canada (22). In a recent study of 2035 *E. coli* urinary isolates recovered from outpatients presenting to Canadian outpatient clinics and emergency rooms, 99.2% were found to be fully susceptible to fosfomycin (16). Of the isolates with AMR, 205 were categorized as MDR (95.1%) and 96.1% of these MDR isolates were susceptible to fosfomycin (16).

Between 2007 and 2016, three highly resistant *E. coli* isolates were identified from the CANWARD collection with fosfomycin MIC of values >512 µg/mL (103). Two of these isolates were isolated from urine and one was isolated from blood (GenBank accession numbers EC623771-EC623773). In this chapter, we characterize the *fosA* genes from these three fosfomycin-resistant isolates using the fosfomycin-susceptible, laboratory strain *E. coli* K-12 BW25113 for expression. Based on this analysis, we also propose and describe a novel sub-family of FosA proteins, which we have named FosA7.5. Here, we discuss their phylogenetic relationship to previously identified FosA1-A12 members in the context of these novel FosA7.5 enzymes. Lastly, homology models of these Fos proteins were created to assess the possible role of structural alterations in drug binding and enzyme activity.

3.2. Results and Discussion

3.2.1. Phylogenetic analysis of *fos* genes reveals multiple *fosA* types in Canadian isolates.

Whole genome sequence analysis revealed that *fosA* genes were present in all three *E. coli* clinical isolate genomes **(Table 3.1)**. The *E. coli* EC623771 *fosA* gene (417 bp) had 100% sequence similarity to *fosA3* (28), and the *E. coli* EC623773 *fosA* gene (426 bp) had 100% sequence similarity to *fosA8* (26) **(Figure 3.1)**. The *E. coli* EC623772 *fosA* (423 bp) gene was not identical

to any previously characterized *fosA* sequence, but it demonstrated >99% sequence identity to two publicly deposited sequences in NCBI/GenBank; a *fosA* gene from a canine isolate of *E. coli* (WP_094163054.1) and a sequence annotated as *fosA7.5* (WP_000941933.1) (**Table S1** in **Appendix A).** We decided to name the novel *E. coli* EC623772 *fosA* variant and the *E. coli* WP_094163054.1 variant *fosA7.5*, following the numbering convention previously used for *fosA7* gene annotation in the NCBI Bacterial Antimicrobial Resistance Reference Gene Database (Accession: PRJNA313047). Phylogenetic trees were generated using the Neighbor-Joining clustering method for these novel FosA sequences with previously described FosA1 to FosA12 protein sequences confirmed the similarity of the three FosA7.5 sequences **(Figure 3.1A-B)** (26–28, 113–119). Notable findings from this analysis are discussed below.

Relative to FosA7.5 from *E. coli* WP_000941933.1, the FosA7.5 from the clinical isolate *E. coli* EC623772 had a Q86E amino acid residue change. In contrast, the FosA7.5 from *E. coli* WP_094163054.1 showed a W92G residue change at a highly conserved amino acid position in the FosA alignment **(Figure 3.2, Table S1** in **Appendix A)**. Hence, we refer to the reference "wild-type" *fosA7.5* sequence as $fosA7.5^{WT}$ (WP_000941933.1), the novel *E. coli* EC623772 *fosA* variant as $fosA7.5^{Q86E}$ and the canine GenBank accession number WP_094163054.1 variant as $fosA7.5^{W92G}$. Despite its name, all FosA7.5 sequences examined herein were distinct from the canonical FosA7 sequence and differ from other FosA7 members at amino acid sites G35, S56, and K62 in the alignment (**Figure 3.2**). FosA7 was originally identified in *Salmonella enterica* serovar Heidelberg (118) and its most closely related variants are associated with *S. enterica*, whereas $FosA7.5^{WT}$, $FosA7.5^{Q86E}$, and $FosA7.5^{W92G}$ variants are all identified from *E. coli*. FosA7.5 sequences are also distinct from FosA7-like sequences from *Klebsiella* spp., and *Citrobacter* spp. shown in **Figure 3.1.**

Twelve FosA variants (FosA1 to FosA12) have been previously described in peer–reviewed publications (26–28, 113–119) and were included in the phylogenetic analysis of FosA protein sequences shown in **Figure 3.1**. There is inconsistency in the FosA literature regarding the naming of FosA enzyme variants. Notably, FosA7, FosA8, FosA9, and FosA10 have each been used twice to describe different variants (26, 113, 118, 143, 144). After the published description of FosA7 in *Salmonella* Heidelberg, Mathur *et al.* 2018 described six FosA variants in *K. pneumoniae* and named them FosA7 through FosA12 (referred to in **Figure 3.1**, **Table S1** in

Table 3.1. Resistance genes and plasmids identified in the three *E. coli* CANWARD isolates.

Strain	MLST	Resistance genes	Plasmids
E. coli EC623771	ST-131	*aac(3)-IId, blaCTX-M-65, blaTEM-1B,* ***fosA3***	IncFIA, IncFIB, IncFII, IncN
E. coli EC623772	ST-354[a]	*aac(3)-IId, aph(3'')-Ib, aph(6)-Id, blaCMY-2, qnrB19, sul2, tet(A),* ***fosA7.5***	Col(pHAD28), IncC, IncFIA, IncFIB
E. coli EC623773	ST-457	*aac(3)-IId, aadA1, aadA2, aph(3'')-Ib, aph(6)-Id, blaTEM-1B, cmlA1, dfrA12, floR, sul2, tet(A),* ***fosA8***	Col(MG828), Col8282, ColpVC, IncFIB, IncFII, IncN, IncX1, p0111

[a]Not in PubMLST Achtman Database, novel ST within the ST-354 clonal complex
Abbreviations: MLST; Multi-locus sequence typing

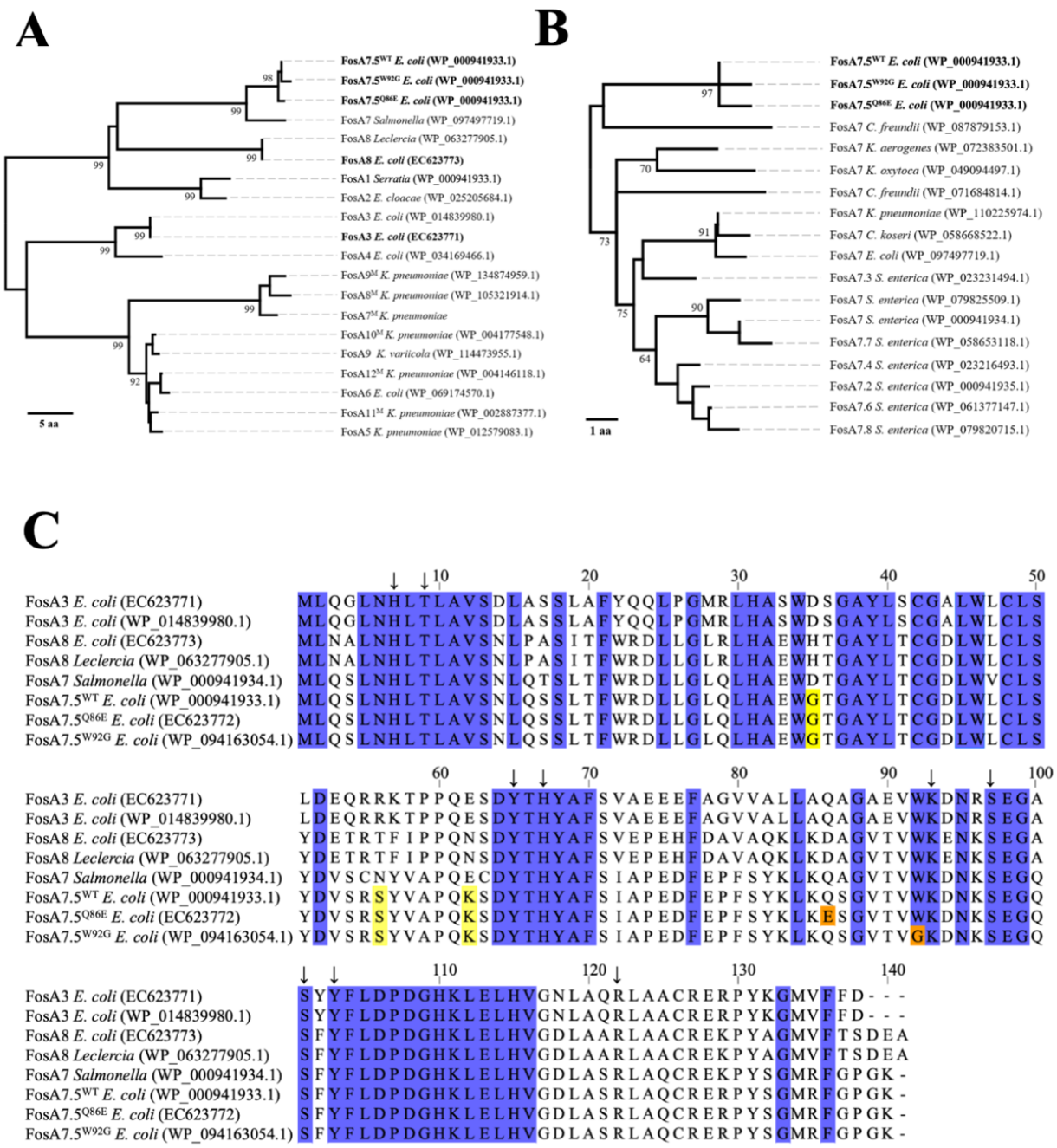

Figure 3.1. Phylogenetic and sequence analysis of clinically isolated *E. coli* FosA sequences and their comparison to previously identified FosA variants. **A)** Phylogenetic analysis of FosA1–FosA12 protein sequences using the Neighbor-Joining distance-based method. Branch lengths represent amino acid differences as distance (scale bar). **B)** Phylogenetic comparison of FosA7 and FosA7.5 family protein sequences using the same method as described in panel A. **C)** Multiple sequence alignment of FosA3, FosA8, and FosA7.5 protein sequence variants. Blue colouring in

the alignment indicates conserved residues identified amongst FosA1–13 family members. Amino acid differences that distinguish the FosA7.5 group from FosA7 are shown in yellow. Differences among FosA7.5 sequences are highlighted in orange. Arrows indicate active site residues. The alignment was generated using Jalview version 2.10.5 (138).

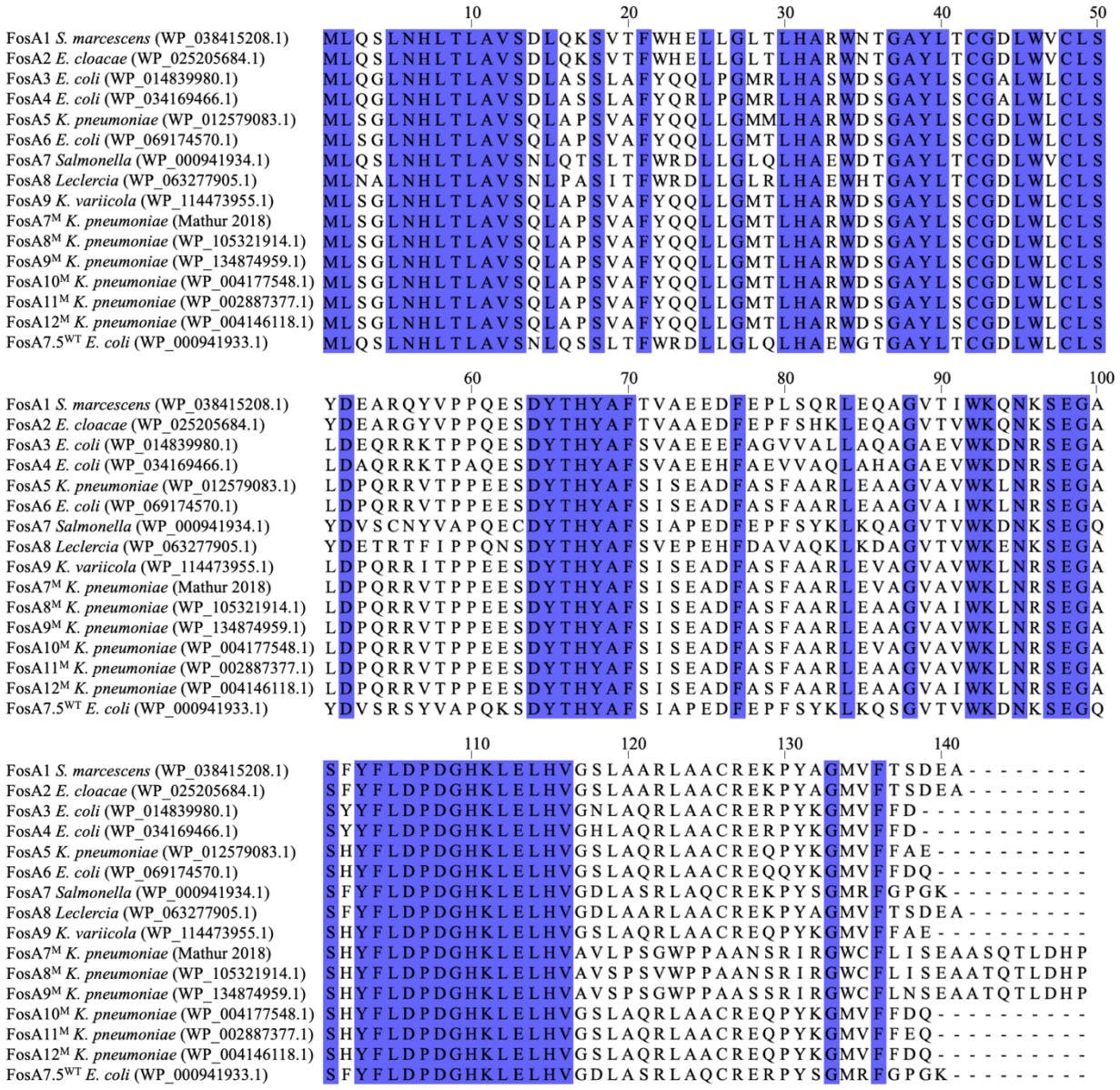

Figure 3.2. Multiple sequence alignment of FosA1-A12 protein sequence variants. Blue colouring in the alignment indicates conserved residues identified amongst all FosA1–12 family members. The alignment was generated using Jalview version 2.10.5 (138).

Appendix A and the following text as FosA7^{M} to FosA12^{M}) (113). Phylogenetic analysis suggests that FosA7^{M}, FosA8^{M}, and FosA9^{M} may comprise a distinct branch of FosA enzymes, but it is unclear if three separate designations are warranted **(Figure 3.1A)**. More recently, *E. coli* FosA8, FosA9, and FosA10 genes were described in three separate papers (26, 119, 144). Based on our phylogenetic tree and sequence alignments in **Figure 3.1,** FosA10^{M}, FosA11^{M}, and FosA12^{M} share 98.6% amino acid sequence identity while FosA5, FosA6 and the newer FosA9 allele have 95.7 to 97.8% sequence similarity (143). Notably, the original descriptions of FosA5 (116), FosA6 (117), and FosA9 (119) indicate that they were mobilized to *E. coli* from *Klebsiella*. Thus, all of these alleles may represent a family of genes derived from *Klebsiella.*

Based on our whole genome sequencing analysis, the *fosA3* (EC623771) and *fosA8* (EC623773) genes identified in our isolates are associated with plasmid sequences, which is consistent with previous reports (26, 28). The *fosA7.5*^{Q86E} allele in *E. coli* EC623772 is flanked on both sides by insertion sequences that confounded our initial attempts to determine the location of this gene. Available genome assemblies (e.g., *E. coli* Ec40743 [GenBank CP041919.1] and *E. coli* 210205630 [GenBank CP015912]) would suggest that the *fosA7.5*^{WT} allele is located on the *E. coli* chromosome. However, resequencing of *E. coli* EC623772 with a MinION system (Oxford Nanopore Technologies) and assembly with Flye (v.2.8.1) (112) revealed that *fosA7.5*^{Q86E} is located on a 103 kb plasmid. Sequence comparison using publicly available databases shows that the backbone of this 103 kb plasmid, excluding the *fosA7.5*^{Q86E} region, is conserved in other plasmids from *E. coli*, *Salmonella* and *Klebsiella*, where 81-82% of the 103 kb plasmid coverage is conserved with >99% sequence identity to GenBank plasmids CP044142.1, JN983043.1, and MF582638.1. Hence, *fosA7.5* genes can spread via plasmids and can be acquired by uropathogenic *E. coli* strains in addition to other Enterobacterales pathogens.

3.2.2. *fosA* genes confer similar fosfomycin resistance MIC values

To verify that the genes from the three Canadian clinical isolates conferred resistance to fosfomycin, *fosA3* (EC623771)*, fosA8* (EC623773) and the three *E. coli fosA7.5* sequences were individually cloned into the low copy expression vector pMS119EH (106). All *fosA* genes were cloned with a C–terminal hexahistidine affinity tag (His_6–tag), then transformed and over–expressed in the *E. coli* K-12 strain BW25113 with IPTG induction **(Table 2.1)**. Western blotting of extracted whole cell proteins demonstrated successful FosA protein expression and

accumulation of each *E. coli* transformant **(Figure 3.3)**. Each transformant underwent fosfomycin AST using agar dilution and disk diffusion methods according to CLSI standards (131, 132), as well as an Etest (bioMérieux, Marcy l'Etoile, France), and the results are shown in **Table 3.2**. The *fosA3*, *fosA8*, and *fosA7.5*^{Q86E} genes cloned from the Canadian clinical isolates, as well as the wild-type *fosA7.5*^{WT} allele all conferred resistance to fosfomycin at MIC values of >512 µg/mL and >1024 µg/mL for agar dilution and Etest, respectively. The only exception was *E. coli* transformed with the *fosA7.5*^{W92G} variant, which remained susceptible to fosfomycin at MIC values of 32 µg/mL and 2 µg/mL using agar dilution and Etest methods, respectively. This indicates that the highly conserved Trp92 residue plays an important role in fosfomycin-inactivation for FosA7.5 enzymes.

3.2.3. FosA homology models demonstrate close overall alignment to each other

As we noted in the section above, key amino acid differences distinguish FosA7.5 members. We generated homology models of FosA3, FosA8, and the three FosA7.5 variants using the I-TASSER webserver (141) to determine how any protein residue structural alterations may potentially impact the FosA drug binding active site and explain why the *fosA7.5*^{W92G} transformant was susceptible to Fosfomycin **(Figure 3.4)**. Enzymatically active FosA forms a protein homodimer, where its active site is comprised of several residues from both monomers that bind fosfomycin (Y9, Y65, K93, S97, S101, Y103, R122) as well as an Mn^{2+} ion needed for enzymatic activity (H7, H67, E113) (21). In our study, dimeric FosA protein homology models were generated from the FosA1 *Serratia marcescens* (PDB: 1nbp) crystal structure to model the complete active site spanning the dimer interface. All FosA7.5 variant models demonstrated close overall alignment to previously characterized FosA3 and FosA8 based on their lowest RMSD values (1.722 to 2.011 Å). The W92G amino acid replacement in FosA7.5^{W92G} (WP_094163054.1) generated a larger drug binding pocket near the fosfomycin binding site when aligned and compared to other FosA7.5 models. This suggests that the replacement of tryptophan by a smaller glycine residue expands the drug binding region and may reduce the enzymatic activity of this variant **(Figure 3.4)**. FosA7.5^{W92G} may allow greater substrate movement or amino acid flexibility within the enzyme's fosfomycin binding site and the replacement this conserved tryptophan with a glycine in this residue position (**Figure 3.2**).

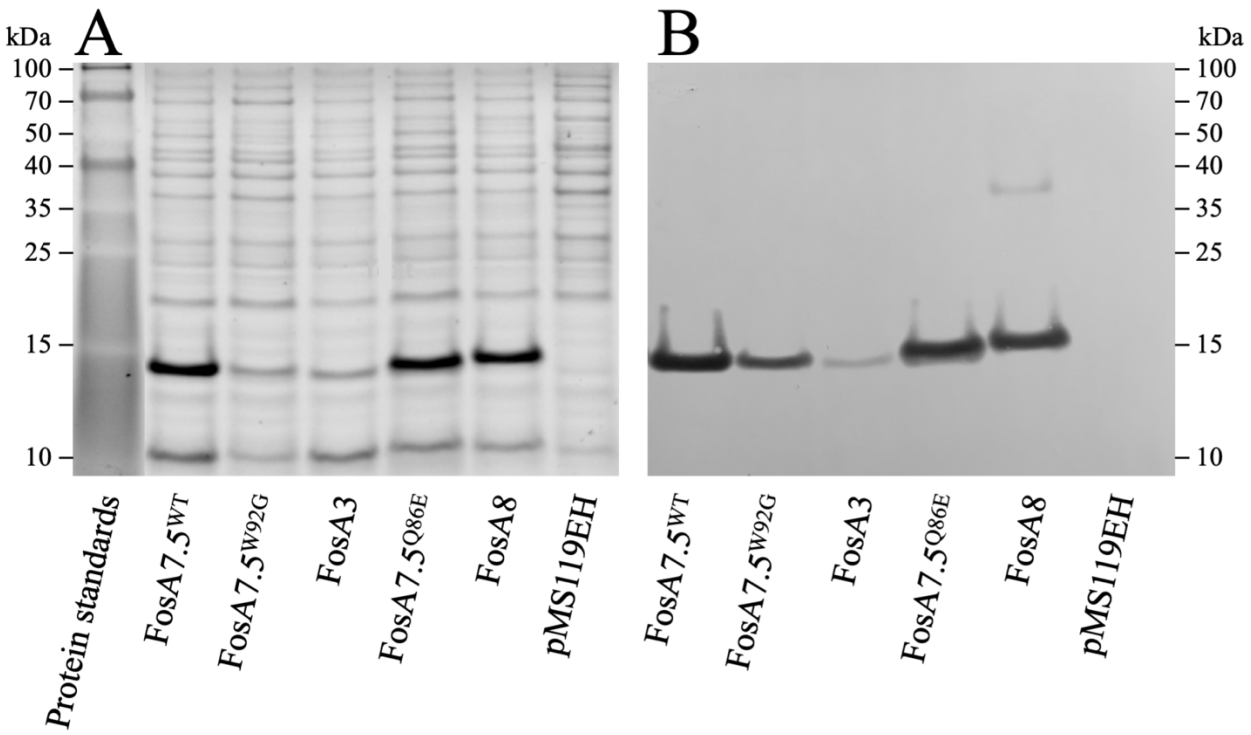

Figure 3.3. Induction of FosA proteins in *E. coli* transformants. A) TCE–visualized whole cell protein extracts. Proteins were fractionated on a 12% acylamide SDS–PAGE gel containing 0.5% (v/v) TCE and visualized under ultraviolet light (310 nm) (129). 10 µL of protein extracts (approximately 10 µg total protein) was loaded into each lane, and 20 µL of Spectra™ Multicolor Broad Range Protein Ladder (Thermo Fisher Scientific) was used to determine protein molecular weights. B) Western blot of protein extracts (130). Proteins were detected using a 1/1000 dilution of the His probe–HRP–conjugated antibody and the HRP conjugate substrate kit (Bio–Rad).

Table 3.2. Fosfomycin susceptibility testing results for *E. coli* transformants.

E. coli plasmid transformants[a]	Agar dilution MIC (μg/mL)	Disk diffusion zone diameter	Etest MIC (μg/mL)	Result
FosA3	>512	6mm[b]	>1024	Resistant
FosA8	>512	6mm	>1024	Resistant
FosA7.5^{WT}	>512	6mm	>1024	Resistant
FosA7.5^{Q86E}	>512	6mm	>1024	Resistant
FosA7.5^{W92G}	32	30mm[c]	2	Susceptible
pMS119EH	2–4	30mm	0.5	Susceptible

[c]All transformants were induced with 1 mM IPTG
[b]6 mm is equivalent to no zone diameter
[c]CLSI 30mm, EUCAST 36mm

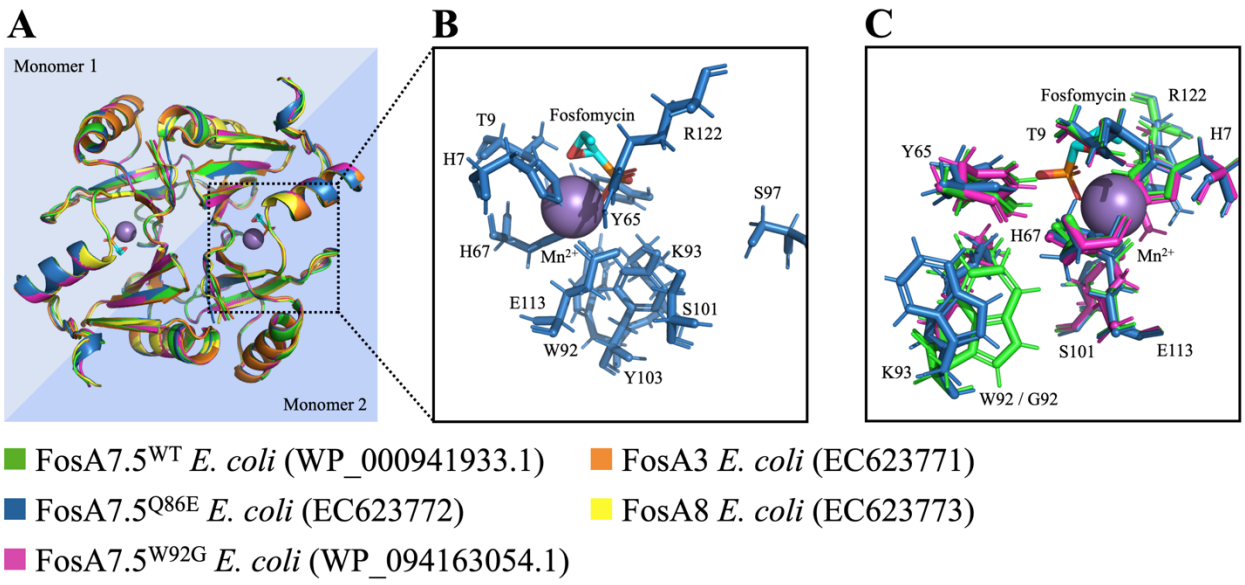

Figure 3.4. Structural visualization of FosA protein homology models generated by I-TASSER. **A)** An overview of aligned superimposed FosA protein dimers are shown where a bound fosfomycin and Mn^{2+} ion are shown as a colored stick diagram and sphere respectively. **B)** A zoomed in stick diagram view of the active site of FosA7.5^{Q86E} from *E. coli* EC623772. **C)** A stick diagram of superimposed active sites from FosA7.5^{WT}, FosA7.5^{Q86E}, and FosA7.5^{W92G} rotated 120 degrees from panel B. These images were created using the program PyMOL version 2.2.3 (142). Colors listed below each panel correspond to FosA sequences shown in all panels.

3.3. Conclusions

In summary, three *fosA* genes from *E. coli* clinical isolates (EC623771-EC623773) recovered from Canadian patients were identified, cloned, and functionally characterized. In addition to confirming the role of *fosA3* and *fosA8* as determinants of fosfomycin resistance (26, 28), we identified and characterized multiple variants of *fosA7.5*. Unlike other *fosA7* alleles which are associated with *Salmonella*, distribution of *fosA7.5* appears to be primarily restricted to *E. coli.* Ongoing surveillance of fosfomycin resistance and the dissemination of *fosA* sequences in *E. coli* is crucial to ensure that fosfomycin remains effective as a treatment option for urinary tract infections.

4. Chapter 4: Characterization of the *Mycobacterium tuberculosis* Mmr efflux pump in *M. smegmatis* reveals a macrolide selectivity when compared to other small multidrug resistance efflux pump family members

4.1. Introduction

M. tuberculosis is a bacterial pathogen primarily responsible for causing the respiratory disease TB, and it has become a serious global health concern due to the emergence of AMR isolates to important first- and second-line TB antimicrobial therapeutics (30). AMR in *M. tuberculosis* leads to longer, less effective, and more expensive treatment courses for M/XDR strains, which can last up to 24 months for M/XDR-TB patients that fully comply with treatment as compared to treatment of pansusceptible strains for 6-9 months (30). Hence, understanding intrinsic AMR mechanisms that are emerging in mycobacteria is important in order to improve *M. tuberculosis* antimicrobial therapies and explore alternative treatments. Macrolides such as clarithromycin are used to treat non-tuberculosis mycobacteria (NTM) infections such as *Mycobacterium avium* (145), and have been investigated for use against *M. tuberculosis* infections (146–148). The core chemical structure of macrolides consists of a 12 to 16-membered lactone ring with one or more deoxy sugars attached (146). Macrolides inhibit protein synthesis by binding to the P-site on the 50S ribosomal subunit, and they possess many desirable pharmacological properties that make them an ideal second line agent for the treatment of drug resistant *M. tuberculosis* infections (146, 148). However, the clinical effectiveness of macrolides against *M. tuberculosis* remains unclear due to poorly understood intrinsic resistance mechanisms. *In vivo* activity of macrolides (bacterial clearance or positive treatment outcomes) does not correlate well with *in vitro* efficacy.

Resistance to macrolides in bacteria occurs through several mechanisms including ribosomal modifications, drug inactivation, and efflux pumps (146). Constitutive or induced expression of rRNA methyltransferase *erm* genes (erythromycin ribsosomal methylase) in mycobacteria causes methylation of the 50S ribosomal subunit, resulting in decreased macrolide binding affinity (148, 149). In *M. tuberculosis*, *erm*(37) is induced in response to macrolide exposure and causes mono-methylation of 23S rRNA, which contributes to intrinsic macrolide resistance in this organism (150, 151). Efflux pumps have also been associated with intrinsic/adaptive macrolide resistance in mycobacteria (*Mycobacterium abscessus*, *Mycobacterium avium*, and *M. tuberculosis*) as well as for Gram-positive organisms such as

Streptococcus pyogenes, *S. pneumoniae*, and *Staphylococcus aureus* (146, 152–154). The induction of clarithromycin-selective efflux pumps in *M. abscessus* is associated with the Actinobacteria transcription factor *whiB7* (152, 155). In *M. tuberculosis*, *whib7* regulates the expression of several efflux pumps, including the ABC transporter Rv1473 which was shown in a previous study to confer reduced susceptibility to macrolides (153). This suggests that efflux pump induction may play a significant role in the intrinsic resistance of *M. tuberculosis* to macrolide antimicrobials. As discussed in chapter 1, other *M. tuberculosis* efflux pumps (such as ABC family Rv1217c-1218c, MFS family Rv1258c, and RND family Rv2942) have been implicated in reduced susceptibility to important antituberculosis drugs (66, 156, 157). However, there is currently a gap in knowledge as to what degree SMR family efflux pumps (specifically Mmr/Rv3065) contribute to the transport of clinically relevant antimicrobials in mycobacteria.

In this study, we examined how the SMR family efflux pump Mmr (Rv3065) contributes to macrolide resistance in mycobacteria. The *M. tuberculosis* Mmr efflux pump was the focus of this study based on previous reports that SMR members in other bacterial species confer reduced susceptibility to erythromycin when expressed (80, 104). Phylogenetic and amino acid sequence analysis of *M. tuberculosis* Mmr was performed to assess the similarity and differences of the Mmr efflux pump to other previously characterized SMR representatives. The *mmr* gene from *M. tuberculosis* H37Rv was cloned in the expression vector pYUB28b and over-expressed in the model organism *M. smegmatis* $mc^2$4517 for antimicrobial susceptibility testing. *M. smegmatis* was chosen to express *mmr* based on its similar genetic background and closer cell membrane architecture to *M. tuberculosis*, as well as its faster generation time, lower biosafety risk group designation, and its higher transformability (95). To compare the substrate specificity of *M. tuberculosis mmr* to other SMR members, we cloned and expressed eight SMR representatives into *E. coli* and *B. subtilis* using the pMS119EH and pHT01 vectors for expression. CLSI broth microdilution AST was performed on each transformant to assess the role of these SMR efflux pumps in conferring reduced susceptibility to macrolides. We also tested these SMR proteins against the lincosamide clindamycin, since antimicrobials belonging to the macrolide-lincosamide-streptogramin (MLS) group have a shared mechanism of action, and resistance to macrolides often confers cross resistance to other MLS agents (158). The outcome of this study shows that *M. tuberculosis* Mmr is selective for macrolide and lincosamide agents when compared

to other SMR members. Additionally, Mmr sequence analysis highlights potential regions of the SMR amino acid motif that may distinguish macrolide substrate selection.

4.2. Results and Discussion

4.2.1. Mmr is closely related to members of the small multidrug pump (SMP) SMR subclass

Although *M. tuberculosis* Mmr is predicted to be an SMR efflux pump family member, we wanted to specify which SMR family subclass Mmr shares the closest homology with. Maximum Likelihood phylogenetic analysis was performed with Mmr and SMR proteins representing the major known SMR subclasses (**Figure 4.1)**. SMR efflux pumps are classified into three major subfamilies based on their substrate selectivity, function, and homology as follows: 1) the small multidrug pump (SMP) subclass of which the *E. coli* EmrE is the archetypical SMR member, 2) the suppressor of *groEL* mutations subclass (SUG) recently renamed as the riboswitch-regulated guanidinium-exporter (GDM) subclass, and 3) the paired SMR (PSMR) subclass which requires expression of two genes to confer efflux resistance (75). Maximum likelihood analysis using PhyML (139) demonstrated that Mmr was located in the SMP subclass cluster, along with *E. coli* EmrE and other established integron-associated Gram-negative SMP members such as QacE and QacF (**Figure 4.1**) (123). SMP proteins are characterized by their ability to confer reduced susceptibility to a broad range of cationic and lipophilic compounds, including various quaternary ammonium compounds (104, 129). Mmr is also phylogenetically related to two SMR proteins identified from *M. smegmatis* mc^2155; MSMEG_3670 (ABK74464.1) and MSMEG_3672 (ABK71834.1). Analysis of these *M. smegmatis* SMR genes show they form a putative PSMR operon in the *M. smegmatis* genome. BLASTp searches revealed homologs of these paired genes exist in other rapidly growing mycobacteria such as *M. fortuitum* and *M. peregrinum*.

To explore the relationship of *M. tuberculosis* Mmr to similar SMR proteins found in Actinobacteria, Maximum Likelihood phylogenetic analysis was performed using PhyML. *M. tuberculosis* Mmr is closest to SMR orthologs from slowly growing mycobacteria, sharing 99.1% sequence identity to *Mycobacterium canettii*, 85.1% sequence identity to *Mycobacterium intracellulare*, and 73.8-84.1% sequence identity to SMR sequences found in other slowly growing mycobacterial species (*Mycobacterium ulcerans, Mycobacterium marinum, Mycobacterium gordonae, Mycobacterium kansasii, Mycobacterium simiae, Mycobacterium avium,* and

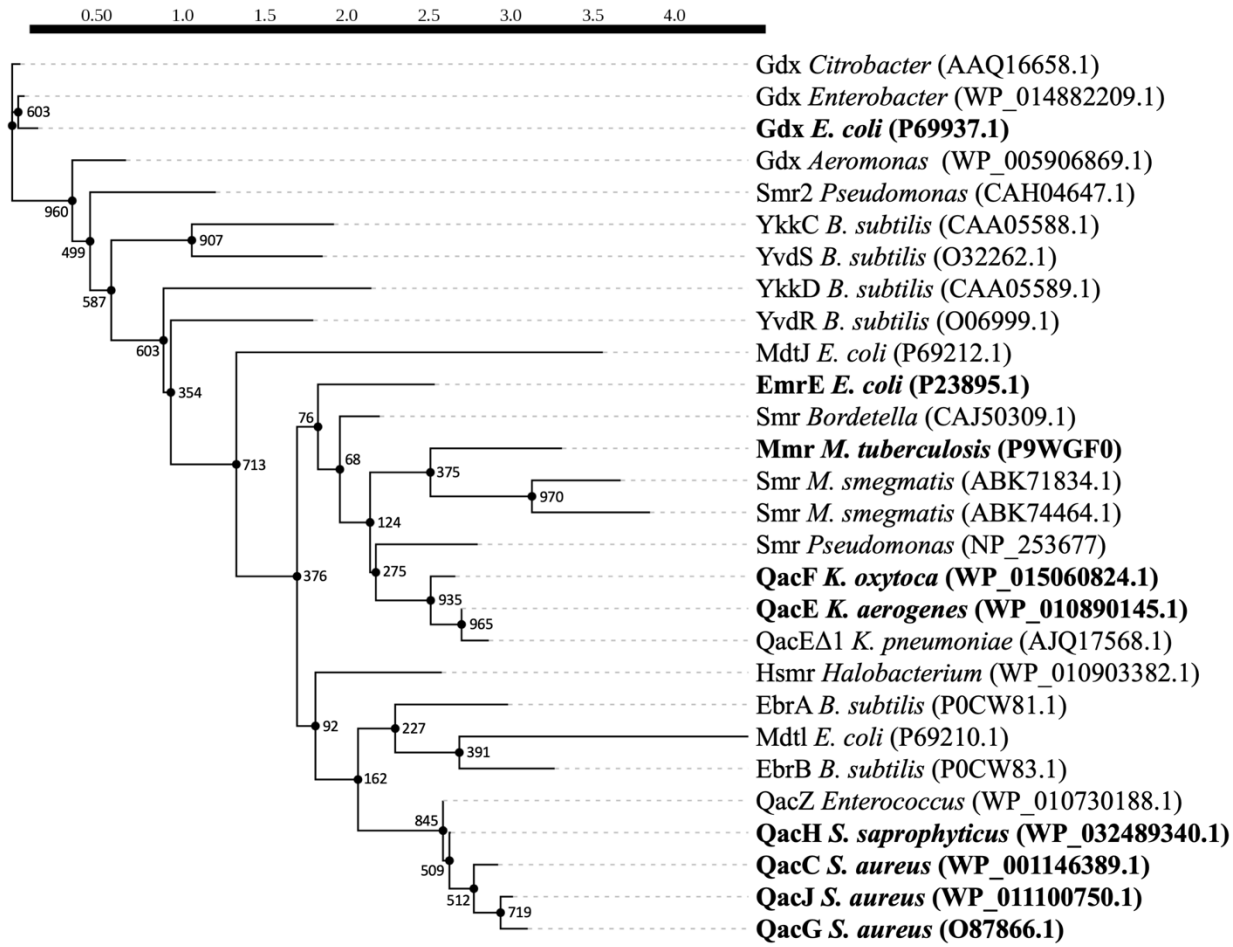

Figure 4.1. Phylogenetic tree of SMR efflux pump family variants. Proteins cloned, over-expressed, and tested for antimicrobial susceptibility in this study are highlighted in bold. Branch node confidence values were determined with 1000 bootstrap replicates using PhyML version 3.0 (139).

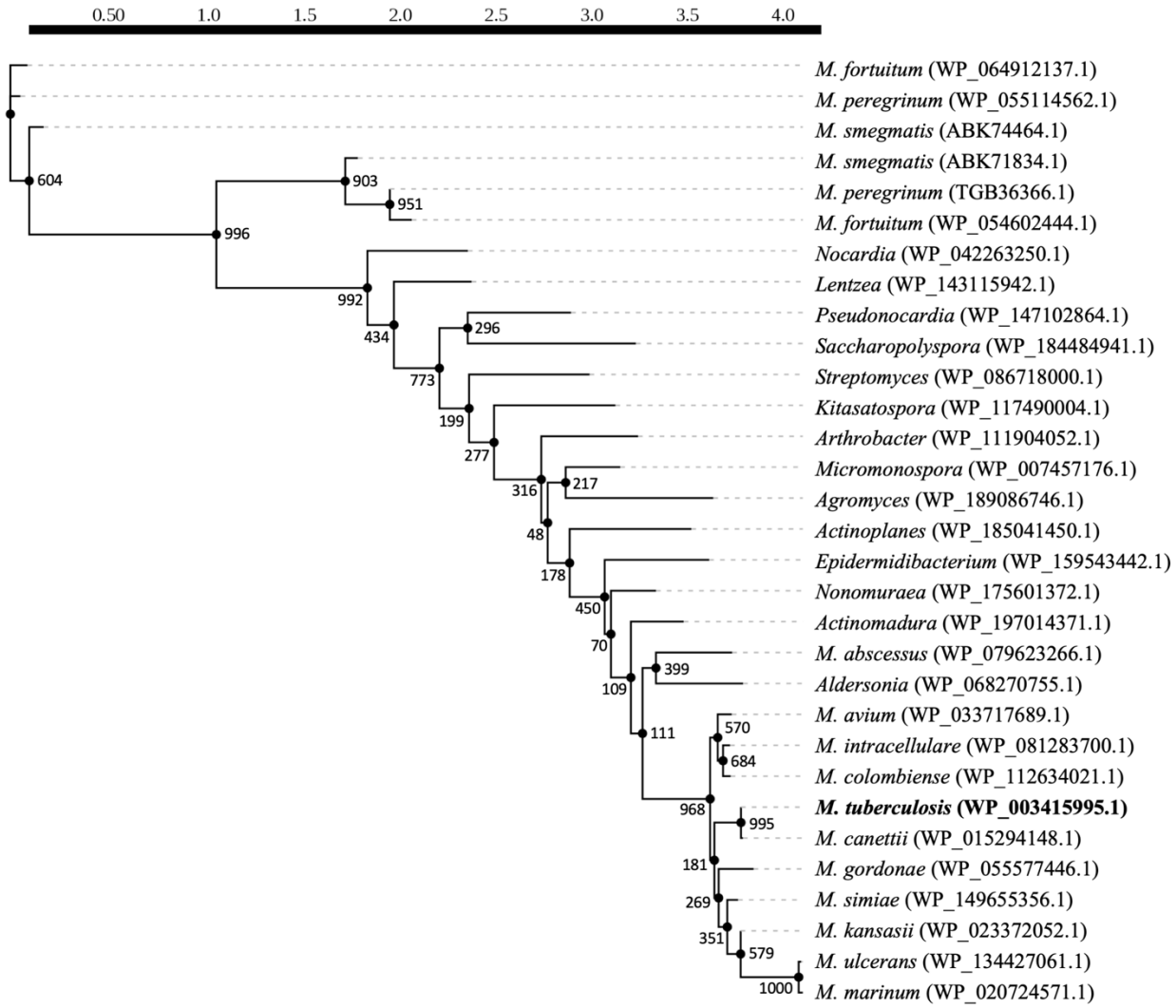

Figure 4.2. Phylogenetic tree of representative Mmr homologs from Actinobacteria. Mmr from *M. tuberculosis* is highlighted in bold. Branch node confidence values were determined with 1000 bootstrap replicates using PhyML version 3.0 (139).

Mycobacterium colombiense) (**Figure 4.2**). In contrast, SMR proteins in the phylogenetic tree from rapidly growing mycobacteria were distantly related to *M. tuberculosis* Mmr. For example, an SMR protein found in *M. abscessus* shares 61.7% sequence identity to *M. tuberculosis* Mmr and was located in a separate cluster from the slowly growing mycobacteria. Importantly, the putative PSMR proteins found in *M. smegmatis*, *M. fortuitum*, and *M. peregrinum* are also dissimilar from other SMR members in Actinobacteria and clustered together in an outlying clade in the phylogenetic tree (**Figure 4.2**). Additionally, *M. tuberculosis* Mmr only shares 35.2% and 39.3% sequence identity with the two PSMR proteins encoded by the *M. smegmatis* genome (MSMEG_3670 and MSMEG_3672, respectively) (**Figure 4.2**), which is the model organism chosen for cloning, over-expression, and AST of Mmr in this study. This suggests that these *M. smegmatis* SMR proteins may have a distinct substrate selectivity different from the other isogenically expressed mycobacterial *mmr* sequences.

4.2.2. Mmr possesses key residue differences suggesting it may confer altered substrate selectivity as compared to other characterized SMP subclass members

Amino acid sequence alignments of *M. tuberculosis* Mmr using Clustal Omega (137) showed sequence identity values ranging from 32.4% to 46.2% based on pairwise sequence alignment comparisons to other representative SMR members (**Figure 4.3**). *M. tuberculosis* Mmr has 41.5% sequence similarity to the archetypical SMR member, *E. coli* EmrE, and shares several key conserved residues implicated in substrate binding (A9, I10, E13, T17, Y39, Y60, W63, Mmr numbering) (86–91), as well as transporter multimerization (G90, G97) (76, 77) noted in previously published SMR and SMP motif studies. Despite the identification of key conserved residue similarities, *M. tuberculosis* Mmr notably differs from EmrE by possessing an alanine residue at S42 (Mmr numbering) on transmembrane helix 2 (TMH2). In a previous study, replacement of alanine with serine in Mmr and an SMR homolog from *Bacillus pertussis* enabled them to transport methyl viologen (93). Additionally, *M. tuberculosis* Mmr differs from other representative SMP members at many other positions. Mmr possesses a glutamine residue at amino acid position 55 replacing a semi-conserved proline residue in turn 1 (T1). Mmr also possesses aspartic acid at the G/S/N57 motif position in TMH3, and possesses a serine residue at the Q/E/D81 position in loop 2 (L2), all of which are notable SMP motif residues. There are also several amino

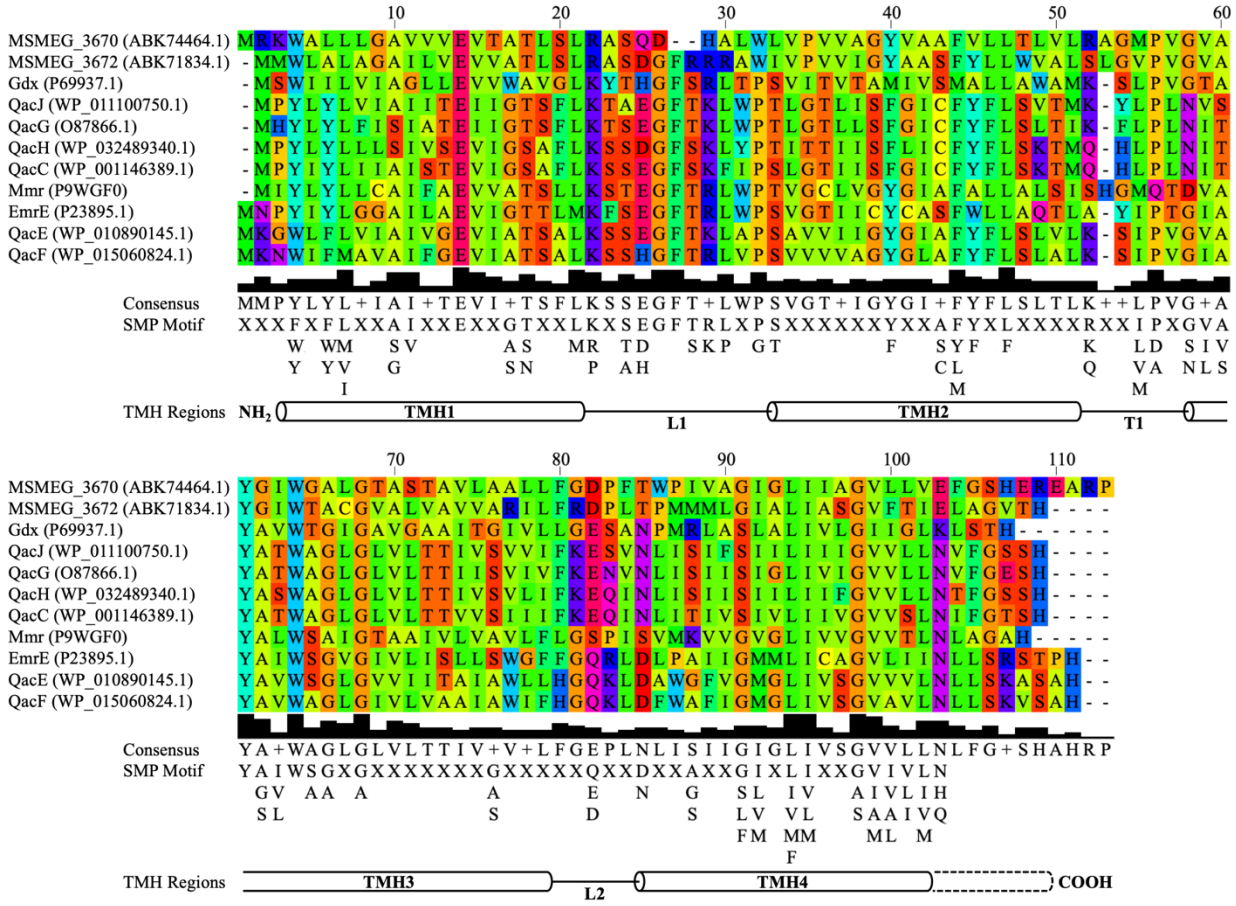

Figure 4.3. Multiple sequence alignment of SMR proteins cloned and analyzed in this study. The alignment was generated using Clustal Omega (137) and amino acids were coloured according to the Taylor scheme in Jalview software version 2.10.5 (138). Transmembrane helices (TMH) are shown as a cylinder cartoon separated by loops (L1-L2) and turns (T1) of the SMR protein secondary structure. The amino acid consensus for each residue position in the alignment is shown as a bar plot.

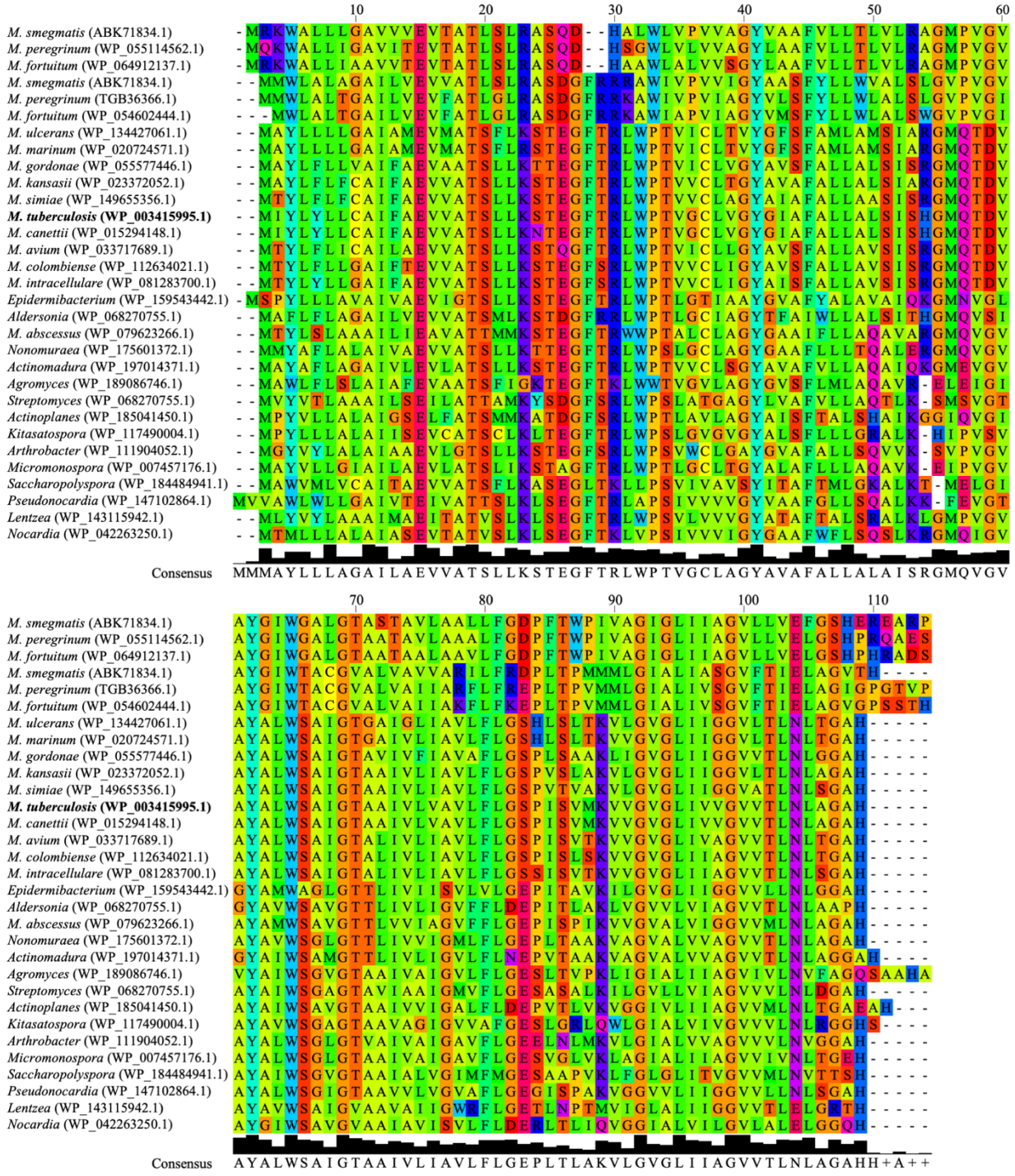

Figure 4.4. Multiple sequence alignment of Mmr homologs from Actinobacteria representatives. The alignment was generated using Clustal Omega (137), and amino acids are coloured according to the Taylor scheme in Jalview software version 2.10.5 (138). The amino acid consensus for each residue position in the alignment is shown at the bottom of the figure as a bar plot.

acids not present in the SMP motif but which uniquely distinguish Mmr from other SMP members, such as C8 on TMH1, C35 and S49 on TMH2, or T68, A69, A70 and V72 on TMH3 (Mmr numbering) (**Figure 4.3**).

As discussed, *M. tuberculosis* Mmr shares between 73.8-99.1% sequence identity with the SMR proteins found in slowly growing mycobacteria (**Figure 4.4**). These orthologs of Mmr and the PSMR proteins present in rapidly growing mycobacteria share many of the aforementioned residues present in Mmr and EmrE. The *M. smegmatis* putative PSMR proteins MSMEG_3670 and MSMEG_3672 share 20.1 to 37.0% and 25.2 to 40.2% sequence similarity to other representative SMR members, respectively (**Figure 4.3**). Despite belonging to the PSMR subclass, they have low pairwise sequence identity to other known PSMR members such as *E. coli* MdtIJ (22.4-33.1%) or *B. subtilis* YkkCD (24.3-29.8%) based on pairwise sequence alignment comparisons (**Figure 4.1**). Furthermore, nBLAST and PhyML analysis of the 500 nucleotide upstream untranslated region of MSMEG_3670 and MSMEG_3672 in the *M. smegmatis* genomic failed to detect any significant homology to any known guanidinium-binding riboswitches (types I-III) that regulate GDM gene expression (159). Both *M. smegmatis* MSMEG_3670 and MSMEG_3672 are at the end of a larger operon containing a 362 amino acid hypothetical gene (WP_011729248.1) and acetyl-CoA dehydrogenase family protein (WP_011729247.1). Hence, the *M. smegmatis* PSMR sequences MSMEG_3670 and MSMEG_3672 are unique and quite distinct from the isogenic Mmr sequence.

4.2.3. Mmr confers reduced susceptibility to macrolides and lincosamides in *M. smegmatis*

In order to assess the substrate specificity of *M. tuberculosis mmr* and compare it to other efflux pumps in the SMP sub-family, we cloned the gene into the expression vector pYUB28b and electroporated this plasmid into *M. smegmatis* $mc^2$4517 for over-expression and AST. To ensure a thorough comparison of SMP and GDM family representatives, we cloned eight other SMR members into plasmids for transformation and over-expression in *E. coli* and *B. subtilis*. Gram-negative SMR representatives (SMP; *emrE*, *qacE*, *qacF* and GDM; *gdx*) were cloned into the expression vector pMS119EH then transformed into *E. coli* K-12 BW25113 strain, and Gram-positive representatives (SMP; *qacC*, *qacG*, *qacH*, *qacJ*) were cloned into the vector pHT01 and electroporated into the *B. subtilis* MGNA-A001 strain. Efflux pump accumulation was verified by isolating the membranes of each transformant, and protein production was visualized using SDS-

tricine-PAGE (**Figure 4.5**) (129). Expression of *mmr* in *M. smegmatis* was also detected by Western blotting (130), since *M. tuberculosis mmr* was cloned with a C-terminal *myc*-hexahistidine affinity tag for verification.

SMR transformants were tested for antimicrobial susceptibility according to CLSI broth microdilution methods (109, 133), and the results are shown in **Table 4.1**. *M. smegmatis* transformed with pMmr consistently conferred 4-fold reduced susceptibility to erythromycin, clarithromycin, azithromycin, and clindamycin, and 2-fold reduced susceptibility to roxithromycin. The pMmr transformant also exhibited and 2-fold reduced susceptibility to acriflavine and ethidium bromide, as shown in a previous study (80). No MIC value differences were observed for pMmr transformant AST with known antituberculosis compounds rifampin, isoniazid, ethambutol, bedaquiline, moxifloxacin, or linezolid (**Table 4.1**). *E. coli* (*emrE*, *qacE*, *qacF*, *gdx*) and *B. subtilis* (*qacC*, *qacG*, *qacH*, *qacJ*) SMR transformants did not exhibit increased resistance to macrolides or clindamycin. However, the *E. coli* and *B. subtilis* transformants had 4-32 fold higher MIC values for the common efflux pump substrate ethidium bromide as compared to their respective empty vector controls, with the exception of *E. coli* pQacE and pGdx. Based on these results, macrolides and clindamycin appear to be specific substrates selected by *M. tuberculosis* Mmr pumps but not for other species SMR efflux pumps tested in this study.

Over-expression of *mmr* in *M. smegmatis* conferred reduced susceptibility to erythromycin in a previous study (80), which was consistent with our results. This indicates that *mmr* expression may contribute towards intrinsic macrolide resistance in *M. tuberculosis* in addition to the known *erm*(37)-mediated macrolide resistance mechanism (150). In comparison, expression of *emrE* in *E. coli* resulted in a 2-fold decrease in the MICs of erythromycin and other macrolides using CLSI broth dilution (109), which was consistent with previous AST experiments performed in our laboratory (160). However, this result differed from other studies; *E. coli emrE* expression was associated with reduced susceptibility to erythromycin using disk diffusion AST methods in one study (104), and a W63G variant of EmrE conferred resistance to erythromycin using agar dilution AST in a different study (161). The observed 2-fold decrease in the MICs of erythromycin, clarithromycin, azithromycin, roxithromycin, and clindamycin for *E. coli* pEmrE in our study may attributed to the differences in broth versus agar AST methods, or the result of fitness costs associated with efflux pump over-expression on the bacterial cells using the pMS119EH expression system.

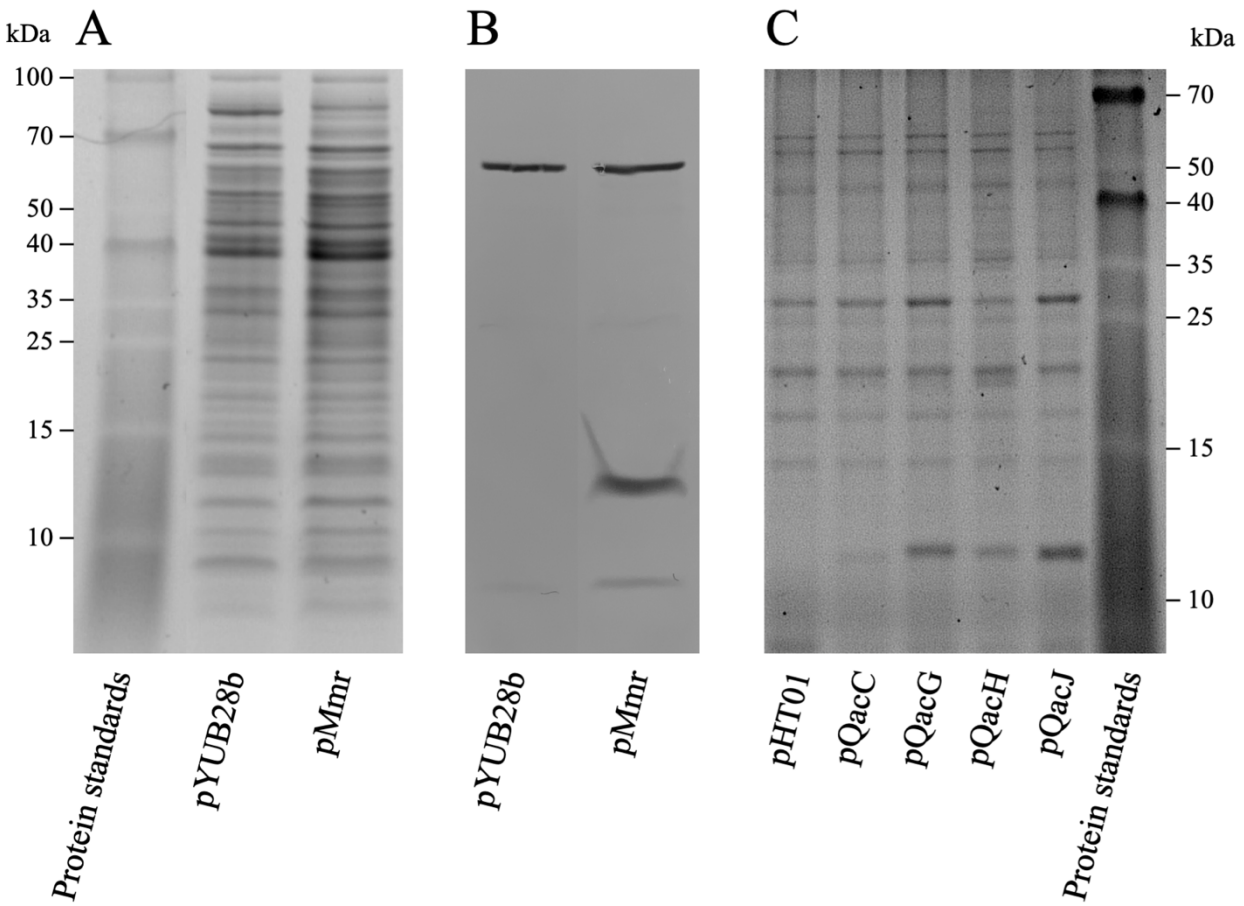

Figure 4.5. Induction of SMR proteins in *M. smegmatis* and *B. subtilis* transformants. **A)** An image of a TCE–strained and visualized whole membrane extracts from various *M. smegmatis* strains. 10 µL of quantified protein extracts (10-25 µg range) were mixed with 15 µL SDS-tricine-PAGE loading dye (100 mM DTT, 150 mM Tris-HCl [pH 7.0], 12% [w/v] SDS, 30% [v/v] glycerol, 0.05% [w/v] Coomassie brilliant blue G250 dye) and were separated on a 16% SDS–tricine-PAGE gel containing 0.5% (v/v) TCE and visualized under ultraviolet light (310 nm) for 5-10 min prior to imaging (129). **B)** Western blot of *M. smegmatis* membrane protein extracts (130). Hexahistidine affinity tagged membrane proteins were detected using a His probe–HRP–conjugated antibody (1/1000 dilution) and the HRP conjugate substrate kit (Bio–Rad). **C)** 16% SDS-tricine-PAGE gel of membrane extracts from *B. subtilis* transformants. Proteins were visualized using the same TCE staining method described in panel A. *E. coli* SMR expression was validated in our lab in previously published work by Slipski *et al*. 2020 and Slipski *et al*. 2021 (75, 123).

Table 4.1. Antimicrobial susceptibility testing results for *M. smegmatis*, *E. coli*, and *B. subtilis* SMR transformants.

	MIC (μg/mL)[a]												
Transformant	ERY	CLR	AZM	ROX	CLI	EBR	ACR	RIF	INH	EMB	BDQ	MXF	LZD
M. smegmatis pYUB28b	16	4	64	32	8	4	1	128	32	1	0.03	0.04	4
M. smegmatis pMmr	**64**[b]	**16**	**256**	64	**32**	8	2	128	32-64	1	0.03-0.06	0.04	4

Transformant	ERY	CLR	AZM	ROX	CLI	EBR
E. coli pMS119EH	32	32	2	128	32	128
E. coli pEmrE	16	16	1	64	16	**512**
E. coli pQacE	32	32	2	128	32	**512**
E. coli pQacF	32	32	2	128	32	128
E. coli pGdx	32	32	2	128	32	128
B. subtilis pHT01	0.25	0.125	1-2	2	ND	4
B. subtilis pQacC	0.25	0.125	1	2	ND	**64**
B. subtilis pQacG	0.25	0.125	1	2	ND	**128**
B. subtilis pQacH	0.25	0.125	1	2	ND	**64**
B. subtilis pQacJ	0.25	0.125	1	2	ND	**64**

[a]Abbreviations: Erythromycin (ERY), Clarithromycin (CLR), Azithromycin (AZM), Roxithromycin (ROX), Clindamycin (CLI), Ethidium bromide (EBR), Acriflavine (ACR), Rifampin (RIF), Isoniazid (INH), Ethambutol (EMB), Bedaquiline (BDQ), Moxifloxacin (MXF), Linezolid (LZD)

[b]MIC changes greater than 2-fold relative to the control strain are highlighted in bold

4.2.4. Homology modelling of Mmr demonstrates structural relatedness to other SMR protein homology models

To assess whether any structural differences between Mmr and other representative SMP proteins may explain the observed differences in macrolide selectivity, homology models of Mmr and SMR protein representatives (EmrE, Gdx, QacC/E/F/G/H/J; **Figure 4.6**) were generated using the I-TASSER webserver (141). To date, the highest resolution X-ray crystal structure of the GDM subclass member Gdx-clo (PDB: 6WK8) (79) was selected by I-TASSER as the closest threading template for all SMR proteins we modeled. SMR sequences had sufficiently low RMSD values (2.1 ± 1.6 Å to 3.4 ± 2.4 Å) and high C-score values (ranging from 0.39 to 1.07) to be used for further protein structural comparisons. An overlapped superposition of each modeled SMR protein and a view of the Mmr drug binding (active) site with bound phenylguanidinum (as the substrate-bound example) generated using PyMOL software version 2.2.3 (142) is shown in **Figure 4.6**.

SMR family efflux pumps belonging to the SMP subclass are known to transport the widest range of structurally dissimilar antimicrobials including antiseptics, quaternary ammonium compounds, and dyes with a cationic charge (74, 80, 81, 104). Members with homology to GDM have a very narrow substrate selectivity, specifically for guanidine analogs and cationic detergents (75). Positively charged substrates selected by various SMR proteins such as tetraphenylphosphonium, methyl viologen, and guanidine have been shown bind and interact at a single highly conserved and negatively charged glutamate residue (E13 in Mmr) located in TMH1 (**Figure 4.3**) (88). Similar to these permanently charged cationic substrates, at physiological pH macrolides have a positive charge, since the dimethylamino group on the desoamine sugar in macrolides has a pK_a of around 8.3-8.9 (162–164). Likewise, clindamycin has a pK_a of 7.6 and also exists predominately in a protonated state (165), suggesting macrolides and lincosamides may be selected by the active SMR glutamate residue. In addition to E13, several conserved active site residues are shared between *M. tuberculosis* Mmr and the well characterized SMP subclass protein *E. coli* EmrE; these conserved active site residues are implicated in both substrate selectivity and H^+ antiport (A9, I10, E13, T17, Y39, Y60, W63, Mmr numbering) (86–91). As shown in **Figure 4.6** and **Figure S1 in Appendix C**, only the Mmr homology model showed a significantly larger drug-binding pocket surrounding bound phenylguanidinium within conserved active site residues by comparison to EmrE and other Qac/Gdx homology models. Differences in unconserved (non-

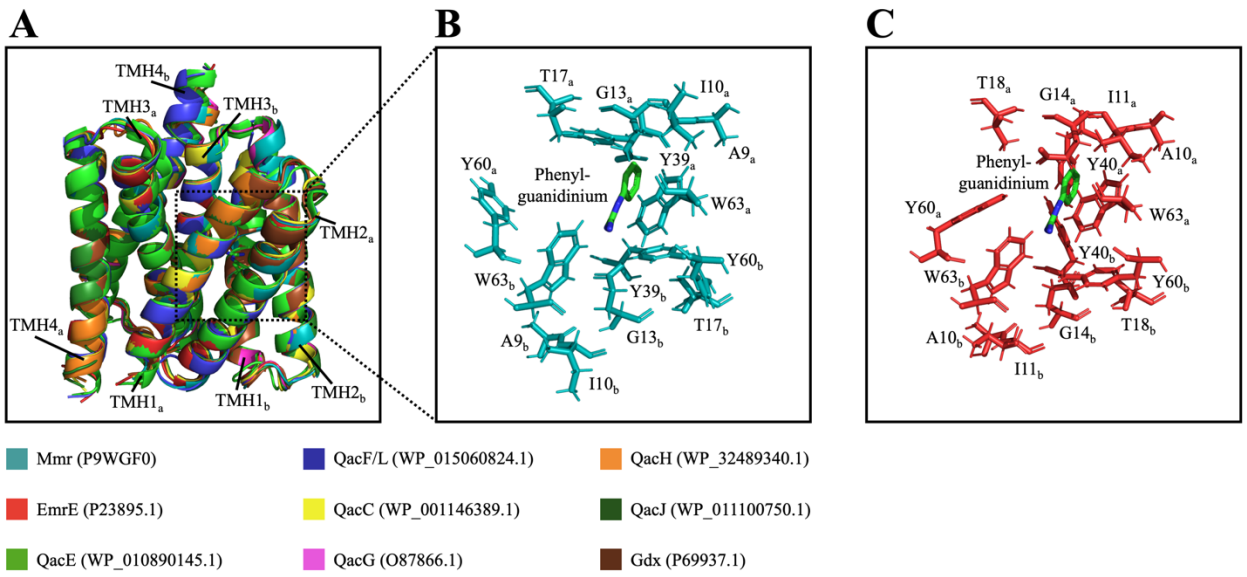

Figure 4.6. Structural visualization of Mmr and related SMR efflux protein homology models generated by I-TASSER. **A)** An overlaid alignment of superimposed SMR protein dimers with a bound substrate (phenylguanidinium) shown as a colored stick diagram. Transmembrane helices (TMH) 1-4 are labeled for each monomer as a and b. Proteins are aligned to the Gdx-clo (PDB: 6WK8) structure from *Clostridiales bacterium* oral taxon 876 str. F0540 (79). **B)** A closer view of residues in the defined region (as a dashed line box) shown as the aquamarine-colored stick diagram view of the active site residues of Mmr from *M. tuberculosis* H37Rv (P9WGF0) with bound phenylguanidinium (as green and dark blue stick diagram). **C)** Zoomed in stick diagram view of active site residues of EmrE from *E. coli* K-12 (P23895) with bound phenylguanidinium (as green and dark blue stick diagram) from the same region as panel A. All structural images were generated using the program PyMOL version 2.2.3 (142). Colours listed below the panel in the legend indicate particular SMR dimers.

SMP motif) positions surrounding the Mmr conserved active site residues likely explain why Mmr can recognize and expel macrolides and lincosamides much better than any other SMR we modelled, as these sequence variations allows the protein dimer active site more room to accommodate larger substrates than other proteins.

Mmr differs from other SMR members at several amino acid positions including C8, C35, S49, Q55, D57, T68, A69, A70, V72, and S81. Notably, P55 and G57 in EmrE (Q55 and D57 inMmr) are known to be associated with protein folding and stability (89, 92). Additionally, when S72 in EmrE (V72 in Mmr) was replaced with cysteine in a previous study, it decreased the MICs of benzalkonium chloride, cetalkonium chloride, and dequalinium chloride and increased the MICs of ethidium bromide and pyronin Y relative to the wild-type EmrE control (92). This indicates that EmrE S72 has a role in substrate binding, and that the V72 variation in Mmr may affect substrate selectivity (92). Lastly, in our homology models C8 and D57 are proximal to the Mmr active site's drug binding pocket and are located near other conserved residues that play a role in substrate binding (E13, Y60, and W63) (86–91). It is possible that the altered orientation of nearby active site residues by the presence of C8 or D57 may have an impact on the ability of Mmr to bind and transport macrolides (**Figure 4.6**).

In addition to structural and amino acid sequence differences between Mmr and other SMR members, the differences in drug selectivity differences we observed herein may be due to the characteristics of the mycobacterial cell envelope and how it influences membrane protein folding and activity. Since membrane structure and composition plays an important role in the folding and orientation of membrane proteins (166), it is possible that the unique architecture of the *M. smegmatis* and/or *M. tuberculosis* cell envelope plays a role in the function of Mmr and other efflux pumps (167). For example, phosphatidyl-*myo*-inositol mannosides are a unique constituent of the *M. tuberculosis*/mycobacterial membrane (168), and the main lipid comprising the inner membrane of *M. smegmatis* (diacyl phosphatidylinositol dimannoside) was suggested in a previous study to decrease the fluidity of the lipid bilayer (169). As a result, the multimerization of efflux pumps and their substrate transport capabilities may be affected by this unique composition of the mycobacterial inner membrane. Alternatively, individual residue replacements can play an important role in SMR substrate selectivity (such as S43A and other residues in *E. coli* EmrE, as noted in previous studies) (92). Therefore, it is possible that one or more of the amino acid

differences discussed between Mmr and the other SMR efflux pumps tested (**Figure 4.3**) may contribute to the observed differences in AST results.

4.3. Conclusions

Mmr is related to other members of the SMP subclass and is phylogenetically and structurally related to other archetypical SMR proteins such as EmrE from *E. coli*. Macrolides and clindamycin appear to be specific substrates of *M. tuberculosis* Mmr and suggest that Mmr may contribute towards intrinsic and/or inducible macrolide resistance in *M. tuberculosis*. Amino acid differences in Mmr when compared to other SMP members (C8, C35, S49, Q55, D57, T68, A69, A70, V72, and S81) may explain its ability to confer macrolide selectivity. Future research on *M. tuberculosis* efflux pumps should explore the role of Mmr in reducing susceptibility to macrolides in *M. tuberculosis.* Understanding how efflux pumps and other factors lead to macrolide resistance in *M. tuberculosis* may help improve the design of antimicrobial regimens for the treatment of drug resistant TB and the design of efflux pump inhibitors specific for mycobacteria to improve treatment outcomes. The associated transcriptional regulatory mechanisms that control Mmr expression should also be explored further to help us understand how efflux pumps become up-regulated in response to antimicrobial exposure. In the future, the use of efflux pump inhibitors in antimicrobial regimens for TB may improve treatment outcomes and make macrolides such as clindamycin more effective.

5. Chapter 5: Discussion of Chaper 3-4 findings, concluding remarks, and future directions

5.1. Summary and impact of Chapters 3 and 4 findings

The emergence of AMR in bacteria represents a major global health challenge (1). This thesis characterizes the AMR genes from two different species of bacteria recognized by the WHO as pathogens of concern; *E. coli* and *M. tuberculosis* (1). What ties these studies together is the similar methodological approaches that were employed for the characterization of two important AMR genes from each pathogen. Despite the recent shift towards next-generation sequencing approaches and the genomic prediction of AMR, culture-based phenotypic characterization techniques such as gene cloning and AST remain the gold standard for AMR gene characterization due to their superior accuracy, precision, and correlation with *in vivo* outcomes when compared to genomic-driven bioinformatic prediction methods (170, 171).

In Chapter 3 of this thesis, three *fosA* genes were cloned and characterized from three separate *E. coli* clinical isolates recovered from Canadian patients. Each cloned *fosA* gene was shown to confer resistance to the phosphoenolpyruvate analogue fosfomycin. Oral fosfomycin is currently recommended by the Infectious Diseases Society of America as a first-line treatment of uncomplicated bacterial cystitis (16), highlighting the importance of new research on AMR mechanisms that confer fosfomycin resistance. In addition to confirming the role of *fosA3* and *fosA8* as determinants of fosfomycin resistance (26, 28), we identified and characterized a novel *fosA7.5* sub-family of *fosA* gene variants. Characterization of novel fosfomycin resistance mechanisms and surveillance of disseminating *fosA* sequences from clinical isolates of *E. coli* (especially UPEC strains) is important to ensure that fosfomycin remains an effective treatment option for urinary tract infections.

In Chapter 4 we characterized the SMR family efflux pump *mmr* from *M. tuberculosis* H37Rv and compared its activity to other representative Gram-positive (*qacC, qacG, qacH*, *qacJ*) and Gram-negative (*emrE, qacE, qacF*, and *gdx*) SMR genes. The results of this chapter helped to address gaps in knowledge related to how Mmr may contribute towards AMR of clinically relevant compounds. Mmr was shown to be phylogenetically and structurally related to other members of the SMP subclass of SMR family efflux pumps. Additionally, *M. tuberculosis* Mmr conferred reduced susceptibility to macrolides and clindamycin when over-expressed in the model organism *M. smegmatis*, while other SMR transformants did not exhibit any increases in the MIC of these agents. These findings suggest that *M. tuberculosis* Mmr has the unique ability to transport

macrolides and clindamycin, and that Mmr may contribute towards an intrinsic/adaptive macrolide resistance phenotype in *M. tuberculosis*. Sequence analysis highlighted residue differences of Mmr (C8, C35, S49, Q55, D57, T68, A69, A70, V72, and S81) compared to other efflux pumps belonging to the SMP subclass, which may account for the observed differences in macrolide selectivity. Understanding how efflux pumps and other factors lead to macrolide resistance in *M. tuberculosis* can help to improve the design of antimicrobial regimens for the treatment of drug resistant TB and aid future research on mycobacterial efflux pump inhibitors.

5.2. Study limitations

There are a few limitations of this study that should be mentioned. To begin, the C-terminal affinity tags added to the cloned *mmr* and *fosA* genes may have had an impact on their overall function and folding (172–174). While the hexahistidine tags used for Western blotting of our FosA proteins did not appear to influence their enzymatic activity when compared to similarly tagged representative *fosA* variants, it is difficult to determine whether the *myc*-hexahistidine tag added to *mmr* had any effects on the ability of this pump to transport substrates. We chose to add an affinity tag to *mmr* based on previous validation of this tag in *emrE* (129), and the difficulties associated with lysing and extracting material from the thick mycobacterial cell envelope. The anti–hexahistidine HRP-conjugated antibody improves the sensitivity of protein detection even with low yields of membrane protein extractions, which made it easier to confirm protein expression in *M. smegmatis* pMmr. However, we acknowledge that the use of an untagged version of *mmr* would also improve confidence in our AST results, and the decision to use a tagged version was based on weighing the potential risks versus clear benefits. In a previous study, tagged and un-tagged versions of EmrE had minor differences in multimerization and resistance profiles (174). Therefore, affinity tags are expected to have some minor influences on overall membrane proteins, but their benefits for downstream analysis in this study outweigh their limitations.

Secondly, the addition of IPTG, acetamide, and antimicrobials added to express or maintain plasmid selection during AST of our *fosA*/SMR transformant bacteria may be possible confounding factors. Although these compounds were also included in the media for our empty plasmid control transformants, they may have exhibited synergistic or antagonistic activities with the antimicrobials tested during AST procedures (175), which was not investigated due to time limitations. Furthermore, efflux pump over-expression could have had unintended toxic effects on

cell growth. As a result, we only included IPTG and acetamide in media used during AST procedures and did not culture bacteria transformants prior to AST with any induction to reduce toxic over-expression phenotypes.

Lastly, the presence of *M. smegmatis* SMR family proteins MSMEG_3670 (ABK74464.1) and MSMEG_3672 (ABK71834.1) as well as the presence of the *erm*(38) gene in *M. smegmatis* mc^2155 (176) were possible confounding factors for macrolide resistance, as they may have exhibited a compounding additive effect on *mmr* activity. However, as discussed in Chapter 4 the *M. smegmatis* PSMR proteins are genetically distinct from *M. tuberculosis* Mmr, suggesting that these proteins likely have significant differences in substrate selectivity, as observed for many PSMR representatives (73). Also, while *erm*(38) is associated with intrinsic macrolide resistance in *M. smegmatis*, it requires induction by either pre-growing *M. smegmatis* with a sub-inhibitory concentration of a macrolide, or incubating cultures for a long period of time (~14 days) to allow *erm* expression (133, 176). CLSI guidelines recommend a 14 day incubation for AST of select rapidly growing mycobacteria (other than *M. smegmatis*) carrying *erm* genes to allow time for expression and eventual cell growth (133), but we did not incubate cultures for more than 5 days, which helped to reduce confounding errors from *erm*-mediated macrolide resistance.

5.3. Future directions

Future research on *fosA* and SMR efflux pump AMR mechanisms in *E. coli* and *M. tuberculosis* should explore several key research questions. Firstly, it would be beneficial to elucidate whether fosfomycin-resistant clinical strains of *E. coli* expressing *fosA* could be restored to a susceptible phenotype through the use of an inhibitor. In a previous study, the antiviral agent phosphonoformate was shown to be a competitive inhibitor of fosfomycin binding at the FosA active site at therapeutically achievable concentrations (177). Further studies on the *in vivo* co-administration of inhibitor compounds with fosfomycin (analogous to β-lactamase inhibitors for β-lactam antimicrobials) such as phosphonates would be a valuable area of research to help improve clinical outcomes for infections with fosfomycin-resistant pathogens (177).

For *M. tuberculosis* protein Mmr, testing its susceptibility to other MLS antimicrobials, such as streptogramin B would help to broaden our understanding of this protein's full substrate profile. Additionally, further research exploring the role of residue replacement using site-directed mutagenesis and/or differences in cell membrane architecture on the substrate specificity of SMR

transporters such as Mmr would help us to understand the function of SMR proteins across different mycobacterial, Gram-positive, and Gram-negative species. For example, do other SMR family members such as EmrE confer reduced susceptibility to macrolides and clindamycin when expressed in *M. smegmatis*, or is this phenotype specific for Mmr? As well, would Mmr's substrate specificity change when over-expressed in a different organism such as *E. coli*? Such experiments could potentially involve troubleshooting due to the problems associated with cross-species protein expression in bacteria but could potentially help to answer important questions about SMR function. Next, follow-up experiments to our study should explore the role of *mmr* expression in conferring reduced susceptibility to macrolides in *M. tuberculosis* itself. Although *M. tuberculosis* is more difficult to genetically manipulate, experiments that improve our understanding of *mmr* activity in *M. tuberculosis* and the associated transcriptional regulatory mechanisms that control *mmr* expression would provide insights on the possible role of this efflux protein in macrolide resistance. Lastly, the use of an animal model to study the treatment efficacy of macrolides on *M. tuberculosis* infection would be beneficial to assess whether *mmr* expression or other intrinsic resistance mechanisms can be linked to *in vivo* treatment outcomes.

5.4. Conclusion

In conclusion, we cloned and characterized important AMR genes from the bacterial pathogens *E. coli* and *M. tuberculosis* and provided novel insights into their AMR phenotypes and phylogenetic/structural relationships to AMR proteins characterized in previous studies. For *E. coli*, the *fosA* genes from Canadian *E. coli* clinical isolates were confirmed as determinants of fosfomycin resistance when expressed in the laboratory strain of *E. coli* K-12 BW25113, and one protein was found to belong to a novel subfamily called FosA7.5. For *M. tuberculosis*, the SMR family efflux pump *mmr* was shown to confer reduced susceptibility to macrolides and clindamycin when over-expressed in the model organism *M. smegmatis* $mc^2$4517. Mmr was also found to be phylogenetically and structurally related to SMR members of the SMP subclass.

Future research should explore the *in vitro* co-administration of inhibitor compounds with fosfomycin to improve clinical outcomes in patients infected with *fosA*-harboring *E. coli*. Additionally, further studies on residue replacement and expression of *mmr* in *M. tuberculosis* will help us to better understand the contribution of this efflux pump to intrinsic macrolide resistance and will aid the design of second-line M/XDR-TB antimicrobial regimens.

References

1. **Geneva: World Health Organization**. 2017. Prioritization of pathogens to guide discovery, research and development of new antibiotics for drug-resistant bacterial infections, including tuberculosis. https://www.who.int/medicines/areas/rational_use/prioritization-of-pathogens/en/.

2. **Geneva: World Health Organization**. 2014. Antimicrobial resistance: Global report on surveillance 2014 summary. https://apps.who.int/iris/bitstream/handle/10665/112647/WHO_HSE_PED_AIP_2014.2_eng.pdf.

3. **Sharma M, Thibert L, Chedore P, *et al.*** 2011. Canadian multicenter laboratory study for standardized second-line antimicrobial susceptibility testing of *Mycobacterium tuberculosis*. J Clin Microbiol **49**:4112–4116.

4. **Christaki E, Marcou M, Tofarides A**. 2020. Antimicrobial resistance in bacteria: mechanisms, evolution, and persistence. J Mol Evol **88**:26–40.

5. **Blount ZD**. 2015. The unexhausted potential of *E. coli*. Elife **4**:1–12.

6. **Baba T, Ara T, Hasegawa M, *et al.*** 2006. Construction of *Escherichia coli* K-12 in-frame, single-gene knockout mutants: the Keio collection. Mol Syst Biol **2**:1–11.

7. **Croxen MA, Finlay BB**. 2010. Molecular mechanisms of *Escherichia coli* pathogenicity. Nat Rev Microbiol **8**:26–38.

8. **Pitout JD**. 2012. Extraintestinal pathogenic *Escherichia coli*: an update on antimicrobial resistance, laboratory diagnosis and treatment. Expert Rev Anti Infect Ther **10**:1165–1176.

9. **Hooton TM**. 2012. Uncomplicated urinary tract infection. N Engl J Med **367**:1028–1037.

10. **Flores-Mireles AL, Walker JN, Caparon M, *et al.*** 2015. Urinary tract infections:

epidemiology, mechanisms of infection and treatment options. Nat Rev Microbiol **13**:269–284.

11. **Denisuik AJ, Lagacé-Wiens PRS, Pitout JD, *et al.*** 2013. Molecular epidemiology of extended-spectrum β-lactamase-, AmpC β-lactamase- and carbapenemase-producing *Escherichia coli* and *Klebsiella pneumoniae* isolated from Canadian hospitals over a 5 year period: CANWARD 2007-11. J Antimicrob Chemother **68**:57–65.

12. **McDanel J, Schweizer M, Crabb V, *et al.*** 2017. Incidence of extended-spectrum β-Lactamase (ESBL)-producing *Escherichia coli* and *Klebsiella* infections in the United States: A systematic literature review. Infect Control Hosp Epidemiol **38**:1209–1215.

13. **Detweiler K, Mayers D, Fletcher SG**. 2015. Bacteruria and urinary tract infections in the elderly. Urol Clin North Am **42**:561–568.

14. **Falagas ME, Vouloumanou EK, Samonis G, *et al.*** 2016. Fosfomycin. Clin Microbiol Rev **29**:321–347.

15. **Zhanel GG, Walkty AJ, Karlowsky JA**. 2015. Fosfomycin: a first-line oral therapy for acute uncomplicated cystitis. Can J Infect Dis Med Microbiol **2016**.

16. **Karlowsky JA, Lagacé-Wiens PRS, Adam HJ, *et al.*** 2019. *In vitro* susceptibility of urinary *Escherichia coli* isolates to first- and second-line empirically prescribed oral antimicrobials: CANWARD surveillance study results for Canadian outpatients, 2007–2016. Int J Antimicrob Agents **54**:62–68.

17. **Gupta K, Hooton TM, Naber KG, *et al.*** 2011. International clinical practice guidelines for the treatment of acute uncomplicated cystitis and pyelonephritis in women: A 2010 update by the Infectious Diseases Society of America and the European Society for Microbiology and Infectious Diseases. Clin Infect Dis **52**:103–120.

18. **Kaye KS, Rice LB, Dane AL, *et al.*** 2019. Fosfomycin for injection (ZTI-01) versus piperacillin-tazobactam for the treatment of complicated urinary tract infection including acute pyelonephritis: ZEUS, a phase 2/3 randomized trial. Clin Infect Dis **69**:2045–2056.

19. **Venkateswaran PS, Wu HC**. 1972. Isolation and characterization of a phosphonomycin-resistant mutant of *Escherichia coli* K-12. J Bacteriol **110**:935–944.

20. **Karageorgopoulos DE, Wang R, Yu X hong, *et al.*** 2012. Fosfomycin: Evaluation of the published evidence on the emergence of antimicrobial resistance in Gram-negative pathogens. J Antimicrob Chemother **67**:255–268.

21. **Doi Y, Wintrode PL, Mackerell AD**. 2017. Structure and dynamics of FosA-mediated fosfomycin resistance in *Klebsiella pneumoniae* and *Escherichia coli*. Antimicrob Agents Chemother **61**:1–13.

22. **Walkty A, Karlowsky JA, Baxter MR, *et al.*** 2019. Fosfomycin resistance mediated by *fos* genes remains rare among extended-spectrum beta-lactamase-producing *Escherichia coli* clinical isolates recovered from the urine of patients evaluated at Canadian hospitals (CANWARD, 2007–2017). Diagn Microbiol Infect Dis **96**:1–3.

23. **Yang TY, Lu PL, Tseng SP**. 2019. Update on fosfomycin-modified genes in Enterobacteriaceae. J Microbiol Immunol Infect **52**:9–21.

24. **Kieffer N, Poirel L, Descombes MC, *et al.*** 2020. Characterization of FosL1, a plasmid-encoded fosfomycin resistance protein identified in *Escherichia coli.* Antimicrob Agents Chemother **64:**1-21.

25. **Ito R, Mustapha MM, Tomich AD, *et al.*** 2017. Widespread fosfomycin resistance in Gram-negative bacteria attributable to the chromosomal *fosA* gene. MBio **8**:1–9.

26. **Poirel L, Vuillemin X, Kieffer N, *et al.*** 2019. Identification of FosA8, a plasmid-

encoded fosfomycin resistance determinant from *Escherichia coli*, and its origin in *Leclercia adecarboxylata*. Antimicrob Agents Chemother **63**:1–7.

27. **Rodriguez MM, Ghiglione B, Power P, *et al.*** 2018. Proposing *Kluyvera georgiana* as the origin of the plasmid-mediated resistance gene *fosA4*. Antimicrob Agents Chemother **62**:1–5.

28. **Wachino JI, Yamane K, Suzuki S, *et al.*** 2010. Prevalence of fosfomycin resistance among CTX-M-producing *Escherichia coli* clinical isolates in Japan and identification of novel plasmid-mediated fosfomycin-modifying enzymes. Antimicrob Agents Chemother **54**:3061–3064.

29. **Lawn SD, Zumla AI**. 2011. Tuberculosis. Lancet **378**:57–72.

30. **Geneva: World Health Organization**. 2020. Global tuberculosis report 2020. http://www.who.int/tb/publications/global_report/en/.

31. **Jetty R**. 2021. Tuberculosis among First Nations, Inuit and Métis children and youth in Canada: Beyond medical management. Paediatr Child Heal **26**:E78–E81.

32. **Vachon J, Gallant V, Siu W**. 2018. Tuberculosis in Canada. Can Commun Dis Rep **44**:75–81.

33. **BañUls AL, Sanou A, Van Anh NT, *et al.*** 2015. *Mycobacterium tuberculosis*: ecology and evolution of a human bacterium. J Med Microbiol **64**:1261–1269.

34. **Vergne I, Gilleron M, Nigou J**. 2015. Manipulation of the endocytic pathway and phagocyte functions by *Mycobacterium tuberculosis* lipoarabinomannan. Front Cell Infect Microbiol **4**:1–9.

35. **Menzies D, Elwood K**. 2014. Chapter 5: Treatment of tuberculosis disease. *In* Canadian Tuberculosis Standards, 7th edition. Public Health Agency of Canada and the Canadian

Lung Association/Canadian Thoracic Society.

36. **Christianson S, Jamieson F, Wolfe J, *et al.*** 2014. Appendix D: Tuberculosis and mycobacteriology laboratory standards: Services and policies. *In* Canadian Tuberculosis Standards, 7th edition. Public Health Agency of Canada and the Canadian Lung Association/Canadian Thoracic Society.

37. **Geneva: World Health Organization**. 2018. Technical report on critical concentration for drug susceptibility testing of medicines used in the treatment of drug resistant tuberculosis. https://apps.who.int/iris/handle/10665/260470.

38. **Gygli SM, Borrell S, Trauner A, *et al.*** 2017. Antimicrobial resistance in *Mycobacterium tuberculosis*: mechanistic and evolutionary perspectives. FEMS Microbiol Rev **41**:354–373.

39. **Zheng J, Rubin EJ, Bifani P, *et al.*** 2013. *para*-Aminosalicylic acid is a prodrug targeting dihydrofolate reductase in *Mycobacterium tuberculosis*. J Biol Chem **288**:23447–23456.

40. **Campbell EA, Korzheva N, Mustaev A, *et al.*** 2001. Structural mechanism for rifampicin inhibition of bacterial RNA polymerase. Cell **104**:901–912.

41. **Yadav S, Rawal G, Baxi M**. 2016. Bedaquiline: A novel antitubercular agent for the treatment of multidrug-resistant tuberculosis. J Clin Diagnostic Res **10**:FM01–FM02.

42. **Blondeau JM**. 2004. Fluoroquinolones: Mechanism of action, classification, and development of resistance. Surv Ophthalmol **49**:1–6.

43. **Mingeot-Leclercq MP, Glupczynski Y, Tulkens PM**. 1999. Aminoglycosides: Activity and resistance. Antimicrob Agents Chemother **43**:727–737.

44. **Swaney SM, Aoki H, Ganoza MC, *et al.*** 1998. The oxazolidinone linezolid inhibits

initiation of protein synthesis in bacteria. Antimicrob Agents Chemother **42**:3251–3255.

45. **Shi W, Zhang X, Jiang X, *et al.*** 2017. Pyrazinamide inhibits trans-translation in *Mycobacterium tuberculosis*: a potential mechanism for shortening the duration of tuberculosis chemotherapy. Science **333**:1630–1632.

46. **Zhanel GG, Wiebe R, Dilay L, *et al.*** 2007. Comparative review of the carbapenems. Drugs **67**:1027–1064.

47. **Goude R, Amin AG, Chatterjee D, *et al.*** 2009. The arabinosyltransferase EmbC is inhibited by ethambutol in *Mycobacterium tuberculosis*. Antimicrob Agents Chemother **53**:4138–4146.

48. **Prosser GA, De Carvalho LPS**. 2013. Kinetic mechanism and inhibition of *Mycobacterium tuberculosis* D-alanine:D-alanine ligase by the antibiotic D-cycloserine. FEBS J **280**:1150–1166.

49. **Manjunatha U, Boshoff HI, Barry CE**. 2009. The mechanism of action of PA-824: novel insights from transcriptional profiling. Commun Integr Biol **2**:215–8.

50. **Lewis JM, Sloan DJ**. 2015. The role of delamanid in the treatment of drug-resistant tuberculosis. Ther Clin Risk Manag **11**:779–791.

51. **Laborde J, Deraeve C, Lecoq L, *et al.*** 2016. Synthesis, oxidation potential and anti-mycobacterial activity of isoniazid and analogues: Insights into the molecular isoniazid activation mechanism. ChemistrySelect **1**:172–179.

52. **Mirnejad R, Asadi A, Khoshnood S, *et al.*** 2018. Clofazimine: a useful antibiotic for drug-resistant tuberculosis. Biomed Pharmacother **105**:1353–1359.

53. **Da Silva PEA, Palomino JC**. 2011. Molecular basis and mechanisms of drug resistance in *Mycobacterium tuberculosis*: classical and new drugs. J Antimicrob Chemother

66:1417–1430.

54. **Brown L, Wolf JM, Prados-Rosales R, *et al.*** 2015. Through the wall: extracellular vesicles in Gram-positive bacteria, mycobacteria and fungi. Nat Rev Microbiol **13**:620–630.

55. **Jarlier V, Nikaido H**. 1990. Permeability barrier to hydrophilic solutes in *Mycobacterium chelonei*. J Bacteriol **172**:1418–1423.

56. **Rom WN, Garay SM**. 2019. Tuberculosis, 2nd edition. Wolters Kluwer, Netherlands.

57. **Nasiri MJ, Haeili M, Ghazi M, *et al.*** 2017. New insights in to the intrinsic and acquired drug resistance mechanisms in mycobacteria. Front Microbiol **8**:1–19.

58. **Szumowski JD, Adams KN, Edelstein PH, *et al.*** 2013. Antimicrobial efflux pumps and *Mycobacterium tuberculosis* drug tolerance: evolutionary considerations, p. 81–108. *In* Pathogenesis of *Mycobacterium tuberculosis* and its interaction with the host organism. Springer-Verlag Berlin Heidelberg, New York.

59. **Rengarajan J, Bloom BR, Rubin EJ**. 2005. Genome-wide requirements for *Mycobacterium tuberculosis* adaptation and survival in macrophages. Proc Natl Acad Sci U S A **102**:8327–8332.

60. **da Silva PEA, von Groll A, Martin A, *et al.*** 2011. Efflux as a mechanism for drug resistance in *Mycobacterium tuberculosis*. FEMS Immunol Med Microbiol **63**:1–9.

61. **Burian J, Yim G, Hsing M, *et al.*** 2013. The mycobacterial antibiotic resistance determinant WhiB7 acts as a transcriptional activator by binding the primary sigma factor SigA (RpoV). Nucleic Acids Res **41**:10062–10076.

62. **Jan B, Ramon-Garcia S, Howes CG, *et al.*** 2012. WhiB7, a transcriptional activator that coordinates physiology with intrinsic drug resistance in *Mycobacterium tuberculosis*.

Expert Rev Anti Infect Ther **10**:1037–1047.

63. **Liu J, Shi W, Zhang S, *et al.*** 2019. Mutations in efflux pump Rv1258c (Tap) cause resistance to pyrazinamide, isoniazid, and streptomycin in *M. tuberculosis*. Front Microbiol **10**:1–7.

64. **Brake LHM, Knegt GJ De, Steenwinkel JE De, *et al.*** 2017. The role of efflux pumps in tuberculosis treatment and their promise as a target in drug development: unraveling the black box. Annu Rev Pharmacol Toxicol **58**:271–291.

65. **Li XZ, Elkins CA, Zgurskaya HI**. 2016. Efflux-mediated antimicrobial resistance in bacteria: Mechanisms, regulation and clinical implications. Springer International Publishing, Switzerland.

66. **Wang K, Pei H, Huang B, *et al.*** 2013. The expression of ABC efflux pump, Rv1217c-Rv1218c, and its association with multidrug resistance of *Mycobacterium tuberculosis* in China. Curr Microbiol **66**:222–226.

67. **Balganesh M, Dinesh N, Sharma S, *et al.*** 2012. Efflux pumps of *Mycobacterium tuberculosis* play a significant role in antituberculosis activity of potential drug candidates. Antimicrob Agents Chemother **56**:2643–2651.

68. **Rodrigues L, Machado D, Couto I, *et al.*** 2012. Contribution of efflux activity to isoniazid resistance in the *Mycobacterium tuberculosis* complex. Infect Genet Evol **12**:695–700.

69. **Rossi E De, Aínsa JA, Riccardi G**. 2006. Role of mycobacterial efflux transporters in drug resistance: an unresolved question. FEMS Microbiol Rev **30**:36–52.

70. **Rodrigues L, Baptista P, Veigas B, *et al.*** 2012. Contribution of efflux to the emergence of isoniazid and multidrug resistance in *Mycobacterium tuberculosis*. PLoS One **7**:1–12.

71. **Gupta RS, Lo B, Son J**. 2018. Phylogenomics and comparative genomic studies robustly support division of the genus *Mycobacterium* into an emended genus *Mycobacterium* and four novel genera. Front Microbiol **9**:1–41.

72. **Pasca MR, Guglierame P, Rossi E De, *et al.*** 2005. *mmpL7* gene of *Mycobacterium tuberculosis* is responsible for isoniazid efflux in *Mycobacterium smegmatis*. Antimicrob Agents Chemother **49**:4775–4777.

73. **Bay DC, Turner RJ**. 2016. Small multidrug resistance efflux pumps, p. 45–71. *In* Efflux-mediated antimicrobial resistance in bacteria: mechanisms, regulation and clinical implications. Springer International Publishing, Switzerland.

74. **Kermani AA, Macdonald CB, Gundepudi R, *et al.*** 2018. Guanidinium export is the primal function of SMR family transporters. Proc Natl Acad Sci U S A **115**:3060–3065.

75. **Slipski CJ, Jamieson TR, Zhanel GG, *et al.*** 2020. Riboswitch-associated guanidinium-selective efflux pumps frequently transmitted on Proteobacterial plasmids increase *Escherichia coli* biofilm tolerance to disinfectants. J Bacteriol **202**:e00104-20.

76. **Elbaz Y, Salomon T, Schuldiner S**. 2008. Identification of a glycine motif required for packing in EmrE, a multidrug transporter from *Escherichia coli*. J Biol Chem **283**:12276–12283.

77. **Sharoni M, Steiner-Mordoch S, Schuldiner S**. 2005. Exploring the binding domain of EmrE, the smallest multidrug transporter. J Biol Chem **280**:32849–32855.

78. **Omasits U, Ahrens CH, Müller S, *et al.*** 2014. Protter: Interactive protein feature visualization and integration with experimental proteomic data. Bioinformatics **30**:884–886.

79. **Kermani AA, Macdonald CB, Burata OE, *et al.*** 2020. The structural basis of

promiscuity in small multidrug resistance transporters. Nat Commun **11**.

80. **De Rossi E, Branzoni M, Cantoni R, *et al.*** 1998. *mmr*, a *Mycobacterium tuberculosis* gene conferring resistance to small cationic dyes and inhibitors. J Bacteriol **180**:6068–6071.

81. **Rodrigues L, Villellas C, Bailo R, *et al.*** 2013. Role of the *mmr* efflux pump in drug resistance in *Mycobacterium tuberculosis*. Antimicrob Agents Chemother **57**:751–757.

82. **Battaglia RA, Price IR, Ke A**. 2017. Structural basis for guanidine sensing by the *ykkC* family of riboswitches. RNA **23**:578–585.

83. **Jack DL, Storms ML, Tchieu JH, *et al.*** 2000. A broad-specificity multidrug efflux pump requiring a pair of homologous SMR-type proteins. J Bacteriol **182**:2311–2313.

84. **Higashi K, Ishigure H, Demizu R, *et al.*** 2008. Identification of a spermidine excretion protein complex (MdtJI) in *Escherichia coli*. J Bacteriol **190**:872–878.

85. **Bay DC, Rommens KL, Turner RJ**. 2008. Small multidrug resistance proteins: A multidrug transporter family that continues to grow. Biochim Biophys Acta - Biomembr **1778**:1814–1838.

86. **Elbaz Y, Tayer N, Steinfels E, *et al.*** 2005. Substrate-induced tryptophan fluorescence changes in EmrE, the smallest ion-coupled multidrug transporter. Biochemistry **44**:7369–7377.

87. **Rotem D, Steiner-Mordoch S, Schuldiner S**. 2006. Identification of tyrosine residues critical for the function of an ion-coupled multidrug transporter. J Biol Chem **281**:18715–18722.

88. **Muth TR, Schuldiner S**. 2000. A membrane-embedded glutamate is required for ligand binding to the multidrug transporter EmrE. EMBO J **19**:234–240.

89. **Mordoch SS, Granot D, Lebendiker M, *et al.*** 1999. Scanning cysteine accessibility of EmrE, an H^+-coupled multidrug transporter from *Escherichia coli*, reveals a hydrophobic pathway for solutes. J Biol Chem **274**:19480–19486.

90. **Gutman N, Steiner-Mordoch S, Schuldiner S**. 2003. An amino acid cluster around the essential Glu-14 is part of the substrate- and proton-binding domain of EmrE, a multidrug transporter from *Escherichia coli*. J Biol Chem **278**:16082–16087.

91. **Soskine M, Steiner-Mordoch S, Schuldiner S**. 2002. Crosslinking of membrane-embedded cysteines reveals contact points in the EmrE oligomer. Proc Natl Acad Sci U S A **99**:12043–12048.

92. **Saleh M, Bay DC, Turnera RJ**. 2018. Few conserved amino acids in the small multidrug resistance transporter EmrE influence drug polyselectivity. Antimicrob Agents Chemother **62**:1–12.

93. **Brill S, Sade-Falk O, Elbaz-Alon Y, *et al.*** 2015. Specificity determinants in small multidrug transporters. J Mol Biol **427**:468–477.

94. **Bay DC, Turner RJ**. 2009. Diversity and evolution of the small multidrug resistance protein family. BMC Evol Biol **9**:1–27.

95. **Bashiri G, Baker EN**. 2015. Production of recombinant proteins in *Mycobacterium smegmatis* for structural and functional studies. Protein Sci **24**:1–10.

96. **Goldstone RM, Moreland NJ, Bashiri G, *et al.*** 2008. A new Gateway® vector and expression protocol for fast and efficient recombinant protein expression in *Mycobacterium smegmatis*. Protein Expr Purif **57**:81–87.

97. **Clinical and Laboratory Standards Institute**. 2018. M48 - Laboratory detection and identification of mycobacteria, 2nd edition.

98. **Public Health Agency of Canada**. Canadian biosafety standard, 2nd edition. https://www.canada.ca/en/public-health/services/canadian-biosafety-standards-guidelines/second-edition.html.

99. **Public Health Agency of Canada**. 2021. Pathogen safety data sheets: Infectious substances – *Mycobacterium* spp. https://www.canada.ca/en/public-health/services/laboratory-biosafety-biosecurity/pathogen-safety-data-sheets-risk-assessment/mycobacterium.html#shr-pg0.

100. **Etienne G, Laval F, Villeneuve C, *et al.*** 2005. The cell envelope structure and properties of *Mycobacterium smegmatis* mc^2155: Is there a clue for the unique transformability of the strain? Microbiology **151**:2075–2086.

101. **Wang F, Jain P, Gulten G, *et al.*** 2010. *Mycobacterium tuberculosis* dihydrofolate reductase is not a target relevant to the antitubercular activity of isoniazid. Antimicrob Agents Chemother **54**:3776–3782.

102. **Bashiri G, Rehan AM, Greenwood DR, *et al.*** 2010. Metabolic engineering of cofactor F420 production in *Mycobacterium smegmatis*. PLoS One **5**:1–10.

103. **Denisuik AJ, Garbutt LA, Golden AR, *et al.*** 2019. Antimicrobial-resistant pathogens in Canadian ICUs: Results of the CANWARD 2007 to 2016 study. J Antimicrob Chemother **74**:645–653.

104. **Yerushalmi H, Lebendiker M, Schuldiner S**. 1995. EmrE, an *Escherichia coli* 12-kDa multidrug transporter, exchanges toxic cations and H^+ and is soluble in organic solvents. J Biol Chem **270**:6856–6863.

105. **Kobayashi K, Ehrlich SD, Albertini A, *et al.*** 2003. Essential *Bacillus subtilis* genes. Proc Natl Acad Sci U S A **100**:4678–4683.

106. **Fürste JP, Pansegrau W, Frank R, *et al.*** 1986. Molecular cloning of the plasmid RP4 primase region in a multi-host-range *tacP* expression vector. Gene **48**:119–131.

107. **Nguyen HD, Phan TTP, Schumann W**. 2007. Expression vectors for the rapid purification of recombinant proteins in *Bacillus subtilis*. Curr Microbiol **55**:89–93.

108. **Zhanel GG, Adam HJ, Baxter MR, *et al.*** 2019. 42936 pathogens from Canadian hospitals: 10 years of results (2007-16) from the CANWARD surveillance study. J Antimicrob Chemother **74**:iv5–iv21.

109. **Clinical and Laboratory Standards Institute**. 2018. M07 - Methods for dilution antimicrobial susceptibility tests for bacteria that grow aerobically, 11th edition.

110. **Matthews TC, Bristow FR, Griffiths EJ, *et al.*** 2018. The integrated rapid infectious disease analysis (IRIDA) platform. BioRxiv 1–34.

111. **Gurevich A, Saveliev V, Vyahhi N, *et al.*** 2013. QUAST: Quality assessment tool for genome assemblies. Bioinformatics **29**:1072–1075.

112. **Kolmogorov M, Yuan J, Lin Y, *et al.*** 2019. Assembly of long, error-prone reads using repeat graphs. Nat Biotechnol **37**:540–546.

113. **Mathur P, Veeraraghavan B, Devanga Ragupathi NK, *et al.*** 2018. Multiple mutations in lipid-A modification pathway & novel *fosA* variants in colistin-resistant *Klebsiella pneumoniae*. Futur Sci OA **4**:FSO319.

114. **Navas J, Leon J, Arroyo M, *et al.*** 1990. Nucleotide sequence and intracellular location of the product of the fosfomycin resistance gene from transposon Tn*2921*. Antimicrob Agents Chemother **34**:2016–2018.

115. **Xu H, Miao V, Kwong W, *et al.*** 2011. Identification of a novel fosfomycin resistance gene (*fosA2*) in *Enterobacter cloacae* from the Salmon River, Canada. Lett Appl

Microbiol **52**:427–429.

116. **Ma Y, Xu X, Guo Q, *et al.*** 2015. Characterization of *fosA5*, a new plasmid-mediated fosfomycin resistance gene in *Escherichia coli*. Lett Appl Microbiol **60**:259–264.

117. **Guo Q, Tomich AD, McElheny CL, *et al.*** 2016. Glutathione-S-transferase FosA6 of *Klebsiella pneumoniae* origin conferring fosfomycin resistance in ESBL-producing *Escherichia coli*. J Antimicrob Chemother **71**:2460–2465.

118. **Rehman MA, Yin X, Persaud-Lachhman MG, *et al.*** 2017. First detection of a fosfomycin resistance gene, *fosA7*, in *Salmonella enterica* serovar Heidelberg isolated from broiler chickens. Antimicrob Agents Chemother **61**:1–6.

119. **ten Doesschate T, Abbott IJ, Willems RJL, *et al.*** 2019. *In vivo* acquisition of fosfomycin resistance in *Escherichia coli* by *fosA* transmission from commensal flora. J Antimicrob Chemother **74**:3630–3632.

120. **Snapper SB, Melton RE, Mustafa S, *et al.*** 1990. Isolation and characterization of efficient plasmid transformation mutants of *Mycobacterium smegmatis*. Mol Microbiol **4**:1911–1919.

121. **Strack B, Lessl M, Calendar R, *et al.*** 1992. A common sequence motif, -E-G-Y-A-T-A-, identified within the primase domains of plasmid-encoded I- and P-type DNA primases and the α protein of the *Escherichia coli* satellite phage P4. J Biol Chem **267**:13062–13072.

122. **Winstone TL, Duncalf KA, Turner RJ**. 2002. Optimization of expression and the purification by organic extraction of the integral membrane protein EmrE. Protein Expr Purif **26**:111–121.

123. **Slipski CJ, Jamieson-Datzkiw TR, Zhanel GG, *et al.*** 2021. Characterization of

proteobacterial plasmid integron-encoded *qac* efflux pump sequence diversity and quaternary ammonium compound antiseptic selection in *E. coli* grown planktonically and as biofilms. Antimicrob Agents Chemother doi: 10.1128/AAC.01069-21. Epub ahead of print.

124. **Altschul SF, Gish W, Miller W, *et al.*** 1990. Basic local alignment search tool. J Mol Biol **215**:403–410.

125. **Green R, Rogers EJ**. 2013. Chemical transformation of *E. coli*. Methods Enzymol **529**:329–336.

126. **Meddeb-Mouelhi F, Dulcey C, Beauregard M**. 2012. High transformation efficiency of *Bacillus subtilis* with integrative DNA using glycine betaine as osmoprotectant. Anal Biochem **424**:127–129.

127. **Lowry OH, Rosebrough NJ, Farr AL, *et al.*** 1951. Protein measurement with the folin phenol reagent. J Biol Chem **193**:265–275.

128. **Kurien BT, Scofield RH**. 2019. Electrophoretic separation of proteins: Methods and protocols.

129. **Bay DC, Turner RJ**. 2012. Spectroscopic analysis of small multidrug resistance protein EmrE in the presence of various quaternary cation compounds. Biochim Biophys Acta - Biomembr **1818**:1318–1331.

130. **Towbin H, Staehelin T, Gordon J**. 1979. Electrophoretic transfer of proteins from polyacrylamide gels to nitrocellulose sheets: procedure and some applications. Proc Natl Acad Sci U S A **76**:4350–4354.

131. **Clinical and Laboratory Standards Institute**. 2019. M100 - Performance standards for antimicrobial susceptibility testing, 29th edition.

132. **Clinical and Laboratory Standards Institute**. 2018. M02 - Performance standards for antimicrobial disk susceptibility tests, 13th edition.

133. **Clinical and Laboratory Standards Institute**. 2018. M24 - Susceptibility testing of mycobacteria, *Nocardia* spp., and other aerobic actinomycetes, 3rd edition.

134. **Kumar S, Stecher G, Tamura K**. 2016. MEGA7: Molecular evolutionary genetics analysis version 7.0 for bigger datasets. Mol Biol Evol **33**:1870–1874.

135. **Saitou N, Nei M**. 1987. The neighbor-joining method: A new method for reconstructing phylogenetic trees. Mol Biol Evol **4**:406–425.

136. **Dopazo J**. 1994. Estimating errors and confidence intervals for branch lengths in phylogenetics trees by a bootstrap approach. J Mol Evol **38**:300–304.

137. **Sievers F, Wilm A, Dineen D, *et al.*** 2011. Fast, scalable generation of high-quality protein multiple sequence alignments using Clustal Omega. Mol Syst Biol **7**:1–6.

138. **Waterhouse AM, Procter JB, Martin DMA, *et al.*** 2009. Jalview Version 2-A multiple sequence alignment editor and analysis workbench. Bioinformatics **25**:1189–1191.

139. **Guindon S, Dufayard J françois, Lefort V, *et al.*** 2010. New algorithms and methods to estimate maximim-likelihood phylogenies: assessing the performance of PhyML 3.0. Syst Biol **59**:307–321.

140. **Pakhomova S, Rife CL, Armstrong RN, *et al.*** 2004. Structure of fosfomycin resistance protein FosA from transposon *Tn2921*. Protein Sci **13**:1260–1265.

141. **Yang J, Yan R, Roy A, *et al.*** 2014. The I-TASSER suite: protein structure and function prediction. Nat Methods **12**:7–8.

142. **Schrödinger LLC**. The PyMOL molecular graphics system, version 2.2.3.

143. **Ten Doesschate T, Abbott IJ, Willems RJL, *et al.*** 2019. *In vivo* acquisition of

fosfomycin resistance in *Escherichia coli* by *fosA* transmission from commensal flora. J Antimicrob Chemother **74**:3630–3632.

144. **Huang Y, Lin Q, Zhou Q, *et al.*** 2020. Identification of *fosA10*, a novel plasmid-mediated fosfomycin resistance gene of *Klebsiella pneumoniae* origin, in *Escherichia coli*. Infect Drug Resist **13**:1273–1279.

145. **Guo Q, Chen J, Zhang S, *et al.*** 2020. Efflux pumps contribute to intrinsic clarithromycin resistance in clinical, *Mycobacterium abscessus* isolates. Infect Drug Resist **13**:447–454.

146. **Zhanel GG, Dueck M, Hoban DJ, *et al.*** 2001. Review of macrolides and ketolides: focus on respiratory tract infections. Drugs **61**:443–498.

147. **Luna-herrera J, Reddy VM, Daneluzzi D, *et al.*** 1995. Antituberculosis activity of clarithromycin. Antimicrob Agents Chemother **39**:2692–2695.

148. **Falzari K, Zhu Z, Pan D, *et al.*** 2005. *In vitro* and *in vivo* activities of macrolide derivatives against *Mycobacterium tuberculosis*. Antimicrob Agents Chemother **49**:1447–1454.

149. **Sharma MK, La Y, Janella D, *et al.*** 2020. A real-time PCR assay for rapid identification of inducible and acquired clarithromycin resistance in *Mycobacterium abscessus*. BMC Infect Dis **20**:1–8.

150. **Buriánková K, Doucet-Populaire F, Dorson O, *et al.*** 2004. Molecular basis of intrinsic macrolide resistance in the *Mycobacterium tuberculosis* complex. Antimicrob Agents Chemother **48**:143–150.

151. **Andini N, Nash KA**. 2006. Intrinsic macrolide resistance of the *Mycobacterium tuberculosis* complex is inducible. Antimicrob Agents Chemother **50**:2560–2562.

152. **Guo Q, Chen J, Zhang S, *et al.*** 2020. Efflux pumps contribute to intrinsic clarithromycin

resistance in clinical, mycobacterium abscessus isolates. Infect Drug Resist **13**:447–454.

153. **Duan W, Li X, Ge Y, *et al.*** 2018. *Mycobacterium tuberculosis* Rv1473 is a novel macrolides ABC Efflux Pump regulated by WhiB7. Futur Med **14**:47–59.

154. **Rodrigues L, Sampaio D, Couto I, *et al.*** 2009. The role of efflux pumps in macrolide resistance in *Mycobacterium avium* complex. Int J Antimicrob Agents **34**:529–533.

155. **Ramón-García S, Ng C, Jensen PR, *et al.*** 2013. WhiB7, an Fe-S-dependent transcription factor that activates species-specific repertoires of drug resistance determinants in actinobacteria. J Biol Chem **288**:34514–34528.

156. **Ramón-García S, Mick V, Dainese E, *et al.*** 2012. Functional and genetic characterization of the tap efflux pump in *Mycobacterium bovis* BCG. Antimicrob Agents Chemother **56**:2074–2083.

157. **Pasca MR, Guglierame P, De Rossi E, *et al.*** 2005. *mmpL7* gene of *Mycobacterium tuberculosis* is responsible for isoniazid efflux in *Mycobacterium smegmatis*. Antimicrob Agents Chemother **49**:4775–4777.

158. **Tenson T, Lovmar M, Ehrenberg M**. 2003. The mechanism of action of macrolides, lincosamides and streptogramin B reveals the nascent peptide exit path in the ribosome. J Mol Biol **330**:1005–1014.

159. **Battaglia RA, Ke A**. 2018. Guanidine-sensing riboswitches: How do they work and what do they regulate? Wiley Interdiscip Rev RNA **9**:1–10.

160. **Slipski CJ, Jamieson TR, Lam A, *et al.*** 2019. Plasmid transmitted small multidrug resistant (SMR) efflux pumps differ in gene regulation and enhance tolerance to quaternary ammonium compounds (QAC) when grown as biofilms. BioRxiv.

161. **Brill S, Falk OS, Schuldiner S**. 2012. Transforming a drug/H^+ antiporter into a

polyamine importer by a single mutation. Proc Natl Acad Sci U S A **109**:16894–16899.

162. **Özkal CB, Meriç S**. 2018. A comparative heterogenous photocatalytic removal study on amoxicillin and clarithromycin antibiotics in aqueous solutions. J Water Technol Treat Methods **1**:1–5.

163. **Goldman RC, Fesik SW, Doran CC**. 1990. Role of protonated and neutral forms of macrolides in binding to ribosomes from Gram-positive and Gram-negative bacteria. Antimicrob Agents Chemother **34**:426–431.

164. **Kong FS, Rupasinghe TW, Simpson JA, *et al.*** 2017. Pharmacokinetics of a single 1g dose of azithromycin in rectal tissue in men. PLoS One **12**:1–14.

165. **Porubcan LS, Serna CJ, White JL, *et al.*** 1978. Mechanism of adsorption of clindamycin and tetracycline by montmorillonite. J Pharm Sci **67**:1081–1087.

166. **Bogdanov M, Dowhan W, Vitrac H**. 2014. Lipids and topological rules governing membrane protein assembly. Biochim Biophys Acta - Mol Cell Res **1843**:1475–1488.

167. **Bogdanov M, Mileykovskaya E, Dowhan W**. 2008. Lipids in the assembly of membrane proteins and organization of protein supercomplexes. Subcell Biochem **49**:197–239.

168. **Boldrin F, Anso I, Alebouyeh S, *et al.*** 2021. The phosphatidyl-*myo*-inositol dimannoside acyltransferase PatA is essential for *Mycobacterium tuberculosis* growth *in vitro* and *in vivo*. J Bacteriol **203**:1–12.

169. **Bansal-Mutalik R, Nikaido H**. 2014. Mycobacterial outer membrane is a lipid bilayer and the inner membrane is unusually rich in diacyl phosphatidylinositol dimannosides. Proc Natl Acad Sci U S A **111**:4958–4963.

170. **Su M, Satola SW, Read TD**. 2019. Genome-based prediction of bacterial antibiotic resistance. J Clin Microbiol **57**:e01405-18.

171. **Van Camp PJ, Haslam DB, Porollo A**. 2020. Bioinformatics approaches to the understanding of molecular mechanisms in antimicrobial resistance. Int J Mol Sci **21**:1–8.

172. **Carson M, Johnson DH, McDonald H, *et al.*** 2007. His-tag impact on structure. Acta Crystallogr Sect D Biol Crystallogr **63**:295–301.

173. **Majorek KA, Kuhn ML, Chruszcz M, *et al.*** 2014. Double trouble - Buffer selection and his-tag presence may be responsible for nonreproducibility of biomedical experiments. Protein Sci **23**:1359–1368.

174. **Qazi SJS, Chew R, Bay DC, *et al.*** 2015. Structural and functional comparison of hexahistidine tagged and untagged forms of small multidrug resistance protein, EmrE. Biochem Biophys Reports **1**:22–32.

175. **Dvorak P, Chrast L, Nikel PI, *et al.*** 2015. Exacerbation of substrate toxicity by IPTG in *Escherichia coli* BL21(DE3) carrying a synthetic metabolic pathway. Microb Cell Fact **14**:1–15.

176. **Madsen CT, Jakobsen L, Douthwaite S, *et al.*** 2005. *Mycobacterium smegmatis* Erm(38) Is a reluctant dimethyltransferase. Antimicrob Agents Chemother **49**:3803–3809.

177. **Ito R, Tomich AD, McElheny CL, *et al.*** 2017. Inhibition of fosfomycin resistance protein FosA by phosphonoformate (foscarnet) in multidrug-resistant Gram-negative pathogens. Antimicrob Agents Chemother **61**:1–8.

Appendix A – Accession numbers utilized in this study

Table S1. Accession numbers for FosA and SMR proteins analyzed in this study.

Protein	Species	Sequence ID
FosA1	*Serratia marcescens*	WP_038415208.1
FosA2	*Enterobacter cloacae*	WP_025205684.1
FosA3	*Escherichia coli*	WP_014839980.1
FosA3[a]	***Escherichia coli* (EC623771)**	**[This Study]**
FosA4	*Escherichia coli*	WP_034169466.1
FosA5	*Klebsiella pneumoniae*	WP_012579083.1
FosA6	*Escherichia coli*	WP_069174570.1
FosA7	*Salmonella enterica*	WP_000941934.1
FosA7.2	*Salmonella enterica*	WP_000941935.1
FosA7.3	*Salmonella enterica*	WP_023231494.1
FosA7.4	*Salmonella enterica*	WP_023216493.1
FosA7.6	*Salmonella enterica*	WP_061377147.1
FosA7.7	*Salmonella enterica*	WP_058653118.1
FosA7.8	*Salmonella enterica*	WP_079820715.1
FosA7	*Salmonella enterica*	WP_079825509.1
FosA7	*Klebsiella aerogenes*	WP_072383501.1
FosA7	*Klebsiella oxytoca*	WP_049094497.1
FosA7	*Klebsiella pneumoniae*	WP_110225974.1
FosA7	*Escherichia coli*	WP_097497719.1
FosA7	*Citrobacter koseri*	WP_058668522.1
FosA7	*Citrobacter freundii*	WP_071684814.1
FosA7	*Citrobacter freundii*	WP_087879153.1
FosA7.5^{WT}	***Escherichia coli***	**WP_000941933.1**
FosA7.5^{Q86E}	***Escherichia coli* (EC623772)**	**[This Study]**
FosA7.5^{W92G}	***Escherichia coli***	**WP_094163054.1**
FosA8	*Leclercia adecarboxylata*	WP_063277905.1
FosA8	***Escherichia coli* (EC623773)**	**[This Study]**
FosA9	*Klebsiella variicola*	WP_114473955.1
FosA7^{M}	*Klebsiella pneumoniae*	[Mathur 2018] (113)
FosA8^{M}	*Klebsiella pneumoniae*	WP_105321914.1
FosA9^{M}	*Klebsiella pneumoniae*	WP_134874959.1
FosA10^{M}	*Klebsiella pneumoniae*	WP_004177548.1
FosA11^{M}	*Klebsiella pneumoniae*	WP_002887377.1
FosA12^{M}	*Klebsiella pneumoniae*	WP_004146118.1
Mmr	***Mycobacterium tuberculosis***	**WP_003415995.1**
Mmr	*Mycobacterium canetti*	WP_015294148.1
Mmr	*Mycobacterium avium*	WP_033717689.1
Mmr	*Mycobacterium colombiense*	WP_112634021.1

Mmr	*Mycobacterium intracellulare*	WP_081283700.1
Mmr	*Mycobacterium gordonae*	WP_055577446.1
Mmr	*Mycobacterium kansasii*	WP_023372052.1
Mmr	*Mycobacterium ulcerans*	WP_134427061.1
Mmr	*Mycobacterium simiae*	WP_149655356.1
Mmr	*Mycobacterium marinum*	WP_020724571.1
Smr	*Mycobacterium abscessus*	WP_079623266.1
MSMEG_3670	*Mycobacterium smegmatis*	ABK74464.1
MSMEG_3672	*Mycobacterium smegmatis*	ABK71834.1
Smr	*Mycobacterium fortuitum*	WP_064912137.1
Smr	*Mycobacterium fortuitim*	WP_054602444.1
Smr	*Mycobacterium peregrinum*	WP_055114562.1
Smr	*Mycobacterium peregrinum*	TGB36366.1
Smr	*Streptomyces angustmyceticus*	WP_086718000.1
Smr	*Actinoplanes octamycinicus*	WP_185041450.1
Smr	*Kitasatospora xanthocidica*	WP_117490004.1
Smr	*Lentzea xinjiangensis*	WP_143115942.1
Smr	*Pseudonocardia sulfidoxydans*	WP_147102864.1
Smr	*Nonomuraea rhodomycinica*	WP_175601372.1
Smr	*Agromyces mediolanus*	WP_189086746.1
Smr	*Nocardia brasiliensis*	WP_042263250.1
Smr	*Saccharopolyspora gloriosae*	WP_184484941.1
Smr	*Aldersonia kunmingensis*	WP_068270755.1
Smr	*Arthrobacter globiformis*	WP_111904052.1
Smr	*Epidermidibacterium keratini*	WP_159543442.1
Smr	*Actinomadura viridis*	WP_197014371.1
Smr	*Micromonospora lupini*	WP_007457176.1
EmrE	***Escherichia coli***	**P23895.1**
QacC	***Staphylococcus aureus***	**WP_001146389.1**
QacE	***Klebsiella aerogenes***	**WP_010890145.1**
QacEΔ1	*Klebsiella pneumoniae*	AJQ17568.1
QacF/L	***Klebsiella oxytoca***	**WP_015060824.1**
QacG	***Staphylococcus aureus***	**O87866.1**
QacH	***Staphylococcus saprophyticus***	**WP_032489340.1**
QacJ	***Staphylococcus aureus***	**WP_011100750.1**
QacZ	*Enterococcus faecalis*	WP_010730188.1
Smr	*Bordetella avium*	CAJ50309.1
Smr	*Pseudomonas aeruginosa*	NP_253677
Hsmr	*Halobacterium salinarum*	WP_010903382.1
Gdx/SugE	***Escherichia coli***	**P69937.1**
Gdx/SugE	*Citrobacter freundii*	AAQ16658.1
Gdx/SugE	*Enterobacter kobei*	WP_014882209.1
Gdx/SugE	*Aeromonas molluscorum*	WP_005906869.1

Smr2	*Pseudomonas aeruginosa*	CAH04647.1
MdtI	*Escherichia coli*	P69210.1
MdtJ	*Escherichia coli*	P69212.1
EbrA	*Bacillus subtilis*	P0CW81.1
EbrB	*Bacillus subtilis*	P0CW83.1
YkkC	*Bacillus subtilis*	CAA05588.1
YkkD	*Bacillus subtilis*	CAA05589.1
YvdS	*Bacillus subtilis*	O32262.1
YvdR	*Bacillus subtilis*	O06999.1

[a]Proteins cloned and over-expressed in this study are highlighted in bold

Appendix B – Fasta files for gene synthesis

Fasta files for BioBasic gene synthesized plasmids used in this study. Lowercase letters indicate restriction sites and affinity tags.

```
>FosA7.5WT_E.coli_WP_000941933.1
gaattcaggagaaataatATGCTTCAATCTCTGAACCACTTAACGCTTGCTGTCAGTAATTTGCAAAGTAGCCTGAC
     ATTCTGGCGCGATTTGCTGGGGTTGCAGTTACATGCTGAGTGGGGTACAGGTGCTTACCTTACCTGTGGTGA
     CCTTTGGCTCTGTCTTTCTTATGACGTATCCCGTAGCTACGTGGCCCCACAGAAAAGTGACTATACCCATTA
     CGCATTCAGCATTGCGCCAGAAGATTTTGAGCCGTTCTCATATAAGCTGAAACAGTCGGGAGTGACGGTCTG
     GAAAGACAATAAAAGCGAAGGGCAATCTTTCTATTTTCTTGACCCGGATGGCCACAAGCTGGAGCTGCATGT
     GGGAGATTTAGCATCTCGACTGGCGCAGTGCCGGGAGAGGCCTTACTCTGGAATGCGTTTTGGTCCTGGTAA
     AggcggctctcatcatcatcatcatcattctTAAtctaga
>FosA7.5Q86E_E.coli_EC623772
gaattcaggagaaataatATGCTTCAATCTCTGAACCACTTAACGCTTGCTGTCAGTAATTTGCAAAGTAGCCTGAC
     ATTCTGGCGCGATTTGCTGGGGTTGCAGTTACATGCTGAGTGGGGTACAGGTGCTTACCTTACCTGTGGTGA
     CCTTTGGCTCTGTCTTTCTTATGACGTATCCCGTAGCTACGTGGCCCCACAGAAAAGTGACTATACCCATTA
     CGCATTCAGCATTGCGCCAGAAGATTTTGAGCCGTTCTCATATAAGCTGAAAGAGTCGGGAGTGACGGTCTG
     GAAAGACAATAAAAGCGAAGGGCAATCTTTCTATTTTCTTGACCCGGATGGCCACAAGCTGGAGCTGCATGT
     GGGAGATTTAGCATCTCGACTGGCGCAGTGCCGGGAGAGGCCTTACTCTGGAATGCGTTTTGGTCCTGGTAA
     AggcggctctcatcatcatcatcatcattctTAAtctaga
>FosA7.5W92G_E.coli_WP_094163054.1
gaattcaggagaaataatATGCTTCAATCTCTGAACCACTTAACGCTTGCTGTCAGTAATTTGCAAAGTAGCCTGAC
     ATTCTGGCGCGATTTGCTGGGGTTGCAGTTACATGCTGAGTGGGGTACAGGTGCTTACCTTACCTGTGGTGA
     CCTTTGGCTCTGTCTTTCTTATGACGTATCCCGTAGCTACGTGGCCCCACAGAAAAGTGACTATACCCATTA
     CGCATTCAGCATTGCGCCAGAAGATTTTGAGCCGTTCTCATATAAGCTGAAACAGTCGGGAGTGACGGTCGG
     GAAAGACAATAAAAGCGAAGGGCAATCTTTCTATTTTCTTGACCCGGATGGCCACAAGCTGGAGCTGCATGT
     GGGAGATTTAGCATCTCGACTGGCGCAGTGCCGGGAGAGGCCTTACTCTGGAATGCGTTTTGGTCCTGGTAA
     AggcggctctcatcatcatcatcatcattctTAAtctaga
>FosA3_E.coli_EC623771
gaattcaggagaaataatATGCTGCAGGGATTGAATCATCTGACGCTGGCGGTCAGCGATCTGGCGTCAAGCCTGGC
     ATTTTATCAGCAGTTACCTGGAATGCGCCTGCACGCCAGCTGGGATAGCGGAGCCTATCTCTCCTGTGGGGC
     GCTGTGGCTGTGCTTGTCGCTGGATGAGCAGCGGCGTAAAACGCCCCCTCAGGAAAGCGACTATACCCACTA
     CGCCTTCAGCGTGGCGGAAGAAGAGTTTGCCGGGGTGGTGGCTCTGCTGGCGCAGGCGGGGGCTGAGGTATG
     GAAAGATAACCGCAGTGAAGGGGCGTCTTACTATTTTCTCGACCCTGACGGCCATAAGCTGGAGCTGCATGT
     GGGGAATCTGGCGCAGCGGCTGGCCGCCTGTCGCGAACGCCCCTACAAGGGGATGGTCTTTTTTGATggcgg
     ctctcatcatcatcatcattctTGAtctaga
>FosA8_E.coli_EC623773
gaattcaggagaaataatATGCTTAACGCCCTTAACCATCTGACCCTTGCTGTCAGCAACTTGCCTGCCAGCATCAC
     TTTCTGGCGCGATCTTCTTGGCCTGCGCCTGCACGCCGAATGGCACACCGGAGCTTACCTTACCTGTGGCGA
     TCTCTGGCTCTGCCTGTCTTATGACGAGACGCGGACATTCATCCCACCACAGAACAGCGATTACACCCACTA
     CGCCTTTTCTGTTGAACCGGAACACTTTGACGCCGTCGCGCAAAAGCTCAAAGACGCTGGCGTAACGGTCTG
     GAAAGAGAACAAAAGCGAAGGGGCGTCGTTCTATTTTCTCGACCCGGACGGGCACAAACTGGAACTGCATGT
     GGGCGATCTGGCCGCGCGTCTGGCGGCGTGTCGGGAGAAGCCTTACGCGGGAATGGTTTTTACGTCAGATGA
     AGCGggcggctctcatcatcatcatcatcattctTAAtctaga
>EmrE_E.coli_P23895.1
tctagaaggagaaataatATGAACCCTTATATTTATCTTGGTGGTGCAATACTTGCAGAGGTCATTGGTACAACCTT
     AATGAAGTTTTCAGAAGGTTTTACACGGTTATGGCCATCTGTTGGTACAATTATTTGTTATTGTGCATCATT
     CTGGTTATTAGCTCAGACGCTGGCTTATATTCCTACAGGGATTGCTTATGCTATCTGGTCAGGAGTCGGTAT
     TGTCCTGATTAGCTTACTGTCATGGGGATTTTTCGGCCAACGGCTGGACCTGCCAGCCATTATAGGCATGAT
     GTTGATTTGTGCCGGTGTGTTGATTATTAATTTATTGTCACGAAGCACACCACATTAAaagcttggctg
>QacE_E.coli_WP_010890145.1
tctagagggagatatatcATGAAAGGCTGGCTTTTTCTTGTTATCGCAATAGTTGGCGAAGTAATCGCAACATCCGC
     ATTAAAATCTAGCGAGGGCTTTACTAAGCTTGCCCCTTCCGCCGTTGTCATAATCGGTTATGGCATCGCATT
     TTATTTTCTTTCTCTGGTTCTGAAATCCATCCCTGTCGGTGTTGCTTATGCAGTCTGGTCGGGACTCGGCGT
     CGTCATAATTACAGCCATTGCCTGGTTGCTTCATGGGCAAAAGCTTGATGCGTGGGGCTTTGTAGGTATGGG
```

GCTCATAGTTAGTGGTGTAGTAGTTTTAAACTTGCTTTCCAAAGCAAGTGCCCACTAActgcag
>QacF_E.coli_WP_015060824.1
tctagagggagatatatcATGAAGAACTGGATATTTATGGCTGTTGCAATCTTTGGCGAGGTCATCGCAACTTCCGC
ACTGAAGTCTAGCCATGGATTCACTAGGTTAGTTCCTTCCGTTGTAGTTGTGGCTGGCTACGGGCTTGCGTT
CTATTTCTTGTCTCTCGCGCTCAAGTCCATTCCGGTCGGTATTGCTTACGCTGTATGGGCTGGGCTTGGCAT
CGTGCTTGTGGCAGCTATTGCTTGGATTTTCCATGGCCAAAAACTAGACTTCTGGGCGTTCATTGGCATGGG
ACTTATCGTCAGTGGCGTCGCCGTTCTAAACCTGCTATCCAAGGTCAGCGCACATTGActgcag
>Gdx_E.coli_P69937.1
tctagaaggaggtatatcATGTCCTGGATCGTTTTATTAATTGCAGGTTTGCTCGAAGTTGTCTGGGCGATTGGCCT
GAAATACACCCACGGTTTTACGCGTCTTACGCCAAGCATTATCACTATTGCGGCGATGATCGTCAGTATCGC
CATGCTCTCTTGGGCAATGCGCACGTTGCCTGTAGGAACCGCTTATGCGGTCTGGACCGGTATTGGCGCTGT
TGGGGCGGCCATTACAGGGATTTTGCTGCTGGGTGAGTCTGCCAGCCCGGCACGTTTGCTGAGCCTTGGGCT
GATCGTTGCTGGCATTATTGGTCTGAAGCTGAGCACTCACTAActgcag
>QacC_B.subtilis_WP_001146389.1
tctagaaggaggtaatatATGCCTTATATTTATTTAATAATAGCCATAAGTACTGAAGTTATTGGAAGTGCATTTCT
TAAATCTTCAGAAGGCTTTTCAAAATTTATACCATCCTTAGGAACAATAATTTCATTTGGAATTTGTTTCTA
TTTTTTAAGTAAAACAATGCAACACCTACCACTAAATATAACTTATGCAACTTGGGCGGGACTAGGTTTAGT
CTTAACAACCGTAGTCTCAATAATTATTTTCAAAGAACAAATAAATCTAATAACTATAGTATCTATAGTTTT
AATCATAGTCGGCGTAGTTTCGTTAAACATTTTCGGAACATCGCATTAACCCGGGcccggg
>QacG_B.subtilis_O87866.1
tctagaaggaggtaatatATGCATTATTTATATTTATTTATCTCAATTGCAACAGAAATAATCGGAACTAGTTTTTT
AAAAACATCAGAAGGTTTCACAAAGTTATGGCCAACATTAGGTACACTACTTTCGTTTGGAATTTGCTTTTA
TTTTTTAAGTTTAACAATAAAATTTTTGCCCTTAAATATAACTTACGCAACATGGGCAGGTCTAGGATTAGT
ATTAACAACAATAATCTCAGTTATCGTTTTTAAAGAAAATGTTAATTTAATTAGTATAATTTCTATTGGCTT
AATTGTTATAGGTGTAGTGCTCTTAAATGTATTTGGAGAAAGCCATTGAcccggg
>QacH_B.subtilis_WP_032489340.1
tctagaaggaggtatatcATGAAGAACTGGCTCTTTCTGGCTATTGCAATATTTGGTGAGGTCGTCGCAACTTCCGC
ACTGAAGTCCAGCCATGGATTCACCAAGTTAGTTCCTTCTGTTGTAGTTGTGGCTGGCTACGGGCTTGCGTT
CTATTTCCTCTCTCTCGCACTCAAGTCCATCCCGGTCGGCATTGCTTATGCTGTTTGGGCTGGCCTCGGCAT
CGTACTTGTGGCAGCTATCGCTTGGATCTTCCATGGCCAGAAACTAGACTTGTGGGCGTTCGTTGGCATGGG
ACTTATCGTTAGTGGCGTCGCCGTTCTAAATCTGCTATCCAAGGTCAGCGCACATTGActgcag
>QacJ_B.subtilis_WP_011100750.1
tctagaaggaggtaatatATGCCTTACTTATATTTAGTAATAGCGATTATAACTGAAATAATAGGAACTAGTTTCTT
AAAAACAGCAGAAGGATTTACAAAACTTTGGCCAACATTAGGCACACTTATTTCATTCGGGATATGTTTCTA
TTTTTTAAGTGTAACTATGAAATATTTACCACTCAATGTATCTTATGCAACTTGGGCAGGGTTAGGACTAGT
TCTTACAACAATAGTTTCAGTTGTAATTTTCAAAGAAAGCGTCAATTTAATTAGTATATTTTCAATAATCTT
AATTATTATTGGTGTTGTGCTTCTTAACGTTTTTGGATCAAGTCATTAAcccggg
>Mmr_M.smegmatis_WP_003415995.1
ccatgggcATGATCTACCTATACCTCTTGTGCGCGATCTTCGCGGAAGTGGTGGCAACCAGCCTGCTCAAAAGCACG
GAAGGGTTCACTCGGTTGTGGCCCACGGTGGGCTGTCTAGTGGGTTATGGCATCGCTTTCGCGCTGCTGGCC
TTGTCGATCTCGCACGGCATGCAGACGGACGTCGCCTATGCGCTGTGGTCGGCAATCGGTACGGCCGCCATT
GTGCTGGTCGCCGTACTGTTTCTCGGCTCGCCGATATCTGTGATGAAGGTGGTTGGCGTCGGCCTGATTGTC
GTCGGCGTGGTCACGTTGAACCTGGCGGGTGCCCATgaatttgaagcgtacgtcgaacagaaactgatctcg
gaggaagacctcaatagcgccgtcgatcatcaccaccaccatcatTGAggatcc

Appendix C – Homology model active sites

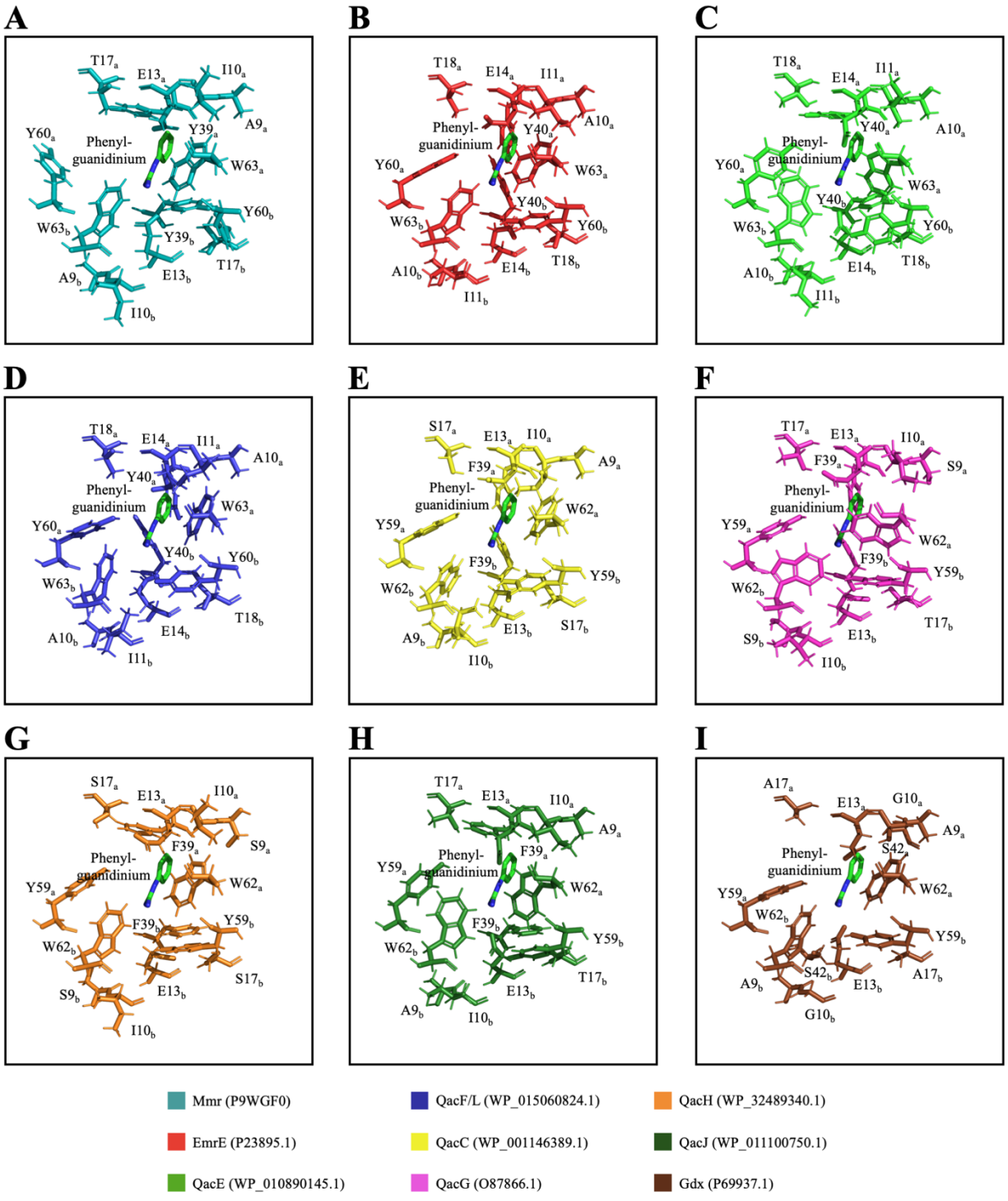

Figure S1. Stick diagrams of SMR efflux protein homology model active sites with bound substrate phenylguanidinium. **A)** Active site of Mmr. **B)** Active site of EmrE. **C)** Active site of QacE. **D)** Active site of QacF. **E)** Active site of QacC. **F)** Active site of QacG. **G)** Active site of

QacH. **H)** Active site of QacJ. **I)** Active site of Gdx. All structural images were generated using the program PyMOL version 2.2.3 (142). Colours listed below the panel in the legend indicate particular SMR dimers.